Characterization of the *Arabidopsis thaliana* RING-type Ubiquitin Ligase XBAT31.1 and its Role in Response to Iron Deficiency Stress

by

Nathieli Beltran Schiavi

Submitted in partial fulfilment of the requirements
for the degree of Master in Science

at

Dalhousie University
Halifax, Nova Scotia
December 2017

© Copyright by Nathieli Beltran Schiavi, 2017

.

TABLE OF CONTENTS

LIST OF TABLES

LIST OF FIGURES

ABSTRACT

Iron (Fe) is a very important micronutrient, specially for animals and plants. In humans, Fe-deficiency can cause anemia, which affects 43% of children, 38% of pregnant woman and 29% of non-pregnant women (World Health Organization et al., 2013). In plants, Fe-deficiency can impact nutritional quality growth and limit crop productivity. As a result, plants must sense Fe deprivation and be capable of balancing Fe-concentration in a homeostatic way, to be able to provide the necessary amounts of the required micronutrient to important process such as respiration and photosynthesis (Briat and Lobreaux, 1997; Hell and Stephan, 2003). The ubiquitin proteasome system (UPS) controls the abundance of important enzymes structural and regulatory proteins. Plants utilize UPS to facilitate changes in cellular protein content required for tolerance of adverse environments, such as micronutrient deficiency. Central to the UPS are the ubiquitin ligase enzymes that govern protein substrate selection. Importantly, a number of RING-type ubiquitin ligases have been shown to regulate proteins involved in iron uptake under iron sufficient (Moroishi et al., 2011) and iron deficient conditions (Kobayashi et al., 2013; Shin et al., 2013). In this study, we demonstrate the role of *Arabidopsis thaliana* XBAT31.1, a RING-type ubiquitin ligase, in response to Fe-deficiency stress. *XBAT31.1* expression is induced under iron deficient conditions. *xbat31-1* seedlings have elevated transcript levels of *Fe-utilization related* genes, such as *FIT, FRO2* and *AHA2* under Fe-deficiency compared to wild type. Unexpectedly, the increase in the transcript level of *IRT1*, which encodes for the major metal transporter responsible for uptake of iron and other metals, was significantly lower compared to wild type. The low levels of *IRT1* transcripts are correlated with *xbat31-1* accumulating less iron, manganese and cobalt in shoots under Fe-deficient condition. Despite the low iron content, *xbat31-1* seedlings are more tolerant to Fe-deficient than wild type seedlings as shown by significant higher root length, fresh weight and chlorophyll content. Based on these results a model is proposed where XBAT31.1 functions as an iron sensor and ubiquitin ligase that indirectly regulates expression of *IRT1* during plant response to Fe-deficiency stress.

Subject Keywords: Iron, Fe-deficiency, plants, Arabidopsis thaliana, ubiquitin proteasome system, ubiquitin ligase.

LIST OF ABBREVIATIONS USED

ABA	Abscisic acid
ABCG37	ATP-BINDING CASSETE SUB-FAMILY C MEMBER 37
ABRC	Arabidopsis Biological Resource Center
ACC	1-AMINOCYCLOPROPANE-1-CARBOXYLIC ACID
AHA2	ADENOSINE TRIPHOSPHATASES H+-ATPase 2
Arabidopsis	*Arabidopsis thaliana*
ATP	Adenosine triphosphate
B	Boron
BAR	Bio-Analytic Resource
bHLH	Basic helix-loop-helix
BP	Bromocresol purple
BRL2	BRASSINOSTEROID-INSENSITIVE LEUCINE-RICH REPEAT RECEPTOR-LIKE KINASE
BTS	BRUTUS
Ca	Calcium
$CaSO_4$	Calcium sulfate
cDNA	Complementary DNA
CHIP	CARBOXYL TERMINUS OF HSC70-INTERACTING PROTEIN
Cl	Chlorine
Col-0	Arabidopsis ecotype Columbia
CP or 20S	Core protease

CPL1	C-TERMINAL DOMAIN PHOSPHATASE-LIKE 1
Cu	Copper
DMSO	Dimethyl sulfoxide
DNA	Deoxyribonucleic acid
DTT	Dithiothreitol
DUBs	Deubiquitinating
E3	Ubiquitin ligase
EDTA	Ethylenediaminetetraacetic acid
EF-1α	ELONGATION FACTOR-1α
FAD7	ω-3 FATTY ACID DESATURASE 7
FDR3	FERRIC REDUCTASE DEFECTIVE 3
Fe	Iron
+Fe	Iron sufficient
-Fe	Iron deficient
Fe(II) or $\mathbf{Fe^{2+}}$	Ferrous oxide
Fe(III) or $\mathbf{Fe^{3+}}$	Ferric oxide
$\mathrm{Fe}(\mathbf{OH})^{\mathbf{2+}}$	Ferrous hydroxide
$\mathrm{Fe}(\mathbf{OH})_{\mathbf{3}}$	Ferric hydroxide
Fe-EDTA	Ferric ethylenediaminetetraacetic acid
FerroZine	3-(2-Pyridyl)-5,6-diphenyl-1,2,4-triazine-p,p′-disulfonic acid monosodium salt hydrate
Fe-S	Iron-sulfide clusters
[2Fe-2S]	2 Iron- 2 sulfide clusters

[3Fe-4S]	3 Iron- 4 sulfide clusters
[4Fe-4S]	4 Iron- 4 sulfide clusters
[8Fe-7S]	8 Iron- 7 sulfide clusters
FIT	FER-LIKE FE DEFICIENCY INDUCED TRANSCRIPTION FACTOR
FPN1	FERROPORTIN 1
FRO2	FERRIC REDUCTASE OXIDASE 2
FRO3	FERRIC REDUCTASE OXIDASE 3
FW	Fresh weight
GA	Gibberellic acid
GST-HIS	Glutathione-S-transferase - poly(His) tag
$\mathbf{H^+}$	Hydrogen ion
$\mathbf{H_2O_2}$	Hydrogen peroxide
HCl	Hydrochloric acid
HECT	Homology to E6-associated Carboxy-Terminus
HRZs	HEMERYTHRIN MOTIF-RINGAND ZINC-FINGER PROTEINS
ICP-MS	Inductively coupled plasma–mass spectrometry
IDE1	FE DEFICIENCY-RESPONSIVE CIS-ACTING ELEMENT
IDEF1	IRON DEFICIENCY-RESPONSIVE ELEMENT-BINDING FACTOR 1
IDF1	IRT1-DEGRADATION FACTOR 1
ILR3	IAA-LEUCINE RESISTANT 3
IPTG	Isopropyl β-D-1-thiogalactopyranoside

IRT1	IRON REGULATED TRANSPORTER 1
K	Potassium
K48	Lysine 48 residues
KCl	Potassium chloride
KDa	Kilodaltons
MA	Mugineic acid
MAPK	MITOGEN ACTIVATED PROTEIN KINASE
MAX2	MORE AUXILLARY BRANCHING 2
MDA	Malondialdehyde
MDa	Megadalton
MES	2-(N-morpholino) ethanesulfonic acid
Mg	Magnesium
$\mathbf{MgCl_2}$	Magnesium chloride
Mn	Manganese
Mo	Molybdenum
MS	Murashige and Skoog media
MYB10	MYELOBLASTOSIS 10
MYB72	MYELOBLASTOSIS 72
N	Nitrogen
NA	Nicotinamide
NaCl	Sodium chloride
NADH	Nicotinamide adenine dinucleotide
NAS	NICOTIANAMINE SYNTHASE

NAS4	NICOTIANAMINE SYNTHASE 4
Ni	Nickel
$^{\cdot}OH$	Reactive hydroxyl radicals
OPT3	OLIGOPETIDE TRANSPORTER 3
OsIRO2	Rice FE-REGULATED bHLH TRANSCRIPTION FACTOR 2
P	Phosphorus
PCR	Polymerase chain reaction
pH	Potential of hydrogen
PM	Plasma membrane
PS	Phytosiderophores
PSI	Photosystem I
PSORT	Protein Subcellular Localization Prediction Tool
PUB44	PLANT U-BOX 44
PYE	POPEYE
PYEL	PYE-like proteins
qRT-PCR	Real-time quantitative reverse transcription polymerase chain reaction
RD29A	RESPONSE-TO-DEHYDRATION 29A
RING	REALLY INTERESTING NEW GENE
Rma1H1	RING MEMBRANE-ANCHOR 1
RNA	Ribonucleic acid
ROS	Reactive oxygen species
RP or 19S	Regulatory particle

RT-PCR	Reverse-transcriptase polymerase chain reaction
S	Sulphur
SAM	S-adenosyl methionine
SDS	Sodium dodecyl sulfate
TCA	Trichloroacetic acid
TGN	Trans-Golgi network
TOM1	TRANSPORTER OF MUGINEIC ACID 1
Tris-HCl	Tris(hydroxymethyl)aminomethane hydrochloride
UBA or E1	Ubiquitin activating enzyme
UBC or E2	Ubiquitin conjugating enzyme
UBQ10	POLYUBIQUITIN 10
UPL1-7	UBIQUITIN-PROTEIN LIGASE 1-7
UPS	Ubiquitin proteasome system
UTR	Untranslated region
WT	Wild type
Xa21	RECEPTOR KINASE-LIKE PROTEIN
XB3	Xa21-BINDING PROTEIN 3
XBAT31	XB3 ortholog 1 in Arabidopsis
XBAT31.1	XB3 ortholog 1 in Arabidopsis splice version XBAT31.1
XBAT31.2	XB3 ortholog 1 in Arabidopsis splice version XBAT31.2
xbat31-1	*XBAT31* T-DNA knockdown
YLS1	YELLOW STRIP-LIKE 1
YSL15	YELLOW STRIP-LIKE 15

ZIF1	ZINC-INDUCED FACILITATOR
Zn	Zinc
26S proteasome	Protease complex

ACKNOWLEDGEMENTS

First, I must thank my lovely life partner, Marciel Gaier, for all care during the last 7 years and specially for the last 2 years. You have been an awesome fiancé and a nice friend since we start grad school. I know how difficult have been to you see me suffering and struggling during grad school, but I promise you; it is going to be worth at the end. I hope you all the best in the next steps of your PhD, my love! Be brave, be strong and be yourself! Let's rock babe!

Secondly, I will say my thank you for my parents (Rute and Vilmar), grandparents (Matilde and João) and two uncles (Leonel and Velarim), you guys are a wonderful family. Even though we are far away, you made almost all my days in the past 2 years with all pictures, videos and conversations! Thank you, guys. I hope I could make you prouder with this Master degree.

Next, I need to say THANK YOU for my lovely supervisor, Sophia Stone. Thank you for being yourself during all my time as your students. You have been a professor, an advisor, a listener and a friend besides of being a supervisor. Thank you for your guidance, support and care since the beginning! I would never had wished a better supervisor for my Master. If I could suggest you one thing, I would say: please never change! I love who you are! I hope we can work together for the next year in the same way we have been working so far! You became my inspiration!

Furthermore, I would like to thank my lab mates and my grad school friends. Specially Dalal, Arthur, Daryl, Mohammad and Victoria. You all have made the last 2 years less difficult for me, with all your kind words in difficult times. I hope I can be there

for you as you were there when I needed you! Thank you so much guys. I hope we all can achieve our goals and become very happy families in the end!

Finally, I would like to thank the girl inside me! I would like to thank myself. I have been fighting against my wishes and desires to become what the people who love me wish me to be and I complete forgot who I am in the middle of this path. I would like to thank myself for advising me last year that this couldn't be my life forever. Thank you, girl, for making me remember. Thank you, girl, for fighting against me to be yourself (or maybe myself!?). You deserve to be everything you want to be, besides other people's wishes. You deserve to be happy! Be brave, be strong and be yourself. That's is the only way you die in peace when the time comes. No regrets ever again, please!

CHAPTER 1: INTRODUCTION

1.1 Mineral nutrient Stress in Plants

Stress is characterized as any external factor that negatively affect plant growth, development, and cause yield loss (Pandey et al., 2017; Xu, 2016). Plant stress is divided in two major categories biotic and abiotic. Biotic stress is defined as one living organism causing damage to other living organism, which could be bacteria, viruses or fungi (Pandey et al., 2017). Abiotic stress is characterized by the change in parameters or resources, which affect plant growth such as water availability, salinity, alkalinity, temperature and mineral nutrients (Pandey et al., 2017).

There are 3 categories of plant stress single, multiple individual or combined. Single stress is represented by plants facing one stress factor at a time. Multiple stress is the impact of two or more stress factors that occur at different time points without overlapping each other, for example, cold and heat stresses occurring in different seasons. Combined stress is similar to the multiple stress category, however the stress factor overlap each other at some point, for example, heat and drought stresses occurrence during summer (Pandey et al., 2017). Biotic and abiotic stress factors can occur with varying combinations, such as biotic-biotic, biotic-abiotic or even abiotic-abiotic.

Despite the importance and occurrence of the other forms of abiotic stress, mineral nutrients stress is one of the most common stress that plants encounter. Mineral nutrients are characterized as macronutrients and micronutrients (Liphadzi and Kirkham, 2006; Rengel, 2015). Macronutrients include nitrogen (N), phosphorus (P), potassium (K), calcium, (Ca), magnesium (Mg) and sulphur (S). Micronutrients include: boron (B),

chlorine (Cl), copper (Cu), iron (Fe), manganese (Mn), molybdenum (Mo), and zinc (Zn). Most sandy or low-organic matter soils are naturally deficient in micronutrients meaning these nutrients are present at lower soluble levels than that required by plants. Arable lands are not usually categorized as micronutrient deficient. However, acidity and alkalinity reduce micronutrient availability and in some cases can even make them unavailable (high pH soils) for uptake by the plant (Liphadzi and Kirkham, 2006).

Plants are able to sense and respond to a variety of abiotic stresses, including micronutrient stress, using a range of mechanisms including the upregulation of gene expression that encode for proteins that ameliorate the damaging effects on cell structure and function (Dorantes-Acosta et al., 2012). For example, in response to increased levels of reactive oxygen species (ROS), MITOGEN ACTIVATED PROTEIN KINASE (MAPK) is activated (Jalmi and Sinha, 2015). MAPKs are part of the most important response against pathogen defense and tolerance against cold, salt and oxidative stress by modifying ROS production levels (Jalmi and Sinha, 2015). However, despite the use of various response mechanisms that maximize survival rate in hostile environments, abiotic stress is responsible for more than 50% of yield loss in major crops (Xu, 2016).

1.2 Iron

Iron (Fe) is one of the most important micronutrient for living organisms due to its redox properties (Lingam et al., 2011). In humans, Fe plays a role in nutritional disorders such as Fe-deficiency anaemia which affects more than 30% of the global population (WHO, 2013). Anemia is assessed by measuring haemoglobin levels in blood samples and it is used as an indicator of Fe-deficiency (WHO, 2013). Haemoglobin is the metalloprotein

transporter containing-iron localized in the red blood cells responsible for carrying oxygen from the respiratory organs to the rest of the body. In human body there is around 3-4g of iron, which 70% is incorporated in hemoglobin (Joosten, 2017). Anemia can be diagnosed in adult men by haemoglobin concentration bellow 13g/dl (grams of haemoglobin per decilitre of blood), in non-pregnant women bellow 12g/dl and in pregnant women bellow 11g/dl since blood volume increases during pregnancy, leading to haemodilution (Joosten, 2017; World Health Organization et al., 2013). Anemia during pregnancy usually reflects in reduction of iron stores in the newborn infant which cause poor cognitive function and motor development (Haniff et al., 2007). For adults the primary source of iron acquisition is diet in which iron could be acquired from two different sources, animals or plants. Worldwide, the major Fe source for human's diet comes from crops, which made Fe-deficiency in plants becoming a very important field to investigation (Martin and Li, 2017). In agriculture, Fe-deficiency can induce chlorosis which causes significant yield loss and poor crop quality, predominantly in high pH soils. Since the nutritional value of a crop can be reduced by Fe-deficiency, important agronomic approaches to overcome Fe availability in soil are available (Hasegawa et al., 2011; Shenker and Chen, 2005). There are 3 major approaches applicable in soils nowadays (1) methods to increase availability of soil-Fe, as reducing soil pH by application of fertilizers; (2) application of external Fe source, as for example Fe-EDTA or other synthetic chelator; and (3) improvement of genetic and breeding techniques to enhance Fe-uptake and translocation efficiency (Shenker and Chen, 2005). These 3 approaches have opened doors to successful production of crops under highly calcareous soils that has been a challenge for farmers in the past decades.

1.2.1 Iron Availability in Soil

Fe is abundant in nature representing 5% of total soil minerals, in contrast to other metals, as for example copper, which represents 0.01%. Even though iron is not a rare compound, iron-deficiency represents a severe problem in the agriculture because 30% of the arable lands consist of calcareous and alkaline soils (high pH soils) (Guerinot, 2001; Guerinot and Yi, 1994). In soil solutions, under a pH range of 4 to 9 (relevant for plant growth), the Fe(III) speciation consists in the most abundant species which are $Fe(OH)^{2+}$ and $Fe(OH)_3$ (Hasegawa et al., 2011; Shenker and Chen, 2003). The sum of all hydrate forms of Fe(III), when in equilibrium with $Fe(OH)_3$, in a pH range of 7.4 to 8.5 is around 10^{-10} (Shenker and Chen, 2003). The hydrate oxides states are poorly absorbed by plant roots causing substandard plant growth (Cohen et al., 1998; Guerinot and Yi, 1994). In contrast, acidic soils are more likely to contain an excess of solubilized Fe(II) which is easily taken up by the roots and can lead to iron toxicity. Fe can react with reduced oxygen forms, creating ROS by Fenton reaction, which is responsible for the conversion of hydrogen peroxide (H_2O_2) into reactive hydroxyl radicals ($^{\cdot}OH$) that are cell damaging reactive molecules able to promote oxidative stress (Jean et al., 2005; Kobayashi and Nishizawa, 2014). ROS can damage cellular components causing cell death (Briat and Lobreaux, 1997; Brumbarova and Bauer, 2009). In wetlands, Fe can form plaques (insoluble ferric hydroxide) in the rhizosphere of aquatic plants, resulting in reduced uptake of nutrients including Fe, Mn, Zn, Cu, P, Pb and Cd (Hasegawa et al., 2011).

1.2.2 Iron in Plants

Most plants require a soluble concentration of Fe in soil from 10^{-8} to 10^{-4} M in order to achieve normal growth and development (Briat and Lobreaux, 1997). However, in neutral or alkaline soils the total soluble Fe (which is available for uptake) is approximately 10^{-17} to 10^{-10}M, respectively (Briat and Lobreaux, 1997). Since Fe is essential for different cellular and molecular processes, such as photosynthesis (in the plastids) and respiration (in the mitochondria), plants require high input of Fe. Plants have developed active mechanisms to efficiently extract iron from soil avoiding Fe-deficiency (Briat et al., 1995; Guerinot and Yi, 1994). Fe-uptake and transport is also tightly regulated at the transcript levels to prevent high input of iron (Briat and Lobreaux, 1997; Selote et al., 2015).

Fe is required for the assembly of nonheme iron and inorganic sulfide (Fe-S) clusters (Brumbarova and Bauer, 2009; Mai et al., 2016). Fe-S clusters can contain [2Fe-2S], [3Fe-4S], [4Fe-4S] or [8Fe-7S] core units, all involved in electron transfer. The ability of Fe-S clusters carrying away electrons make them very important for mediating electron transport and for being, in whole or in part, the sites for substrate-binding of redox and non-redox enzymes (Johnson et al., 2005).

Fe-S clusters participate in many process, such as DNA replication and repair, chlorophyll catabolism, ribosome biogenesis, sulfur and nitrogen assimilation, and [4Fe-4S] clusters are involved in the photosynthetic electron transport chain by transferring their electrons directly to stromal ferredoxins in the photosystem I (PSI) or by regulation of gene expression and substrate binding, activation or reduction (Couturier et al., 2013; Fuss et al., 2015).

Iron plays a role as an active cofactor of many enzymes, being necessary for plant hormone synthesis as ethylene by the activation of 1-AMINOCYCLOPROPANE-1-CARBOXYLIC ACID (ACC) OXIDASE (Romera et al., 1996). It is also necessary for abscisic acid (ABA) production by controlling the activity of PHYTOENE DESATURASE (Rout and Sahoo, 2015).

1.2.3 Iron Sensors in Plants

Iron sensors are defined by Kobayashi and Nishizawa (2014) as biomolecules that can (1) bind Fe directly or indirectly; (2) change its function as an outcome of binding, and (3) regulate Fe homeostasis. By using these criteria's, 2 Fe-sensors have been described for rice which are rice *Oryza sativa* IRON DEFICIENCY-RESPONSIVE ELEMENT-BINDING FACTOR 1 (IDEF1) and HEMERYTHRIN MOTIF-REALLY INTERESTING NEW GENE (RING) AND ZINC-FINGER PROTEINS (HRZs) (Kobayashi and Nishizawa, 2014). The two rice HRZs are homologous to the previously identified *Arabidopsis thaliana* (Arabidopsis) BRUTUS (BTS) which is the only iron sensor that meets the same criteria to be named as an iron sensor in Arabidopsis (Long et al., 2010). *IDEF1* was identified in rice as a transcription factor, which binds to *FE DEFICIENCY-RESPONSIVE CIS-ACTING ELEMENT (IDE1)* and promotes the expression of rice *FE-REGULATED bHLH TRANSCRIPTION FACTOR 2 (OsIRO2)* during the early stages of Fe deficiency response (Kobayashi et al., 2009, 2007; Ogo et al., 2006; Zheng, et al., 2010). Even though *IDEF1* plays an important role in response to Fe-deficiency, its transcript levels do not change under such conditions, suggesting that IDEF1 is located upstream of

the stress-induced transcription cascade (Kobayashi et al., 2009, 2007). IDEF1 also binds Fe, Zn, Cu and Ni ions, which makes it a candidate for Fe sensing (Kobayashi et al., 2012; Kobayashi and Nishizawa, 2014).

HZRs/BTS transcripts increase in response to Fe-deficiency stress (Long et al., 2010; Selote et al., 2015). The encoded multifunctional protein possess a hemerythrin domain, which is a binding-site for Fe and Zn ions, and a RING domain that imparts ubiquitin ligase activity responsible for ubiquitinating and targeting proteins for degradation by 26S proteasome (Kobayashi et al., 2013). The fact that HZR/BTS can bind iron suggests that the protein may function as a Fe sensor and also regulate the abundance of other iron related proteins (Kobayashi and Nishizawa, 2014).

1.2.4 Iron Uptake Strategies

Oxygenic photosynthetic organisms, such as plants, always face the double challenge of acquiring iron from an inorganic environment and make it available in different bound organic forms (Hell and Stephan, 2003). To promote iron uptake by roots, under different soil conditions, plants developed two major strategies chelation strategy and reduction strategy.

Chelation strategy or Strategy II, is used by graminaceous monocotyledons, for example barley, corn and rice. These plants are able to take up Fe(III) directly from the soil by secreting phytosiderophores (PS) into the rhizosphere, specifically mugineic acid (MA) (Figure 1). MA is a high-affinity Fe(III) chelating compound of low molecular weight (Hasegawa et al., 2011; Mulligan and Choryt, 2017). MA is exported by TRANSPORTER

OF MUGINEIC ACID 1 (TOM1) and forms Fe(III)-MA complex which is recognized and imported to the cytoplasm by YELLOW STRIP-LIKE 1 (YLS1) in barley or YSL15 (YELLOW STRIP-LIKE 15) in rice (Connorton et al., 2017; Schmidt and Buckhout, 2011) (Figure 1). The chelation strategy is sensitive to changes in soil pH since high alkaline soils can reduce solubility of Fe(III) oxides and hydroxides, controlling directly its concentration. Since the concentration of PS, in the rhizosphere, is related with the capability of chelation and solubilization of Fe(III), PS is the most important component of this strategy (Brumbarova and Bauer, 2009). Under Fe-deficient condition, PS are able to form organic complexes or chelates with Fe(III) which helps to increase the movement of iron in soil (Hasegawa et al., 2011).

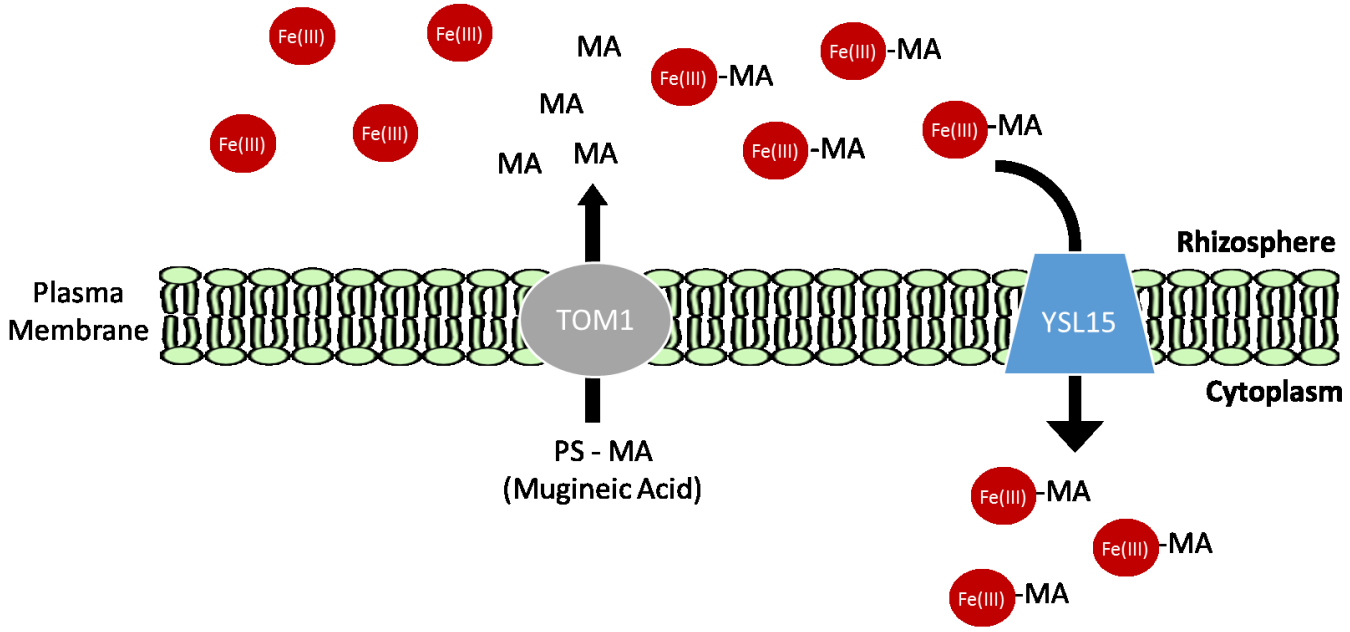

Figure 1 - Iron Uptake Chelation-based Strategy Machinery in Rice.

In the absence of iron, two transporters are upregulated, TRANSPORTER OF MUGINEIC ACID 1 (TOM1) and YELLOW STRIP-LIKE 15 (YSL15). TOM1 is responsible for transporting the Phytosiderophores - Mugineic Acid (PS-MA) to the rhizosphere, which will chelate Fe(III), forming a Fe(III)-MA complex. The membrane transporter YSL15 will import Fe(III)-MA complex into the cytoplasm.

Reduction strategy or Strategy I, is used by dicotyledons and non-grasses monocotyledons, for example tomato and Arabidopsis. It requires at least three steps to be able to acquire Fe from the rhizosphere. Step 1: acidification of the rhizosphere; step 2: reduction of Fe(III) to Fe(II); and step 3: induction of Fe transporter (Figure 2). This strategy involves increasing the expression of 3 major genes, *FERRIC REDUCTASE OXIDASE 2* (*FRO2*), *ADENOSINE TRIPHOSPHATASES H+-ATPase 2* (*AHA2*) and *IRON REGULATED TRANSPORTER 1* (*IRT1*), with a strong up-regulation of *FRO2* and *IRT1* under Fe deficiency (Colangelo, 2004; Robinson et al., 1999; Selote et al., 2015). The proton translocating AHA2 is responsible for acidifying the apoplast by extrusion of H^+, which facilitates the enzymatic reduction of Fe(III) (Eroglu et al., 2016; Santi and Schmidt, 2009). FRO2 reduces Fe(III) to Fe(II) by transferring electrons from the cytosolic NADH to Fe(III)-chelates (Eroglu et al., 2016; Yi and Guerinot, 1996). Reduction of Fe(III) is needed because the metal ion transporter, IRT1, only uptakes Fe(II) (Selote et al., 2015). IRT1 is membrane localized and strongly expressed in root epidermal cells. IRT1 is also responsible for transportation of other metal ions such as Zn, Mn, Co, Cd and Ni (Hell and Stephan, 2003; Vert et al., 2002). The reduction strategy also requires phenolic compounds, which act as metal chelators able to form Fe(III)-PS complexes (Clemens and Weber, 2016). The major phenolic compounds detected in root exudates of Arabidopsis are coumarins which are transported into the rhizosphere by ATP-BINDING CASSETE SUB-FAMILY C MEMBER 37 (ABCG37) (Schmid et al., 2014).

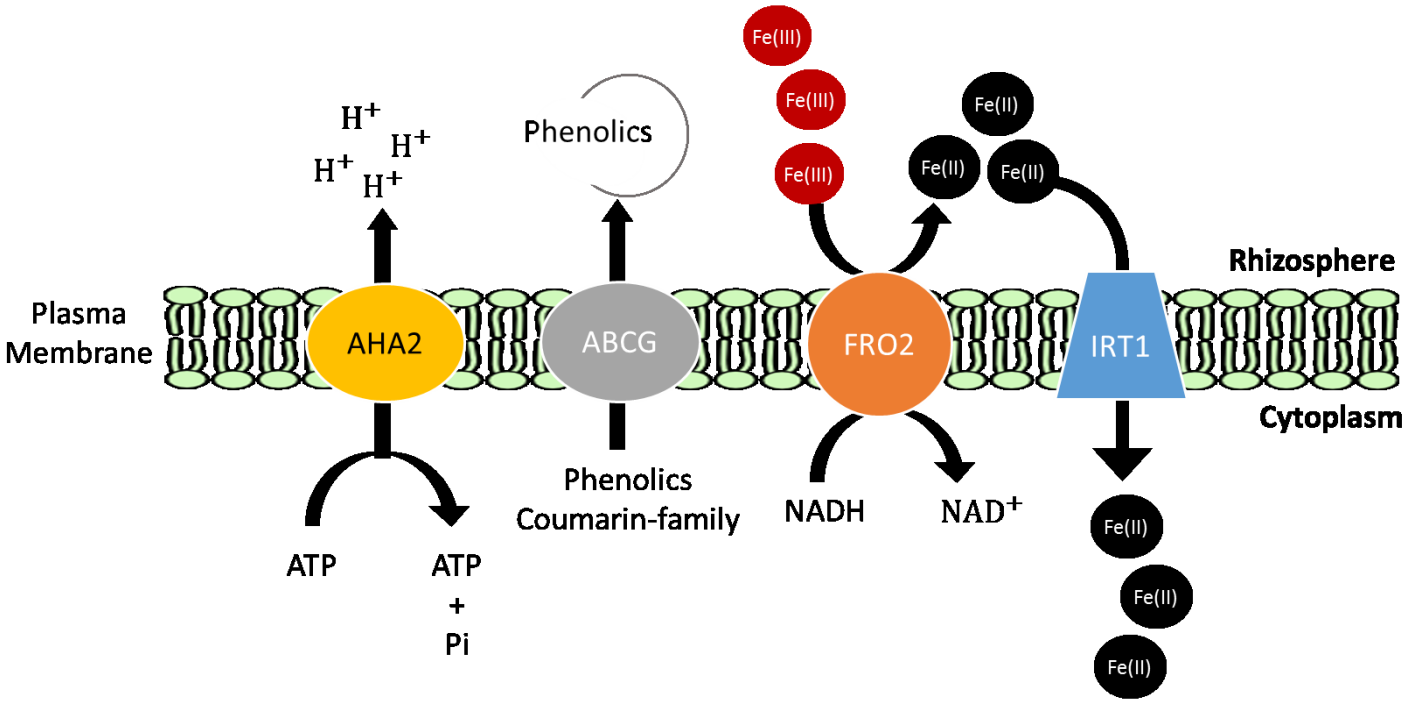

Figure 2 - Iron Uptake Reduction-based Strategy Machinery in *Arabidopsis thaliana*.

In the absence of iron, ADENOSINE TRIPHOSPHATASES H+-ATPase 2 (AHA2) is upregulated, which lowers the soil pH by extruding protons to the rhizosphere, and assist in solubilizing Fe(III). ATP-BINDING CASSETE SUB-FAMILY C MEMBER 37 (ABCG37) will export phenolics to the rhizosphere, which chelates Fe(III). Solubilized and chelate Fe complexes will be recognized by FERRIC REDUCTASE OXIDASE 2 (FRO2) that is going to be responsible for reducing Fe(III)-chelates to Fe(II). Fe(II) is then imported into the cytoplasm by the upregulated transporter IRON REGULATED TRANSPORTER 1 (IRT1).

The main difference between both strategies is the oxidation state of iron, where reduction strategy plants can take up Fe as ferrous (Fe(II) or Fe^{2+}) and chelation strategy plants can take up Fe as ferric (Fe(III) or Fe^{3+}) (Connorton et al., 2017). Both strategies were thought to be used separately by different plant species. However, recent studies have shown that non-graminaceous plants (primary utilize the reduction strategy) possess the ability of export Fe(III) chelators, which is part of the chelation strategy machinery. In addition, graminaceous plants can use the reduction strategy in specific cases to acquire Fe(II). For example, in low oxygen environments, plants with the chelation strategy use a functional homologue of IRT1 to acquire Fe(II) (Kobayashi and Nishizawa, 2014, 2012; Mai et al., 2016). Soils lacking oxygen (for example paddy fields) cause a shift in the equilibrium of Fe, where Fe(III) is less concentrated compared to Fe(II), this shift would cause a problem for rice to acquire Fe(III) if the chelation strategy was the only way to acquire Fe from the soil (Kim and Guerinot, 2007). These findings are relatively new for plants, however the ability to use different strategies to acquire Fe is also observed in other organisms such as, the proteobacteria, *Pseudomonas aeruginosa* (Kreamer et al., 2012). These organisms can uptake Fe(III) using one set of transporters and can uptake Fe(II) using another set of transporters depending on the environment and availability (Lane et al., 2015; Mai et al., 2016; Palmer and Skaar, 2016).

1.2.5 Iron Translocation

Fe (as well as Zn, Co, Mn, Ni and Cd) is transported by IRT into roots where it is complexed to chelators so that it can be moved to other tissues without causing any cell

damage or become insoluble (Connorton et al., 2017) (Figure 3). Nicotinamide (NA) is a chelator of Fe(II) forming Fe(II)-NA complex, which is used to transport iron via the root symplast pathway until Fe reaches the xylem (Figure 3). NA is a non-protein amino acid which is produced by NICOTIANAMINE SYNTHASE (NAS) by using S-adenosyl methionine (SAM) (Morrissey et al., 2009; Zhai et al., 2014). FERROPORTIN 1 (FPN1) is responsible for loading Fe into the xylem (Morrissey et al., 2009; Zhai et al., 2014). The transporter responsible for loading NA into xylem is still unknown (Gayomba et al., 2015). Once Fe(II)-NA complex enters the xylem, Fe(II) will be oxidised becoming Fe(III) which is then chelated with citrate, forming Fe(III)-citrate complex (Figure 3). Citrate is predicted to chelate approximately 99.5% of total iron present in the xylem exudates and it is released into the apoplastic space by FERRIC REDUCTASE DEFECTIVE 3 (FRD3) (Connorton et al., 2017; Durrett et al., 2007; Zhai et al., 2014).

For Fe to be able to enter in the shoots it must be reduced to Fe(II), which is likely to be done by FRO family (Gayomba et al., 2015). Fe(II) will be complexed to NA, forming again Fe(II)-NA, which is able to re-enter the symplast and travel to other sink tissues via the phloem. The loading of Fe(II) into phloem is mediated by OLIGOPETIDE TRANSPORTER 3 (OPT3) (Connorton et al., 2017; Zhai et al., 2014) (Figure 3). The lateral distribution of Fe(II)-NA complexes into sink tissues is done by YELLOW STRIPE LIKE (YSL) transporters in Arabidopsis (Figure 3) (Chu et al., 2010; Connorton et al., 2017; Jean et al., 2005; Zhai et al., 2014). Phloem is also responsible for remobilization of Fe to young leaves and seeds (Gayomba et al., 2015; Kim and Guerinot, 2007).

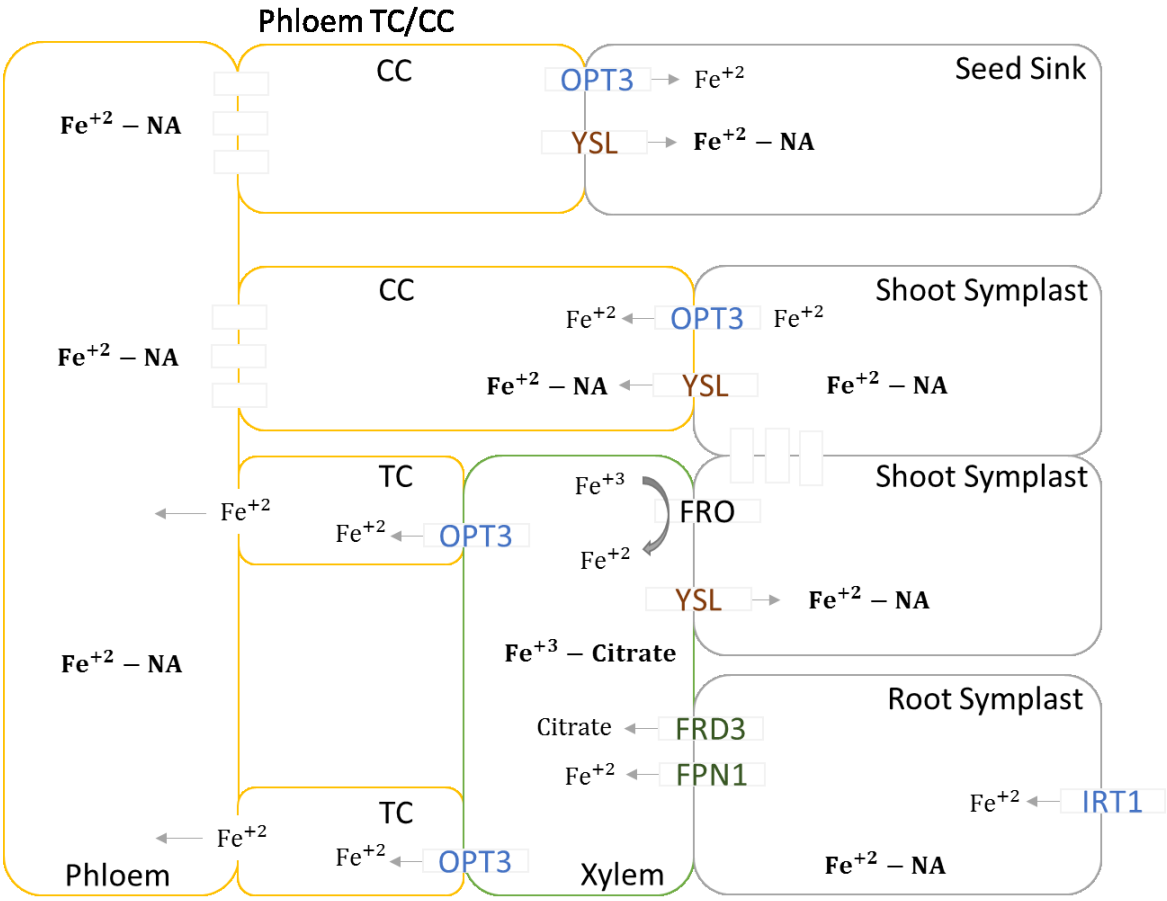

Figure 3 - Simplified Representation of Iron Transportation in *Arabidopsis thaliana*.

Fe^{+2} enters in the root via IRON REGULATED TRANSPORTER 1 (IRT1) and is chelated with nicotianamide (NA) forming Fe^{+2}-NA complex. Fe^{+2} enters in the xylem via FERROPORTIN 1 (FPN1) and is oxidized forming Fe^{+3}. Fe^{+3} is chelated with citrate forming Fe^{+3}-citrate complex. Citrate is loaded into xylem via FERRIC REDUCTASE DEFECTIVE 3 (FRD3). Fe^{+3} is reduce to Fe^{+2} likely by one member of FERRIC REDUCTASE OXIDASE (FRO) family. Fe^{+2} enters the shoot via YELLOW STRIPE 1-LIKE (YSL) when is again complexed to NA forming Fe^{+2}-NA. Fe^{+2}-NA is transported to sink tissues via the phloem. Fe^{+2} is loaded into the phloem by OLIGOPETIDE TRANSPORTER 3 (OPT3) through companion cells (CC) or transfer cells (TC).

1.2.6 Iron-Utilization Related Genes

Since Fe plays an important role in many biological processes in plants, it is important to tightly regulate its homeostasis. Plants have developed a sophisticated regulatory system, which includes transcriptional and posttranscriptional controls (Zhang et al., 2015). Genes involved in Fe uptake, mobilization, or signaling, such as *AHA2, FRO2* and *IRT1*, are called *Fe-utilization-related* genes and are up-regulated under Fe-limited conditions (Kobayashi et al., 2009; Vert et al., 2002) The expression of *Fe-utilization-related* genes under Fe-deficiency is controlled by the basic helix-loop-helix (bHLH) transcription factor *FER-LIKE FE DEFICIENCY INDUCED TRANSCRIPTION FACTOR (FIT)* (Jakoby et al., 2004). *FIT* is induced in the root epidermis that activates the expression of *FRO2* and *IRT1* (Jakoby et al., 2004). *FIT* heterodimerizes with other members of *bHLH* family, such as *bHLH38, bHLH39, bHLH100, bHLH101*, which are also induced under Fe-deficiency condition (Hindt et al., 2017; Sivitz et al., 2012; Wang et al., 2007). *FIT* is known to control the expression of two others transcription factors, *MYELOBLASTOSIS 10 (MYB10)* and *MYELOBLASTOSIS 72 (MYB72)* that are essentials for early Fe-deficiency response and act as regulators of NA synthesis (Palmer et al., 2013).

Another *bHLH* transcription factor *POPEYE (PYE)* plays a role in plant response to Fe-deficiency condition. *PYE* is highly expressed in root pericycle cells; however, its protein is observed in the nuclei of all root cells (Long et al., 2010). This suggest that PYE may move into the root system to link itself to *FIT* network (Rampey et al., 2006; Zhang et al., 2015). In contrast to *FIT, PYE* seems to be repress the expression of its target genes, which include *NICOTIANAMINE SYNTHASE 4 (NAS4), FERRIC REDUCTASE*

OXIDASE 3 (FRO3), and *ZINC-INDUCED FACILITATOR (ZIF1). In vitro* analysis suggested that, similar to FIT, PYE interact with other bHLHs (called PYE-like (PYEL) proteins) including bHLH104, bHLH115, and bHLH105 (also known as IAA-LEUCINE RESISTANT 3 -ILR3) to direct its activity (Rampey et al., 2006). bHLH104 and ILR3 regulate the expression of others *bHLH* genes, such as *bHLH38/39/100/101* and *PYE*, and they act as positive regulators of Fe-deficiency response in plants (Hindt et al., 2017; Zhang et al., 2015).

1.3 The Ubiquitin Proteasome System

The Ubiquitin Proteasome System (UPS) is a highly conserved ATP-dependent proteolysis mechanism, which regulates the abundance of numerous proteins and is therefore involved in almost all aspects of eukaryotic biology (Callis, 2014; Stone, 2014). UPS recognizes specific polyubiquitinated substrates to be degraded. Substrates must have a polyubiquitin chain consisting of at least 4 ubiquitin molecules linked in K48, otherwise the proteasome delivery signal may not be efficient (Pickart and Fushman, 2004; Thrower, 2000). After recognition by the 26S proteasome, the ubiquitin molecules will be released, followed by substrate protein unfolding, cleavage and peptide discharge. The resulting peptides are recycled by the cell (Figure 4).

The 26S proteasome is 2 MDa complex, which consists of 31 subunits divided into two subcomplexes called core protease (CP) and regulatory particle (RP) or 20S and 19S, respectively (Smalle and Vierstra, 2004) (Figure 4). The CP complex is a nonspecific ATP and ubiquitin independent protease. The RP complex is associated with the CP complex, conferring to the proteasome ATP dependence and recognition of polyubiquitinated

substrates (Bedford et al., 2011). The assemble 26S proteasome consists of a CP complex capped on one or both ends by the RP complex (Figure 4) (Bedford et al., 2011).

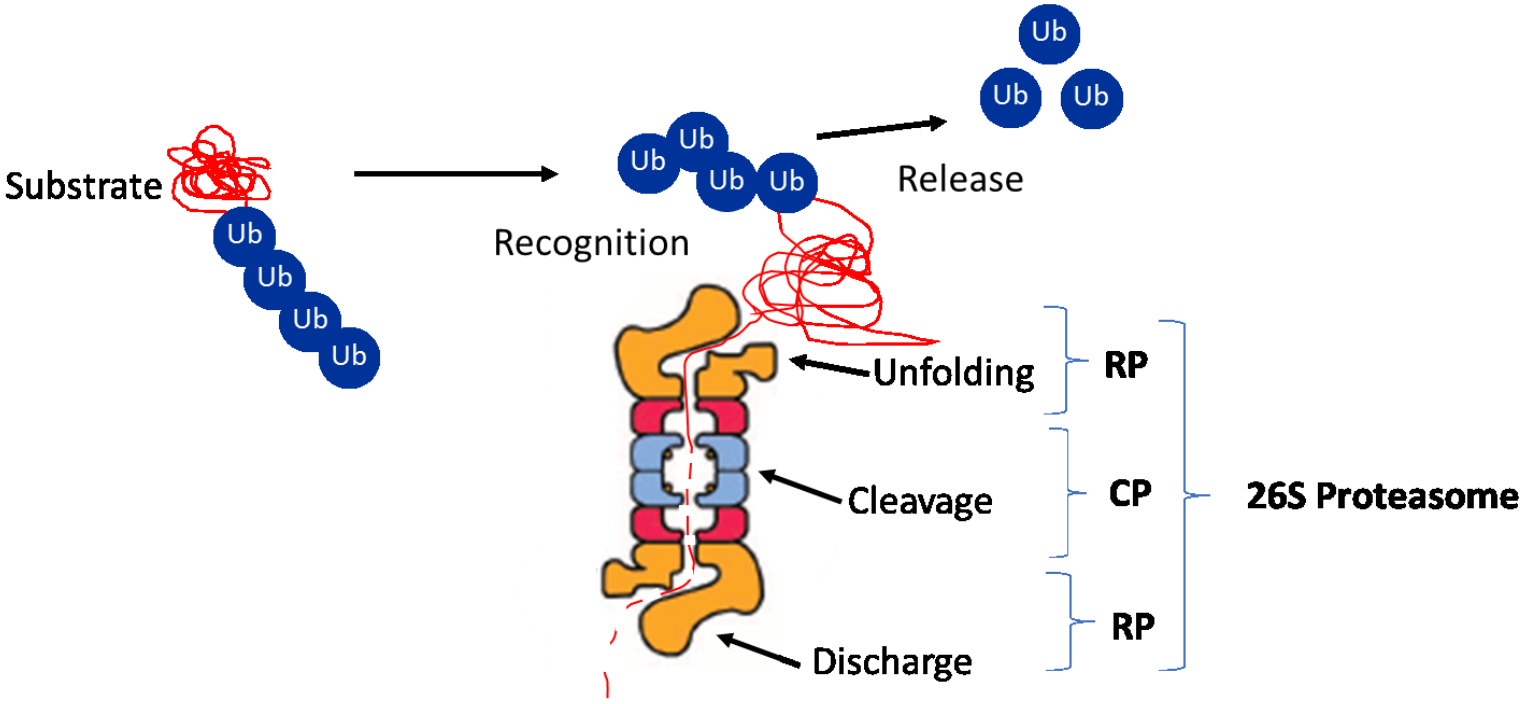

Figure 4 - The Ubiquitin Proteasome System (UPS).

The UPS degrades polyubiquitinated proteins. The polyubiquitinated substrate is recognized by 26S proteasome which unfolds and cleaves the protein into peptides that are discharged. The 26S proteasome consists of multiple sub-complexes; a central core particle (CP, blue and red) and capped on either end by a regulatory particle (RP, yellow). The RP is responsible for polyubiquitin recognition, deubiquitination (release of ubiquitin molecules) and unfolding of the substrate and the CP is responsible for proteolysis.

1.3.1 Ubiquitination

Ubiquitination is the attachment of one (or more) molecule(s) of ubiquitin to a selected protein. Ubiquitin is a 76-amino acids protein characterized as a covalent modifier of other proteins and of itself, being highly conserved and ubiquitously expressed in eukaryotes (Callis, 2014; Stone, 2014). Attachment of ubiquitin to a protein can regulate localization, activity, mobility and abundance (Prasad and Stone, 2010). The versatility of ubiquitin makes this system a very important regulatory pathway central to almost all cellular processes in eukaryotes. Ubiquitin conjugation to a substrate requires three enzymes: ubiquitin activating enzyme (UBA) or E1; ubiquitin conjugating enzyme (UBC) or E2; and ubiquitin ligase or E3. The conjugation of ubiquitin to a substrate begins with the E1 activating and transferring an ubiquitin molecule to an E2, forming a E2-ubiquitin intermediate. The substrate-recruiting E3 then facilitates the transfer of ubiquitin from the E2-ubiquitin intermediate to the substrate (Figure 5). Ubiquitin is attached to an internal lysine residue on the substrate. The outcome of ubiquitin conjugation depends on the number of ubiquitin molecules and the type of modification that occurs on the substrate (Callis, 2014; Stone, 2014).

One type of modification that occurs is the attachment of one molecule of ubiquitin to lysine residues on the substrate, called monoubiquitination (Figure 5). Another type of modification is the attachment of several ubiquitin molecules in a chain to a specific lysine residue in the substrate, called polyubiquitination (Figure 5) (Stone, 2014). The ubiquitin molecule contains seven lysine residues (K6, K11, K27, K29, K31, K48 and K63) that can be used to create different types of ubiquitin linkages to build a chain (Chen and Sun, 2009; Nakasone et al., 2013).

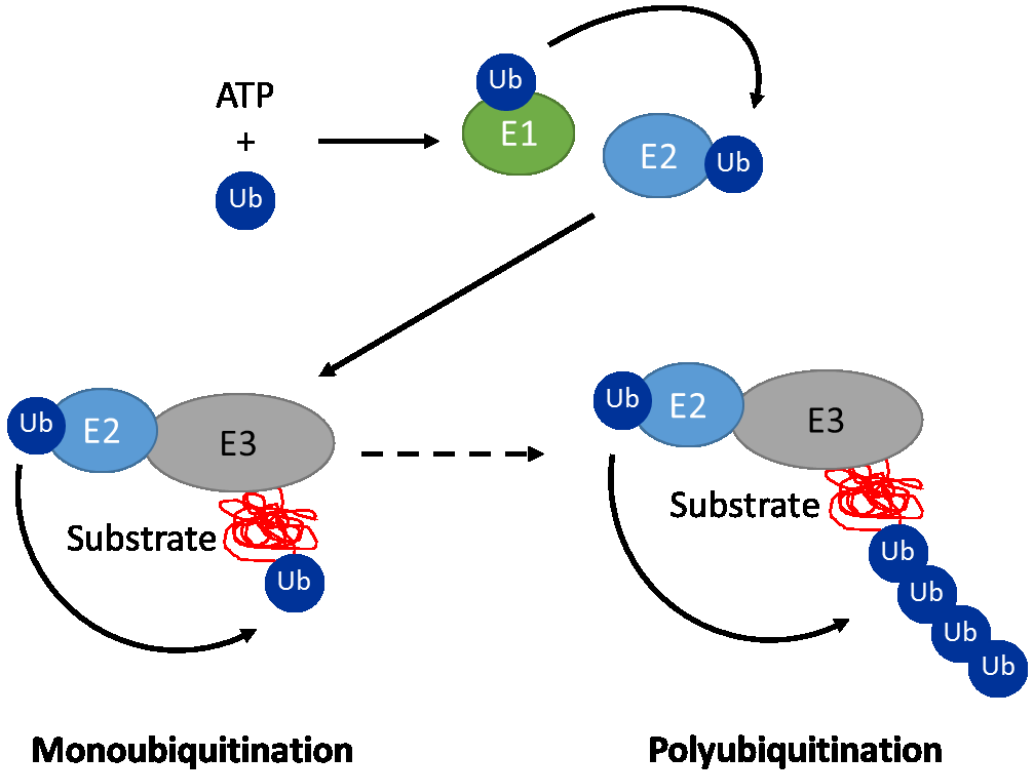

Figure 5 - The Ubiquitination Pathway.

Conjugation of ubiquitin begins with the ATP dependent attachment of a ubiquitin (Ub) molecule to a Ubiquitin Activating enzyme (or E1). Ubiquitin is then transferred to the Ubiquitin Conjugating enzyme (or E2). The E2-Ub complex interacts with the Ubiquitin Ligase (or E3), which also binds the substrate to transfer ubiquitin to the substrate. The process is repeated to build a chain of ubiquitin molecules. The attachment of a single ubiquitin to a substrate is referred to as monoubiquitination, while the conjugation of a polyubiquitin chain is known as polyubiquitination.

The outcome of each type modification is not known. However, it is known that intracellular trafficking or protein activation can be an outcome of the attachment of a polyubiquitination chain generated using K63 (Chen and Sun, 2009). The targeting proteins for degradation by the 26S proteasome (protease complex) is the outcome of a polyubiquitination chain made using K48 (Thrower, 2000). By this selective removal of specific targets, via the covalent attachment of ubiquitin molecules, plants can control many cellular processes, such as response to external stimuli, cell growth and division (Liu and Stone, 2013).

In addition to the ubiquitination pathway being dynamic, it is also a reversible process. Deubiquitinating enzymes (DUBs) can cleave the ubiquitin molecule attached to proteins. DUBs can also process immature ubiquitin molecules, from fusion of ubiquitin with other proteins, to mature ubiquitin molecules (Ueno et al., 2008).

1.3.2 Ubiquitin Ligases (E3s)

Ubiquitin ligases are the central components in the ubiquitination pathway as they are responsible for substrate selection. E3s are abundant in plant proteome, for example, the Arabidopsis genome is predicted to encode for more than 1,400 proteins that function as E3s or components of complex E3 enzymes. In addition, the Arabidopsis genome encodes for two isoforms of the E1 enzyme and 37 different E2 enzymes. All together, the ubiquitin enzymes along with the 26S proteasome account for approximately 6% of the Arabidopsis proteome (Cho et al., 2017).

E3s possess two major functions in the ubiquitination pathway; first they are responsible for interacting with the E2-ubiquitin intermediate and second they are in charge of substrate recognition (Stone et al., 2005; Ueno et al., 2008). Arabidopsis E3s are categorized into 3 major groups based on the presence of a E2 binding domain: HECT (Homology to E6-associated Carboxy-Terminus), U-box or RING domain (Smalle and Vierstra, 2004). U-box-type and RING-type E3s interact noncovalently with E2s, which carry the thioester-linked ubiquitin, and facilitate transfer of the ubiquitin directly to the substrate (Figure 6B). In contrast, HECT-type E3s forms a ubiquitin thioester bond before transferring the ubiquitin molecule to the substrate (Figure 6A) (Stone et al., 2005).

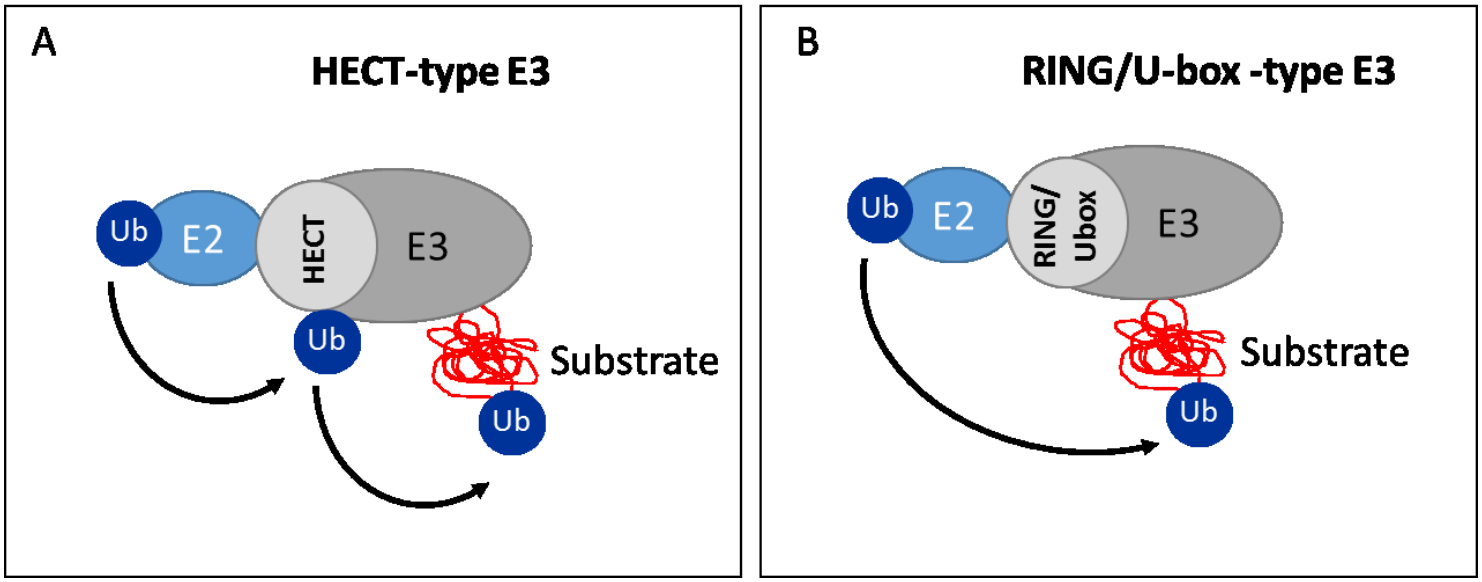

Figure 6 - *Arabidopsis thaliana* Ubiquitin Ligases.

HECT-type E3 (A) forms a covalently linked intermediate with the ubiquitin molecule prior to transfer to the substrate protein. RING or U-box-type E3s (B) facilitate transfer of ubiquitin from the E2-ubiquitin complex directly to the substrate protein.

HECT-type ubiquitin ligases are usually large proteins of more than 100KDa. These are defined by the presence of a conserved 350-amino acids C-terminal E2-binding domain, which was first detected in humans (Downes et al., 2003; Smalle and Vierstra, 2004). They vary in numbers with organisms. For example, humans have 30 HECT-type E3s, while Arabidopsis possess just 7 HECT-type E3s which are named UPL1-7 (UBIQUITIN-PROTEIN LIGASE 1-7) (Chen and Hellmann, 2013). Biological function has been defined for only a few Arabidopsis HECT-type E3s. UPL3 is involved in gibberellic acid (GA) signaling, as *upl3* display a hyper-sensitivity to GA (Downes et al., 2003). UPL5 is assigned a role in the regulation of leaf senescence (Miao and Zentgraf, 2010).

RING and U-box E2 binding domains are similar in structure and function. The cross-brace structure of the RING domain is formed using eight conserved cysteines and histidine's residues bonded with two zinc ions. The U-box domain forms a similar structure but does not chelate zinc ions directly, instead it uses the hydrogen bonds and the salt bridges to maintain its structure (Cho et al., 2017; Smalle and Vierstra, 2004; Stone et al., 2005). In Arabidopsis, there are approximately 480 proteins predicted to contain a RING domain and 64 predicted U-box containing proteins (Smalle and Vierstra, 2004). RING and U-box E3 ligases have been associated in plant development and stress responses (Cho et al., 2017). For example, RING MEMBRANE-ANCHOR 1 (Rma1H1) is associated with tolerances for water/drought/salt, MORE AUXILLARY BRANCHING 2 (MAX2) with shoot and root development, CARBOXYL TERMINUS OF HSC70-INTERACTING PROTEIN (CHIP) with low- or high-temperature stress and PLANT U-BOX 44 (PUB44) with senescence process (Chen and Hellmann, 2013).

1.4 The Ubiquitin Proteasome System and the Iron-deficiency Response

In plants, ubiquitin proteasome system (UPS) is responsible for coordinating responses to abiotic stresses, including Fe-deficiency responses (Sharma et al., 2016). A number of ubiquitin ligases have been described and shown to target specific substrates for degradation under Fe-deficient condition. For example, the RING-type E3 BRUTUS (BTS) is induced by low Fe conditions. *BTS* mutants posses an increase in Fe-deficiency tolerance characterized by continued root growth and increased rhizosphere acidification compared to the WT plants (Selote et al., 2015; Zhang et al., 2015). This demonstrates that BTS is as a negative regulator to Fe-deficiency response (Zhang et al., 2015). It has been shown that BTS targets regulatory components, such as PYEL for degradation by the 26S proteasome (Selote et al., 2015).

Another example of a RING-type E3 involved in controlling of Fe-deficiency response is IRT1-DEGRADATION FACTOR 1 (IDF1), which is involved in the monoubiquitinating IRT1 resulting in depletion of the transporter from the plasma membrane (Brumbarova et al., 2015; Shin et al., 2013). Under Fe deficiency, IRT1 accumulates at the plasma membrane (PM) where executes its function of acquiring metal from the rhizosphere. In addition, IRT1 can accumulate in the trans-Golgi network (TGN) from where it can travel again to PM. PM localized IRT1 can undergo endocytosis which is dependent upon monoubiquitination (Barberon et al., 2011). After IRT1 internalization in the TGN, it can be recycled or sent for degradation.

FIT is a positive regulator of the Fe-deficiency stress response required for increasing the expression of *FRO2* and *IRT1* (Brumbarova et al., 2015). *FIT* is transcriptionally regulated by Fe-deficiency and post-translational regulated by UPS

(Sivitz et al., 2011). Recent studies have demonstrated that degradation of a transcription factor by the UPS could promote/stimulate gene expression under specific conditions (Sivitz et al., 2011). The theory is that degradation of 'exhausted' transcription factor allows for replacement with 'new' transcription factor and this would enhance transcription. Degradation of FIT by the 26S proteasome is thought to enhance activity and promote the expression of *Fe-utilization related* genes under constant Fe stress condition (Sivitz et al., 2011).

1.5 XB3 RING-type Ubiquitin Ligase Family

XA21-BINDING PROTEIN 3 (XB3) is a RING-type ubiquitin ligase identified in rice proteome. XB3 contains 8 Ankyrin repeats followed by a carboxyl-terminal RING domain (Yuan et al., 2013). XB3 interacts with Xa21 (RECEPTOR KINASE-LIKE PROTEIN), a receptor like-kinase responsible for the detection of the proteobacteria, *Xanthomonas oryzae*, and promotion of rice innate immunity (Wang et al., 2006). XB3 has been shown to be essential for Xa21 accumulation and Xa21 mediated-immunity associated with disease/stress tolerance.

In Arabidopsis there are 5 XB3-like proteins, each containing a carboxyl-terminal RING domain and from 2 to 5 Ankyrin repeats (Nodzon et al., 2004; Stone et al., 2005). Those XB-3 like proteins where grouped in one family which was named XB3 ortholog 1 in Arabidopsis (*XBAT31*) to XBAT35 (Prasad et al., 2010; Yuan et al., 2013). So far, XBAT32 and XBAT35 have been defined or predicted roles in ethylene biosynthesis and signaling (Carvalho et al., 2012; Prasad and Stone, 2010). XBAT32 is involved in lateral root development (positive regulator) and XBAT35.1/2 is involved in apical hook

curvature (negative regulator) (Carvalho et al., 2012; Prasad et al., 2010). XBAT35.2 has recently been shown to be involved in cell death induction and pathogen response (Liu et al., 2017). The roles of other members of this family, XBAT31, XBAT33 and XBAT34, have not been characterized.

1.5.1 RING-type Ubiquitin Ligase XBAT31

XB3 ortholog 1 in Arabidopsis (*XBAT31*) is predicted to undergo alternative splicing, producing two isoforms. A longer *XBAT31.1* (At2g28840.1) and a shorter *XBAT31.2* (At2g28840.2) version. *XBAT31.1* is 1371bp in length with a unique start codon (ATG) and *XBAT31.2* is 1329bp in length with the start codon that is also found in the first exon of *XBAT31.1* (Figure 7). Very little is known about the role of the XBAT31 isoforms in planta. Recently published results suggest that *XBAT31* is involved in triggering cell death in *Nicotiana benthamiana* (tobacco) leaves (Huang et al., 2013). Similar to Arabidopsis XBAT31, rice XBOS31 and *Citrus sinensis* XBCT31 can also trigger cell death when overexpressed in tobacco leaves (Huang et al., 2013). Potential interactors identified for XBAT31 include BRASSINOSTEROID-INSENSITIVE LEUCINE-RICH REPEAT RECEPTOR-LIKE KINASE (BRL2) and C-TERMINAL DOMAIN PHOSPHATASE-LIKE (CPL1) (Supplemental Figure 1) (Bang et al., 2008; Ceserani et al., 2009). *BRL2* is expressed in developing leaves of Arabidopsis and play a role in vascular development (Ceserani et al., 2009). *CPL1/RCF2/FRY2* is one of more than 20 members of *CPL* family and has been identified as a negative regulator of the expression of stress-responsive genes, such as *RESPONSE-TO-DEHYDRATION 29A* (*RD29A)* and *ω*-

3 FATTY ACID DESATURASE 7 (*FAD7*) (Bang et al., 2008; Koiwa et al., 2002; Matsuda et al., 2009). *CPL1* is involved in plant response to osmotic, heat and Fe-deficiency stresses (Aksoy and Koiwa, 2013; Jeong et al., 2013; Koiwa et al., 2002; Xiong et al., 2002). These interactions suggest a role for XBAT31 in vascular development and/or possibly response to abiotic stresses, such as heat and Fe deficiency.

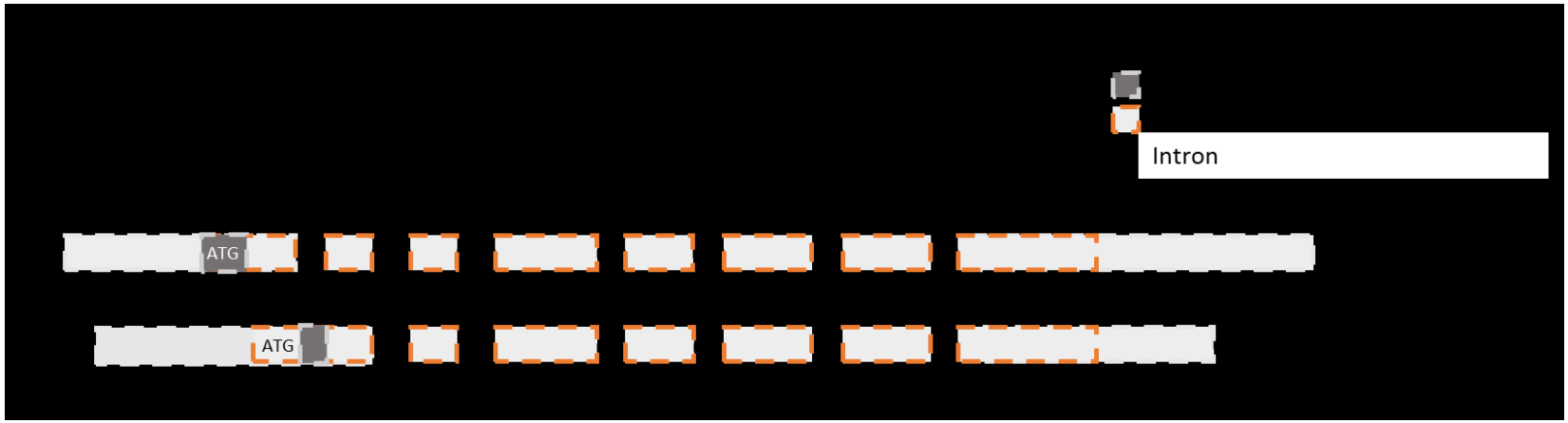

Figure 7 - *XBAT31.1* and *XBAT31.2* Predicted Gene Structure.

XBAT31.1 (A) is 1371bp length within 8 exons. *XBAT31.2* (B) is 1329bp length within 7 exons. The first intron is retained in *XBAT31.2*. The start codon for *XBAT31.1* is further upstream and unique for its sequence.

1.6 Objectives

To maintain iron homeostasis under fluctuating growth conditions, plants must balance iron uptake, modulating intercellular and intracellular iron transport (Long et al., 2010). The major goal of this project is to characterize the role of E3 ligase XBAT31.1 in iron uptake and Fe-deficiency response using phenotypic, physiological and gene expression approaches.

CHAPTER 2: METHODOLOGY

2.1 Plant Materials and Standard Growth Conditions

Seeds of wild type (WT) *Arabidopsis thaliana* (Arabidopsis) ecotype columbia (Col-0) and *XBAT31* mutant (*xbat31-1)* were obtained from Arabidopsis Biological Resource Center (ABRC; https://abrc.osu.edu/). *xbat31-1* (SAIL_142_H06) contains the T-DNA inserted in the *UTR* (*untranslated region)* of AT2G28840. Seeds were surface-sterilized with sterilization solution (30% bleach and 0.02% Triton X-100) for 15min and then washed several times with ddH_2O (double distilled water). Sterilized seeds were plated on half-strength (½) Murashige and Skoog (MS) (Caisson Labs; www.caissonlabs.com) solid medium containing 0.8% agar and 1% sucrose (Sigma-Aldrich; https://www.sigmaaldrich.com). Seeds were stratified at 4°C for 2 days and then germinated under continuous light at 22°C for up to 9 days. Seedlings were transferred to soil and grown under 16h/8h light/dark cycle at 22°C in a growth chamber.

2.2 Iron Sufficient (+Fe) and Iron Deficient (-Fe) Conditions

For iron sufficient (+Fe) conditions, ½ MS (Caisson Labs; www.caissonlabs.com) solid media was supplemented with 100 µM Ferric-ethylenediaminetetraacetic acid (Fe-EDTA; Sigma-Aldrich; https://www.sigmaaldrich.com). Iron deficient (-Fe) conditions, Fe-EDTA free ½ MS (Caisson Labs; www.caissonlabs.com) solid media was supplemented with 150µM of 3-(2-Pyridyl)-5,6-diphenyl-1,2,4-triazine-p,p′-disulfonic acid monosodium salt hydrate – FerroZine (Sigma-Aldrich;

https://www.sigmaaldrich.com). See Table 1 for components of +Fe and Table 2 for components of -Fe ½ MS media. Sterilized seeds were germinated and grown on +Fe solid media for 4 days under continuous light at 22°C. Seedling were then transferred to +Fe and –Fe solid media for an additional 5 days under continuous light at 22°C. Primary root growth, fresh weight and chlorophyll content (see section 2.6) was then assessed. For root length, plates were scanned using CanoScan LiDE120 (Canon; https://estore.canon.ca) and the ImageJ® software (ImageJ®; http://imagej.net) were used for measure root lengths.

For treatment using liquid solutions, seedlings were germinated and grown in +Fe media containing ½ MS (Caisson Labs; www.caissonlabs.com) liquid media supplemented with 100 µM iron ethylenediaminetetraacetic acid (Fe-EDTA; Sigma-Aldrich; https://www.sigmaaldrich.com) for 4 days and then transfer to -Fe conditions containing Fe-EDTA free ½ MS (Caisson Labs; www.caissonlabs.com) liquid media supplemented with 150µM of 3-(2-Pyridyl)-5,6-diphenyl-1,2,4-triazine-*p*,*p'*-disulfonic acid monosodium salt hydrate – FerroZine (Sigma-Aldrich; https://www.sigmaaldrich.com) for additional 5 days.

Table 1 - Components of Fe-sufficiency MS media for *Arabidopsis thaliana* from Caisson Labs (www.caissonlabs.com).

Components (+Fe MS media)	Molar concentration (mol/L)
Ammonium Nitrate (NH_4NO_3)	0.020613920
Boric Acid (H_3BO_3)	0.000100273
Calcium Chloride, Anhydrous ($CaCl_2$)	0.002993386
Cobalt Chloride, Hexahydrate ($CoCl_2 \cdot 6H_2O$)	0.000000105
Cupric Sulfate, Pentahydrate ($CuSO_4 \cdot 5H_2O$)	0.000000100
EDTA, Disodium, Dihydrate ($C_{10}H_{14}N_2Na_2O_8 \cdot 2H_2O$)	0.000100097
Ferrous Sulfate, Heptahydrate ($FeSO_4.7H_2O$)	0.000099996
Magnesium Sulfate, Anhydrous ($MgSO_4$)	0.001501317
Manganese Sulfate, Monohydrate ($MnSO_4 \cdot H_2O$)	0.000099995
Molybdic Acid Sodium Salt, Dihydrate ($Na_2MoO_4 \cdot 2H_2O$)	0.000001033
Potassium Iodide (KI)	0.000005000
Potassium Nitrate (KNO_3)	0.018792902
Potassium Phosphate, Monobasic, Anhydrous (KH_2PO_4)	0.000702625
Zinc Sulfate, Heptahydrate ($ZnSO_4 \cdot 7H_2O$)	0.000029907
Ferric-EDTA ($C_{10}H_{13}FeN_2O_8$)	0.000100000

Table 2 - Components of Fe-deficient MS media for *Arabidopsis thaliana* from Caisson Labs (www.caissonlabs.com).

Components (-Fe MS media)	Molar concentration (mol/L)
Ammonium Nitrate (NH_4NO_3)	0.020613920
Boric Acid (H_3BO_3)	0.000100273
Calcium Chloride, Anhydrous ($CaCl_2$)	0.002993386
Cobalt Chloride, Hexahydrate ($CoCl_2 \cdot 6H_2O$)	0.000000105
Cupric Sulfate, Pentahydrate ($CuSO_4 \cdot 5H_2O$)	0.000000100
Magnesium Sulfate, Anhydrous ($MgSO_4$)	0.001501317
Manganese Sulfate, Monohydrate ($MnSO_4 \cdot H_2O$)	0.000099995
Molybdic Acid Sodium Salt, Dihydrate ($Na_2MoO_4 \cdot 2H_2O$)	0.000001033
Potassium Iodide (KI)	0.000005000
Potassium Nitrate (KNO_3)	0.018792902
Potassium Phosphate, Monobasic, Anhydrous (KH_2PO_4)	0.000702625
Zinc Sulfate, Heptahydrate ($ZnSO_4 \cdot 7H_2O$)	0.000029907

2.3 Identification of Homozygous T-DNA Insertional Plants

Homozygote T-DNA plants were identified by polymerase chain reaction (PCR) and gene expression confirmed by reverse-transcriptase (RT)-PCR. For PCR analysis, Phire Plant Direct PCR Kit (Sigma-Aldrich; https://www.sigmaaldrich.com) was used according to manufacturer's instructions. Primers used are shown in Table 3.

Table 3 - Primers Used to Detect the Presence of T-DNA Insertion in AT2G28840.

Primer name	Description	Primer sequence
LB2	T-DNA specific forward primer	5’-GCTTCCTATTATATCTTCCCAAATTACCAATACA-3’
RP	Gene specific forward primer	5’-TCGCCTATCCTACAATCATCG-3’
LP	Gene specific reverse primer	5’-CTCGATCTGACCATTAGCAGC-3’

For RT-PCR, total RNA was extracted from 9-day-old seedlings using TRIzol reagent (Invitrogen; www.thermofisher.com/) according to the manufacturer's instructions. Purity of RNAs were check by measuring the absorbance 280/230 and 260/230 using NanoDrop (Thermo Fisher; www.thermofisher.com/). Total RNA was reverse-transcribed using SuperScript VILO IV reverse transcriptase (Invitrogen; www.thermofisher.com/) following manufacturer instruction. The resulting cDNA was used in PCR reactions utilizing Taq DNA Polymerase with ThermoPol® Buffer following manufacturer instruction (BioLabs; https://www.neb.ca/) and primers are described in Table 4.

Table 4 - Primers Used to Identify Expression Levels of WT and *xbat31-1* Using RT-PCR.

Gene	Primer Name	Description	Primer Sequence
AT2G28840.1	.1F	XBAT31.1 forward primer	5’- CATCACTATCCGTCGTGTGATGG-3’
AT2G28840.2	.2F	XBAT31.2 forward primer	5’-AGGTTAGTTTCAGTGATATTCTCCG-3’
AT2G28840	R	XBAT31 reverse primer	5’-ACAGGACTTGATTGAGCAGCA-3’
At1g49240	ACTIN8 F	Forward primer	5’-GCGGTTTTCCCCAGTGTTGTTG-3’
At1g49240	ACTIN8 F	Reverse primer	5’-TGCCTGGACCTGCTTCATCATACT-3’

2.4 Quantitative Real-time – PCR (qRT-PCR) Analysis

Total RNA extraction and cDNA synthesis were done as mentioned above (section 2.3). qRT-PCR was performed with iTaq Universal SYBR Green Supermix (BioRad; www.bio-rad.com/) following manufacturer instruction. Primers used are shown in Table 5 and Table 6. Primer specificity was confirmed by analysis the efficiency percentages, melting curves and agarose gel electrophoresis of the PCR products. Normalized gene expression levels were calculated to relative transcript levels by the constitutively expressed *ELONGATION FACTOR-1α* (*EF-1α*) or *POLYUBIQUITIN* 10 (*UBQ10*) genes.

Table 5 - Primers Used in qRT-PCR Analysis.

Gene	Primer Name	Description	Primer Sequence
AT2G28840.1	.1F	*XBAT31.1* forward	5'-TCCGGTCGACTTCCACAG-3'
AT2G28840.2	.2F	*XBAT31.2* forward	5'-GATCTCGCCGGAATCTCGTCGGA-3'
AT2G28840	R	*XBAT31* reverse	5'-CGGAGTCTGCTTGTGACGATTCAA-3'
AT1G01580	FRO2F	*FRO2* forward	5'-TCTTTGTCCTCCACGTCGGCA-3'
AT1G01580	FRO2R	*FRO2* reverse	5'-GAGCAGCGAGCAAGCGAACA-3'
AT4G30190	AHA2F	*AHA2* forward	5'-CCACGCCTTTCCGCTCAAGA-3'
AT4G30190	AHA2R	*AHA2* reverse	5'-TGCGGTTTACGCCAACTGGG-3'
AT4G19690	IRT1F	*IRT1* forward	5'-GGGATCATAGTTCACTCGGTGGTCA-3'
AT4G19690	IRT1R	*IRT1* reverse	5'-CCGCCAAGACCCATGCCTTC-3'
AT2G28160	FITF	*FIT* forward	5'-TGGGACATGCTTCGAACAGAGC-3'
AT2G28160	FITR	*FIT* reverse	5'-TGCAGAACCGGATTTGACTCACG-3'

Table 6 – Housekeeping Genes Primers Used in qRT-PCR Analysis.

Gene	Primer Name	Description	Primer Sequence
AT5G60390	EF1αF	*EF1α* forward	5'-TGAGGCACTTCCCGGTGACA-3'
AT5G60390	EF1αR	*EF1α* reverse	5'-GTTGGCGGCACCCTTAGCTG-3'
At4g05320	UBQ10F	*UBQ10* forward	5'-GGCCTTGTATAATCCCTGATGAATAAG-3'
At4g05320	UBQ10R	*UBQ10* reverse	5'-AAAGAGATAACAGGAACGGAAACATAGT-3'

2.5 Protein Purification and Ubiquitination Assay

XBAT31.1 cDNA was obtained from Arabidopsis Biological Resource Center (ABRC; https://abrc.osu.edu/) and introduced via Gateway into pDEST-527 (Addgene; https://www.addgene.org/11520/) following manufacturer instruction. HIS-GST tag destination vector was used in order to obtain HIS-GST-XBAT31.1 tagged recombinant protein. HIS-GST-XBAT31.1 fusions were expressed in *Escherichia coli* Rosetta (DE3) (Sigma-Aldrich; https://www.sigmaaldrich.com). Transformed cells were grown at 37°C, with shaking, for at least 4h or until OD600 reach 1.0 in liquid LB medium before they were induced with 1mM of Isopropyl β-D-1-thiogalactopyranoside (IPTG). Cells were harvest by centrifugation and lysed by sonication. Lysis buffer used contains 25mM Tris-HCl pH7.5, 500mM NaCl, 0.01% Triton-X-100, 5mM imidazole, 20µg/ml of PMSF and 1 mg/ml of lysozyme. Protein was purified using HIS-Select® Nickel Magnetic Agarose Beads (Sigma-Aldrich; https://www.sigmaaldrich.com) according to the manufacturer's protocols. Bradford assays (Bio-Rad; www.bio-rad.com/) was used to quantify purified proteins.

Ubiquitination assay was carried out as described previously (Stone et al., 2005). Reactions (30µL) containing 4µg ubiquitin (BostonBiochem; www.bostonbiochem.com/), 50ng yeast E1 (BostonBiochem; www.bostonbiochem.com/), 250ng E2 Arabidopsis HIS-AtUBC8, 250ng E3 HIS-GST-XBAT31.1, 2mM ATP, 50mM Tris-HCl pH 7.5, 5mM $MgCl_2$, 50mM KCl, and 1mM DTT were incubated for up to 8 hours at 30ºC. Positive control reactions containing E3 HIS-GST-XBAT35.1 were incubated for 4 hours at 30°C. For negative control, ubiquitin or the E3 was omitted from the reactions. Reactions were stopped by adding 5x SDS loading buffer. Samples were then boiled for 10 minutes and

separated on SDS polyacrylamide gels. Ubiquitin proteins were detected by western blotting with rabbit anti-ubiquitin primary antibodies (1:10000; BostonBiochem; www.bostonbiochem.com/) and anti-rabbit secondary antibodies (1:10000; Sigma-Aldrich; https://www.sigmaaldrich.com). To detect HIS-GST-XBAT31.1/XBAT35.1, western blotting with mouse anti-histidine primary antibodies (1:10000; Sigma-Aldrich; https://www.sigmaaldrich.com) and anti-mouse secondary antibodies (1:10000; Sigma-Aldrich; https://www.sigmaaldrich.com) was carried out.

2.6 Chlorophyll Quantification

Chlorophyll quantification was carried out as described previously (Chappelle et al., 1992). Assay was performed using 9-day-old seedlings. Leaves were collected and treated overnight with dimethyl sulfoxide (DMSO; Fisher Scientific) in the dark at 25°C for 12h. Samples were then centrifuged at 10,000g at 4ºC for 5min. Chlorophyll concentrations were calculated from spectroscopy absorbance measurements at 664nm (chlorophyll a) and 648nm (chlorophyll b), and carotenoids at 470nm using the equations below:

$$\text{Chla} = 12.25(\text{A664}) - 2.79(\text{A648})$$

$$\text{Chlb} = 21.50(\text{A648}) - 5.10(\text{A664})$$

$$\text{Total Chl} = (\text{a} + \text{b})$$

$$\text{Carotenoids} = 1000(\text{A470}) - 1.82(\text{Chla}) - 85.02(\text{Chlb})/198$$

2.7 Rhizosphere Acidification

For rhizosphere acidification quantification using MS media, the experiment was carried out as described previously (Pizzio et al., 2015). Seedlings were germinated on +Fe solid media for 7 days and then transferred to flask containing liquid +Fe or -Fe solution for 2 weeks. Ten seedlings were placed in 3mL of assay solutions containing ¼ +Fe MS and 2mM MES (2-(N-morpholino) ethanesulfonic acid) buffer pH 6.8 or ¼ -Fe MS and 2mM MES buffer pH 6.8. Seedlings were grown for 2 weeks under continuous light and shaking at 22°C. pH was measured and used to determine [H^+] (mole/L) as shown in the equation below:

$$\mathrm{pH} = -\log\,[\mathrm{H}^+]$$

For rhizosphere acidification using bromocresol purple (BP), the experiment was carried out as described previously (Long et al., 2010). For this assay, 9-day-old seedlings from +Fe and -Fe were transfer for 24h to BP plates containing 1% agar, 0.006% bromocresol purple and 0.2mM calcium sulfate ($CaSO_4$) with pH adjusted to 6.5. After 24h plates were scanned using CanoScan LiDE120 (Canon; https://estore.canon.ca) and changing in colour from purple to yellow (indication of rhizosphere acidification) was monitored.

2.8 Determination of Ferric Chelate Reductase (FRO2) Activity

FRO2 activity assay was carried out as described previously (Yi and Guerinot, 1996). Excised roots from 9-day-old seedlings grown under +Fe or -Fe were washed with 0.5mM calcium sulfate ($CaSO_4$) and rinsed with ddH_2O at least 3 times. Roots from 10 seedlings were weight, placed into a test tube containing 1.4mL of assay solution (0.1mM

Fe-EDTA and 0.3mM FerroZine) in the dark at 25°C for 30 min. FRO2 activity was then determined spectrophotometrically by measuring the absorbance (A) at 562nm and quantified using a molar extinction coefficient of 28.6 mM^{-1} cm^{-1} as in the equation below:

$$\frac{(A/28.6)x700}{rootFW/2}$$

2.9 Determination of Fe(II) Allocation in Roots using Pearl Stain

Pearl stain was carried out as described previously (Long et al., 2010). For the assay, 9-day-old seedlings were washed with 10mM ethylenediaminetetraacetic acid (EDTA) (pH 8.0) solution for 5 min and then with ddH_2O 3 times. Next, seedlings were vacuum infiltrated with equal volumes of 4% (v/v) hydrochloric acid (HCl) and 4% (w/v) potassium ferrocyanide (Perls solution) for 30 min at room temperature and then incubated for 30 min at 53°C. Seedlings were then rinsed 3 times with ddH_2O. Staining was examined, and pictures were taken using an Olympus Optical Microscope GX51.

2.10 Tissue Elemental Analysis

9-day-old seedlings grown under +Fe and –Fe conditions were used to collect 300mg of fresh weight. Shoots were washed 5min with ddH_2O and roots were washed with 2mM calcium sulfate ($CaSO_4$) and 10mM ethylenediaminetetraacetic acid (EDTA) for 10 min and then rinsed twice in ddH_2O. Samples were divided into 2 replicates of ~100 mg fresh weight, then dried in a 65°C oven for 48h, and reweighed. Dried samples were digested using 0.6 mL of 70% nitric acid (Sigma Aldrich) at 110°C for 4 h. Samples were then diluted to 6 mL with ddH_2O and sent for analysis by inductively coupled plasma–

mass spectrometry (Clean Water Laboratory, Dalhousie University; http://centreforwaterresourcesstudies.dal.ca/projects/view/5). Measurements were obtained for the following elements: Mg, P, Ca, Mn, Fe, Co, Ni, Cu, Zn and Cd.

2.11 Electrolyte Leakage

Electrolytes leakage was carried out as described previously (Dionisio-Sese and Tobita, 1998). For the assay, 9-day-old seedlings grown under +Fe and –Fe conditions were used to collect 100mg of fresh leaf and root tissue. Shoot samples were submerged in 10mL of ddH20 and incubated at 32ºC for 2h. Initial electrical conductivity (EC1) were measured using an electrical conductivity meter (HQ14D Portable Conductivity meter; https://www.hach.com). After the conductivity measurement, the leaf tissues were autoclaved at 121ºC for 20min to release all electrolytes, cooled to 25ºC, and final electrical conductivity (EC2) was then measured. Electrolytes leakage (EL) were calculated, relatively to leaf fresh weight (FW), using the equation below:

$$\mathrm{EL/FW} = \frac{\mathrm{EC1/EC2 \times 100}}{\mathrm{FW}}$$

2.12 Determination of Lipid Peroxidation

Measurement of malondialdehyde (MDA) was carried out as described previously (Guo et al., 2012). MDA was extract using the 2-thiobarbituric acid (TBA). Seedling leaves (0.1g fresh weight) were ground in a solution of 1.5mL 0.1% trichloroacetic acid (TCA) and 1.5mL 0.5% TBA. Samples were boiled for 10 min, cooled to 25°C and then

centrifuged at 1,400g for 15 min. MDA values were calculated by measuring absorbance at 532nm and 600nm and using a molar absorption coefficient of 1.56 x 10^5 using the equation below:

$$\mathrm{MDA} = \frac{(\mathrm{A532} - \mathrm{A600}) * 3 \times 1000/156]}{FW}$$

2.13 Heat-shock Stress Treatment

1-week-old seedlings grown on solid MS media under standard conditions were used for heat shock treatment. Plates containing at least 50 seedlings of *xbat31-1* or WT were sealed with parafilm and heat shock at 50ºC in water bath for 5, 10, 20, 30 or 40min was performed. Non-heated plates were used as a control. After 7 days of recovery, plates were photographed and open to count surviving (green) seedlings (white seedlings were categorized as dead).

CHAPTER 3: RESULTS

Plants have developed mechanisms to tightly regulate Fe uptake under inconstant environments. They can be facing Fe insolubility due to alkaline soils or Fe overloading due to very acidic or chelate-supplemented soils. To ensure continued growth development and yield productions it is crucial that plants properly balance between positive and negative regulation of the Fe uptake machinery (Brumbarova et al., 2015; Hindt et al., 2017). To have a better understanding of the mechanisms that regulate responses to Fe-deficiency, we investigated the role of XBAT31.1 in this important process.

3.1 Analysis of XBAT31 Sequence and Domain Architecture

XBAT31.1 transcript encodes for a protein consisting in 456 amino acids while *XBAT31.2* transcript encodes a 442 amino acids protein. XBAT31.1 and XBAT31.2 contain a carboxyl-terminal RING domain. XBAT31.1 also contains 5 Ankyrin repeats while XBAT31.2 contains 4 Ankyrin repeats and 2 transmembrane domains (Figure 8A and 8B). By using online prediction platforms such as Protein Subcellular Localization Prediction Tool (PSORT; www.psort.org/) it is possible to predict subcellular localization based on amino acid sequence. XBAT31.1 is predicted to be nuclear localized (79%) with low possibilities of localizing to the mitochondria (13%) or cytoplasm (8%). In contrast, XBAT31.2 is predicted to have an extracellular localization, including cell wall (56%) with low possibilities of localizing to the mitochondria (22%) or nucleus (11%).

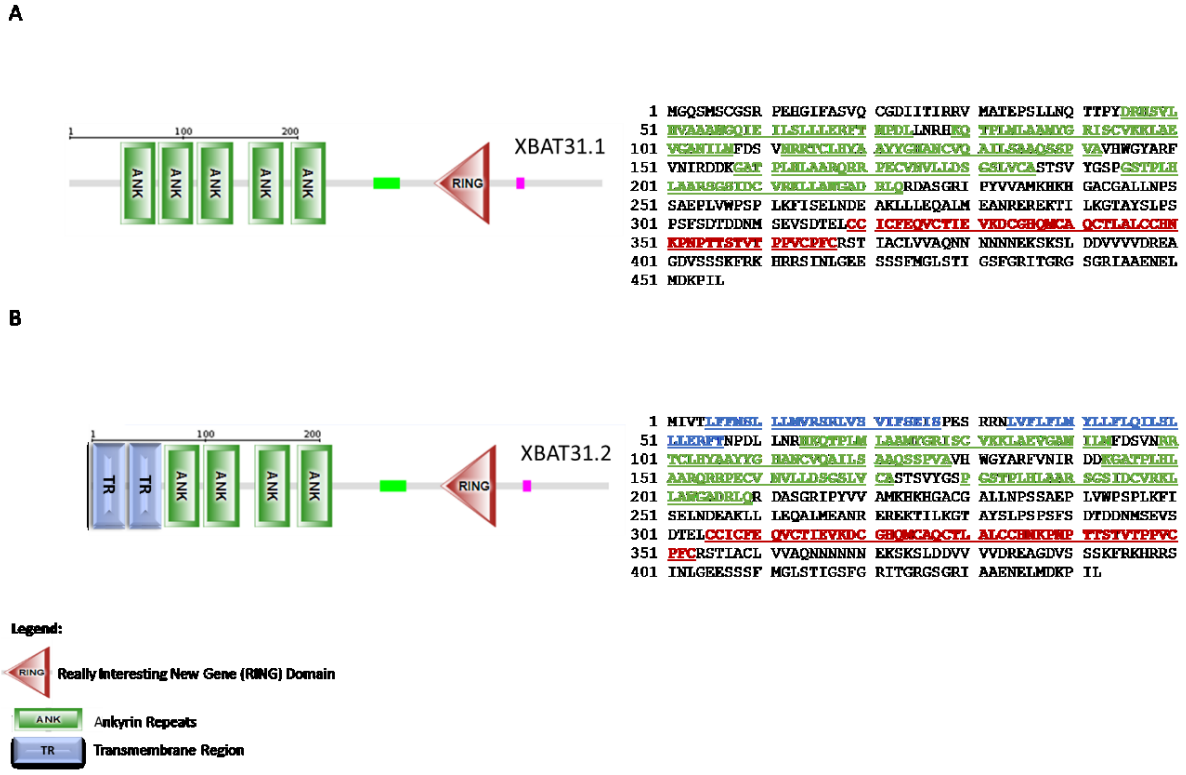

Figure 8 - Domain Architecture and Amino Acid Sequence for XBAT31 Isoforms.

XBAT31.1 (A) posses 5 ankyrin repeat (green) and a RING domain (red); XBAT31.2 (B) posses 2 transmembrane domains (blue), 4 ankyrin repeat (green) and a RING domain (red). Amino acid sequences highlight the ankyrin repeat (green), transmembrane domains (blue) and the RING domain (red). Domain architecture obtained from Simple Modular Architecture Research Tool (SMART; http://smart.embl-heidelberg.de/); amino acid sequences obtained from Arabidopsis Biological Resource Center (ABRC; https://abrc.osu.edu/).

Using databases such as Bio-Analytic Resource (BAR; http://bar.utoronto.ca/) it is possible to retrieve information on gene expression levels in different plant tissue grown under standard or stress conditions (Zimmermann, 2004). *XBAT31* is found to have highest expression in 3 different Arabidopsis tissues which are second internode, mature pollen and senescent leaves under standard growth conditions (Figure 9). The retrieved results for *XBAT31* gene expression, using BAR, are in accordance with published data showing that *XBAT31* is involved in triggering cell death in *Nicotiana benthamiana* leaves (Huang et al., 2013). The same study showed that from the 58 proteins allocated in big *XB3* family over different plant species, 34 are closer related to *XB3* than the others. From those 34, they selected for their study 3 proteins from rice (*XB3*, *XBOS31* and *XBOS37*), one for Arabidopsis (*XBAT31*), 2 for citrus (*XBCT31* and *XBCT32*) and they used *XBAT32* as a negative control, which they indicated as phylogenetically distinct from the other members cited above.

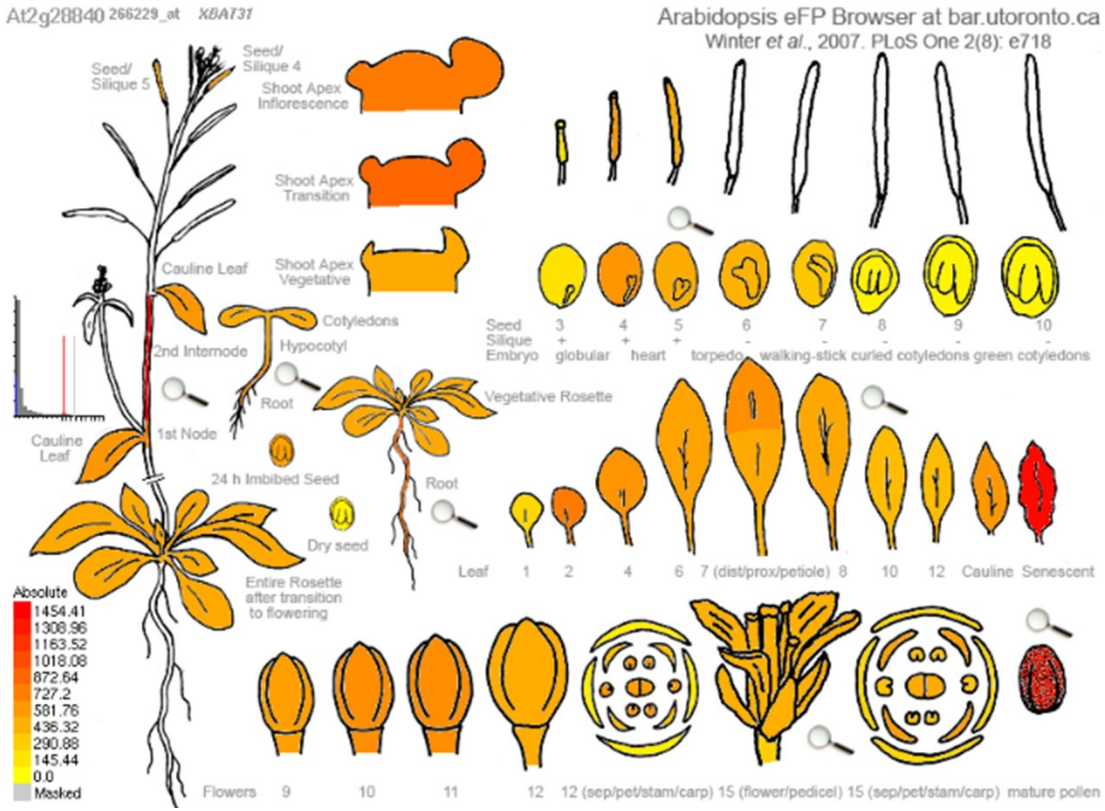

Figure 9 - *XBAT31* Expression in *Arabidopsis thaliana* under Standard Growth Conditions.

Information obtained from Bio-Analytic Resource (BAR) for Plant Biology (http://bar.utoronto.ca/eplant/). BAR doe not state the version of *XBAT31* used for the analysis. Highest expression levels are observed in senescent leaves and mature pollen.

XBAT31 protein, when overexpressed, is able to trigger cell death in tobacco leaves as strong as XB3 protein which is an already known E3 ubiquitin ligase with well defined function. This information all together open space to further investigation of XBAT31 ubiquitin ligase activity and its biological role in Arabidopsis responses to stress.

3.2 XBAT31.1 is a Functional Ubiquitin Ligase

Both *XBAT31* isoforms are predicted to function as ubiquitin ligases involved in protein ubiquitination to promote degradation but neither of them have had its E3 activity demonstrated, either *in vitro* or *in planta*. Stone et al. (2005) had suggested that XBAT31.1 was not a functional E3. The lack of success may have been due to the short incubation time (2h) used for the *in vitro* ubiquitination assay (Stone et al., 2005). Utilizing the same *in vitro* assay with slight difference in buffer composition and with an increase in incubation time to 8h, XBAT31.1 was shown to possess E3 activity (Figure 10 and Supplemental Figure 2). Unfortunately, we were unable to isolate *XBAT31.2* full cDNA sequence, therefore we were not able to obtain the recombinant protein to confirm its activity *in vitro*.

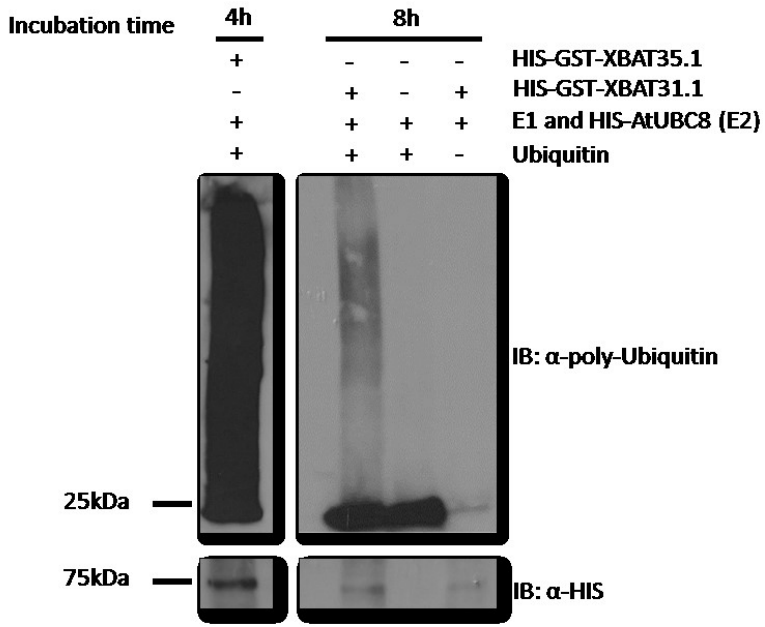

Figure 10 - *In vitro* Ubiquitination Assay Showing XBAT31.1 Ubiquitin Ligase Activity.

HIS-GST-XBAT31.1 was incubated with yeast E1, Arabidopsis E2 HIS-AtUBC8 and ubiquitin. A high molecular weight smear detected by immunoblotting (IB) with ubiquitin antibodies indicates the presence of ubiquitinated proteins (lane 2). The omission of ubiquitin (lane 4) or HIS-GST-XBAT31.1 (lane 3) from the assay prohibited protein ubiquitination. HIS-GST-XBAT35.1 was used as a positive control (lane 1). Anti-HIS was used to demonstrate the presence of the HIS-GST-XBAT31.1 and HIS-GST-XABT35.1 in the assay.

3.3 Identification of *XBAT31* T-DNA Insertion Homozygous Mutant (*xbat31-1*) with Reduced Gene Expression

For *XBAT31* gene, 3 T-DNA mutant lines are available from Arabidopsis Biological Resource Center (ABRC; https://abrc.osu.edu/); *xbat31-1*, SAIL_142_H06; *xbat31-2,* SAIL_705_D09 and *xbat31-3,* SAIL_142_F06. All 3 mutant lines had the T-DNA inserted in the 5'-*UTR* (*untranslated region),* which is predicted to reduce gene expression (Schmidt et al., 2014). Polymerase chain reaction (PCR) utilizing gene and T-DNA specific primers was used to genotype each mutant line and identify plants homozygous for the T-DNA insertion (Figure 11). Plants homozygous for the T-DNA insertion were success identified from the *xbat31-1* (SAIL_142_H06) line but not from *xbat31-2* (SAIL_705_D09) or *xbat31-3* (SAIL_142_F06).

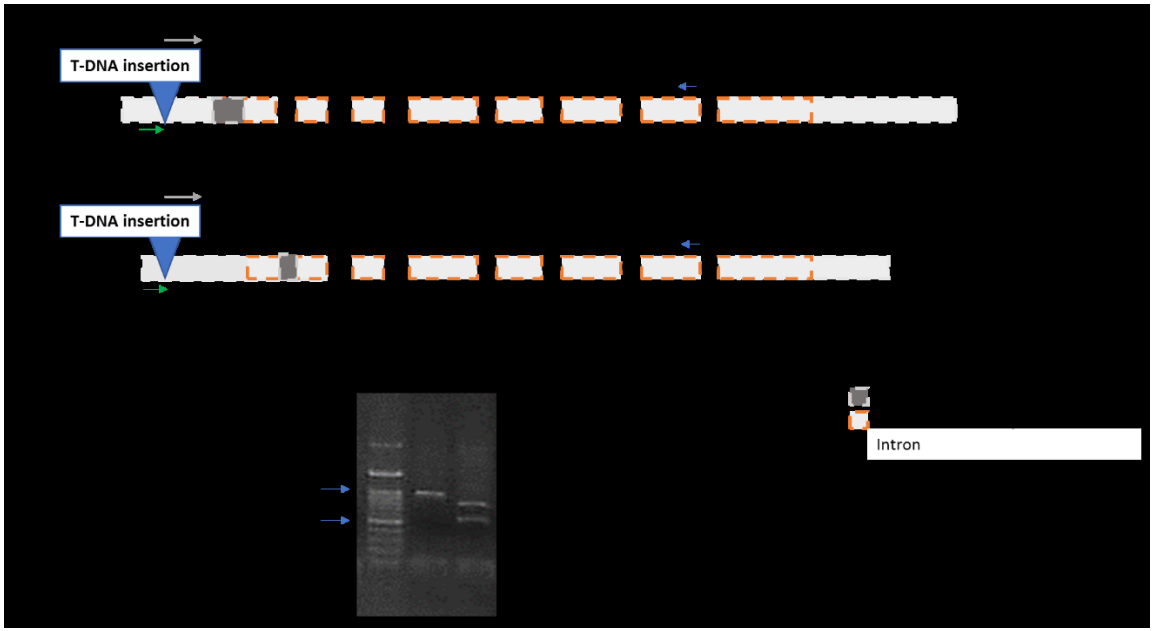

Figure 11 - Genotyping of *xbat31-1* T-DNA Insertion Plant Line.

XBAT31.1 (A) and *XBAT31.2* (B) gene structure showing localization of the T-DNA insertion and primers used for genotyping by polymerase chain reaction (PCR) to identify of homozygous T-DNA lines. Primers used: LP - sequence specific forward primer; LB2 - T-DNA specific left border primer; RP – sequence specific reverse primer. (C) All three primers were used in a single PCR reaction with genomic DNA extracted from wild type (WT) or xbat31-1 seedlings. The presence 1116bp band (produced using LP and RP primers) is indicates the absence of the T-DNA. The presence of a 432 and 732 PCR products (produced using LB2 and LP or RP, respectively) indicates the presence of the T-DNA. The absence of a 1116bp PCR product suggest that *xbat31-1* is homozygote for the T-DNA insertion.

Next, reverse transcription polymerase chain reaction (RT-PCR) and real-time quantitative reverse transcription polymerase chain reaction (qRT-PCR) were used to demonstrate that the mutation leads to reduce expression of *XBAT31.1* and *XBAT31.2.* Sequence specific primers that are able to distinguish between *XBAT31.1* and *XBAT31.2* transcripts were used to perform RT-PCR and qRT-PCR (Figure 12). By using RT-PCR it was possible to visualize a significant reduction in the transcript levels of both *XBAT31.1* and *XBAT31.2* in *xbat31-1* compared to WT. To confirm that *XBAT31.1* and *XBAT31.2* transcripts were significant decreased in *xbat31-1*, qRT-PCR was performed. Again, the transcript level of *XBAT31.1* and *XBAT31.2* were significant less in *xbat31-1* compared to WT (Figure 12).

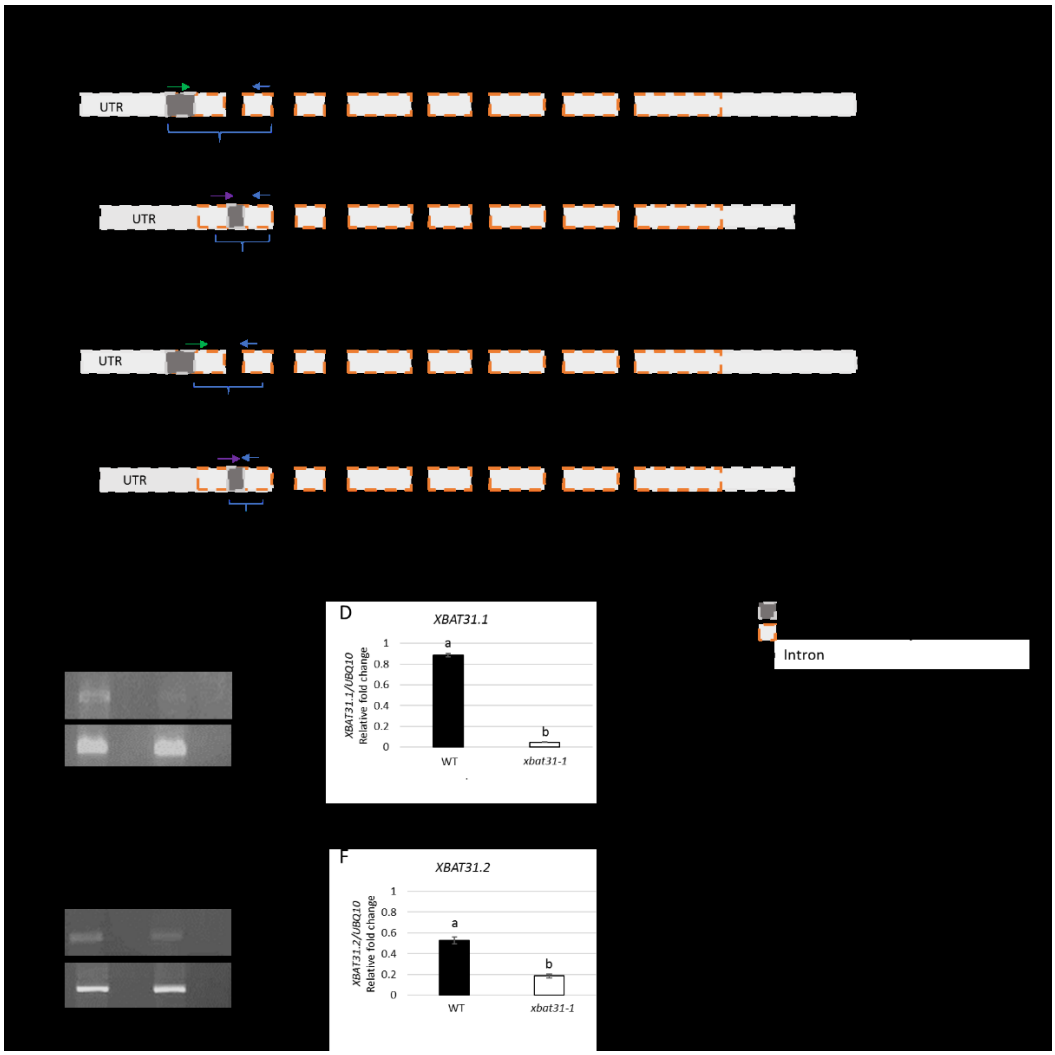

Figure 12 - Expression of *XBAT31* Isoforms.

XBAT31.1 and *XBAT31.2* gene structure showing localization of the primers used for genotyping by reverse transcription polymerase chain reaction RT-PCR (A) or real-time reverse transcription polymerase chain reaction qRT-PCR (B). *XBAT31.1* (C and D) and *XBAT31.2* (E and F) expression analysis using RNA extracted from 9-day-old wild type (WT) and *xbat31-1* seedlings grown under standard conditions (solid MS media). RT-PCR (C and E) analysis with (+) and without (-) the reverse transcriptase (RT) enzyme. Actin8 was used as a control. qRT-PCR (D and F) analysis using *UBQ10* as the housekeeping gene in reactions. Different letters indicate p-value ≤0.05 using One-Way ANOVA Tukey comparison. Error bars indicate ± SE from 4 biological replicates.

3.4 *XBAT31.1*, but not *XBAT31.2*, Expression Increases in Response to Fe-deficiency Conditions

The interaction between XBAT31 and CPL1 suggest a role for the E3 in abiotic stress response (Bang et al., 2008). CPL1 has been shown to be involved in regulating response to different stresses including Fe-deficiency stress (Aksoy et al., 2013). Genes involved in Fe-deficiency stress are up-regulated when iron levels are reduced. To determine if *XBAT31.1* and/or *XBAT31.2* may be involved in plant response to Fe-deficiency, the transcript levels were assessed using RT-PCR and qRT-PCR. The transcripts level analyses were performed using isoform-specific primers (Figure 13 A and B). RNA was extracted from 9-day-old seedlings from WT grown under iron sufficient (+Fe) and iron deficient (-Fe) conditions. RT-PCR analysis showed an increase in *XBAT31.1* transcript levels under -Fe condition (Figure 13 C and Supplemental Figure 3A). No significant increase in *XBAT31.2* transcript levels was observed (Figure 13 E and Supplemental Figure 3B). qRT-PCR analysis confirmed the results obtained by RT-PCR. A significant increase in *XBAT31.1* expression levels under -Fe and a non-significant change in *XBAT31.2* expression under the same condition (Figure 13 D and F). These results suggest that *XBAT31.1* gene expression is up-regulated under -Fe, and in contrast *XBAT31.2* does not respond to Fe-deficiency stress.

Figure 13 - Expression of *XBAT31* Isoforms under Iron-deficient and Iron-sufficient Conditions.

XBAT31.1 and *XBAT31.2* gene structure showing localization of the primers used for transcript quantification by reverse transcription polymerase chain reaction RT-PCR (A) or real-time reverse transcription polymerase chain reaction qRT-PCR (B). Analysis of *XBAT31.1* (C and D) and *XBAT31.2* (E and F) expression using RNA extracted from 9-day-old wild type (WT) seedlings grown with (+) and without (-) Fe. RT-PCR (C and E) EF1α as a control. qRT-PCR (D and F) using *UBQ10* as a housekeeping gene. Different letters indicate p-value ≤0.05 using One-Way ANOVA Tukey comparison. Error bars indicate ± SE from 4 biological replicates.

qRT-PCR was also used to compare the expression of both E3 isoforms in *xbat31-1* and WT seedlings grown under +Fe and -Fe conditions (Figure14). As expected the transcript level of *XBAT31.1* was significantly higher in seedlings grown under –Fe compared to +Fe condition and no change in *XBAT31.2* levels was observed. In all conditions, the transcript levels of both isoforms are lower in *xbat31-1* compared to WT seedlings (Figure 14). Increase in *XBAT31* expression in response to iron deficient conditions was further confirmed by experimental data available on the BAR database (Figure 15). Unfortunately, the *XBAT31* isoform used for this analysis was not stated.

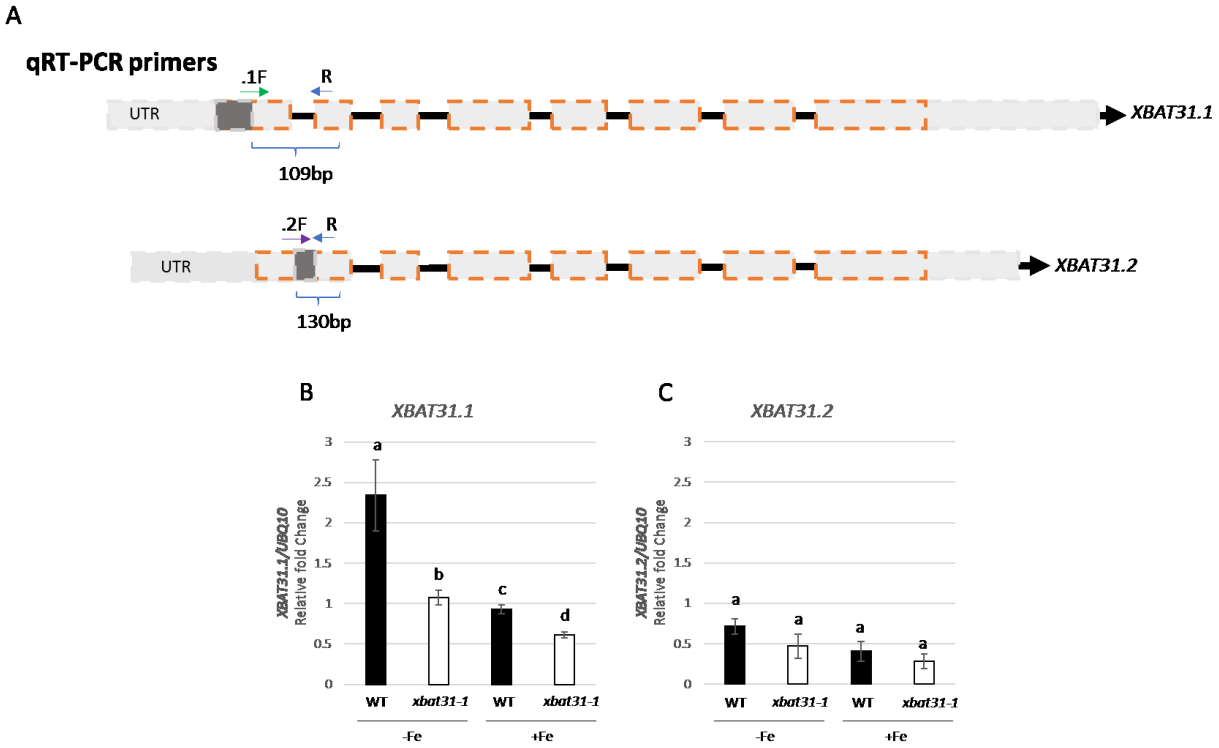

Figure 14 -Expression of *XBAT31* Isoforms in *xbat31-1* Compared to Wild type (WT) Grown under Iron-sufficient and Iron-deficient Conditions.

XBAT31.1 and *XBAT31.2* gene structure showing localization of the primers used for transcripts quantification by real-time reverse transcription polymerase chain reaction qRT-PCR (A). qRT-PCR analysis of *XBAT31.1* (B) and *XBAT31.2* (C) expression with (+) and without (-) Fe. 9-day-old seedlings from WT and *xbat31-1* were used in the reactions with *UBQ10* as a housekeeping gene. Different letters indicate p-value≤0.05 using One-Way ANOVA Tukey comparison Error bars indicate ± SE from 4 biological replicates.

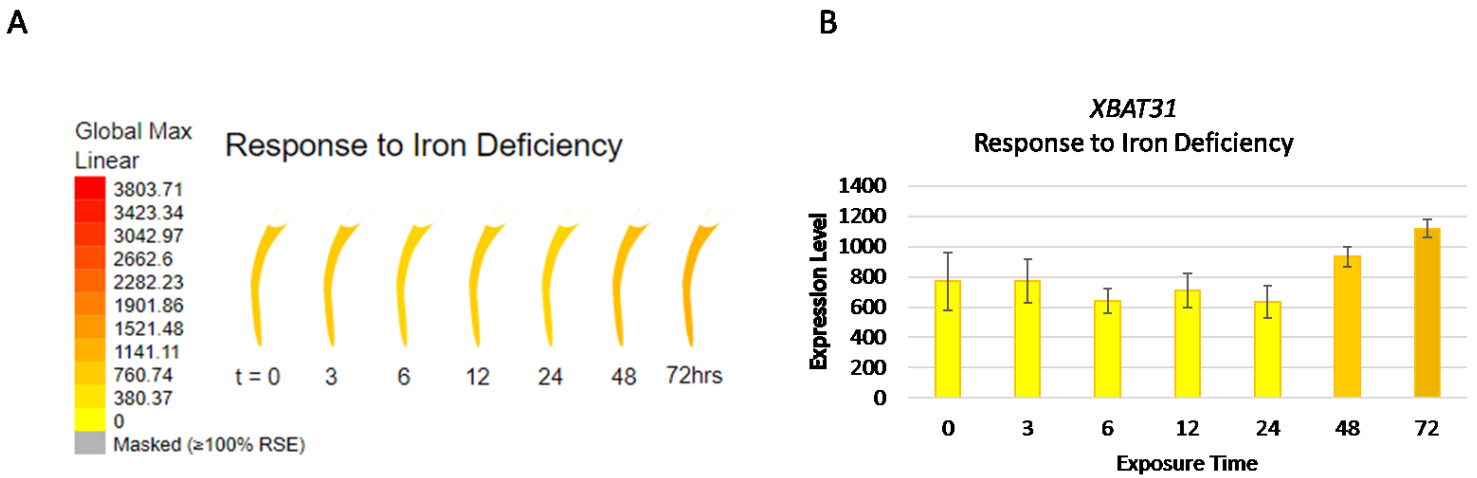

63

Figure 15 -*XBAT31* Expression in Wild Type Roots under Iron-deficiency Stress Condition.

XBAT31 (A) expression in roots in response to Fe deficiency showing increase in transcript levels with 48h and 72h of exposure. Quantification of *XBAT31* (B) expression levels shown in (A). Information obtained from the Bio-Analytic Resource (BAR) for Plant Biology database (http://bar.utoronto.ca/eplant/). BAR does not state the version of *XBAT31* used for the analysis. Values and error bars (SD) showed in the graph are available in BAR online platform. No statistical analysis was provided.

3.5 *Iron-utilization related* genes (*FIT*, *FRO2* and *AHA*2) are Strongly Up-regulated under Fe-deficiency in *xbat31-1* Compared to Wild Type

FIT, *FRO2* and *AHA2* are consider major components of Fe-uptake machinery and are known to be up-regulated under -Fe condition compared to +Fe condition (Brumbarova et al., 2015). To further investigate the role of *XBAT31.1* in Fe-deficiency response, the expression of *Fe-utilization related* genes in *xbat31-1* was compared to WT. To accomplish this, qRT-PCR was performed using 9-day-old WT and *xbat31-1* seedlings grown under +Fe and -Fe conditions. As shown in Figure 16, the expression of *FIT, FRO2* and *AHA2* were significant up-regulated in both *xbat31-1* and WT seedlings grown under -Fe condition. Importantly, the increase in *FIT, FRO2* and *AHA2* expression was greater in *xbat31-1* compared to WT (Figure16). These results indicate that the reduction in *XBAT31* expression in the mutant leads to a more drastic response to Fe-deficiency in these *Fe-utilization related* genes.

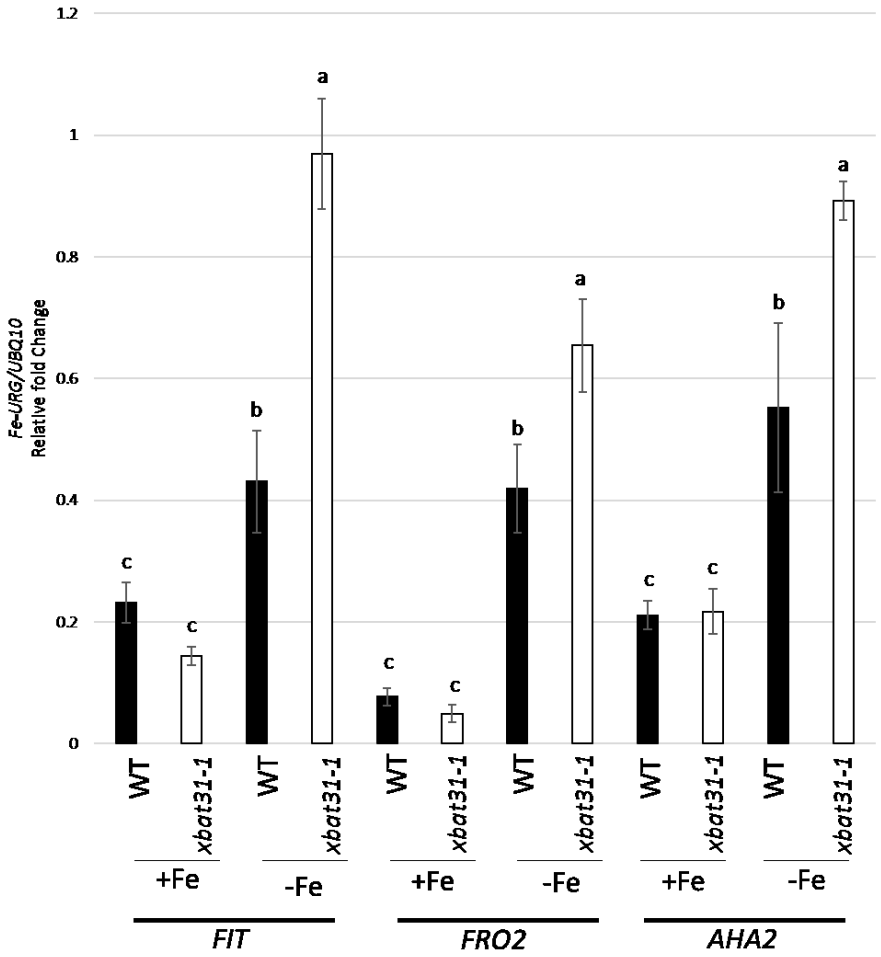

Figure 16 - Expression of *Fe-utilization related* genes (*URGs*) in *xbat31-1* Compared to Wild Type (WT).

qRT-PCR was used to quantify transcript levels of *FIT, FRO2* and *AHA2* in 9-day-old WT and *xbat31-1* seedlings. Seedlings were grown with (+) and without (-) Fe and *UBQ10* was used as a housekeeping gene in reactions. Different letters indicate p-value ≤0.05 using One-Way ANOVA Tukey comparison. Error bars indicate ± SE from 4 biological replicates.

3.6 Up-regulation of *IRT1* under Fe-deficient Condition is Lower in *xbat31-1* Compared to WT

IRT1, the major Fe(II) transporter in Arabidopsis, is strongly up-regulated under Fe-deficient condition (Brumbarova et al., 2015). IRT1 expression is regulated by FIT and since *FIT* transcript levels are elevated in *xbat31-1* it is expected that IRT1 levels should also be strongly upregulated. To determine *IRT1* expression levels in *xbat31-1*, qRT-PCR was performed using 9-day-old WT and *xbat31-1* seedlings grown under +Fe and -Fe conditions. As shown in Figure 17, a significant up-regulation of *IRT1* transcript levels was observed in *xbat31-1* when seedlings were shifted from +Fe to -Fe conditions. However, when compared to WT, the increase in *IRT1* transcript levels was significantly less for *xbat31-1*. This result may be an indication that despite *IRT1* being controlled positively by *FIT*, it may also be controlled by a negative regulator which is affected by the reduction of the E3 in *xbat31-1*.

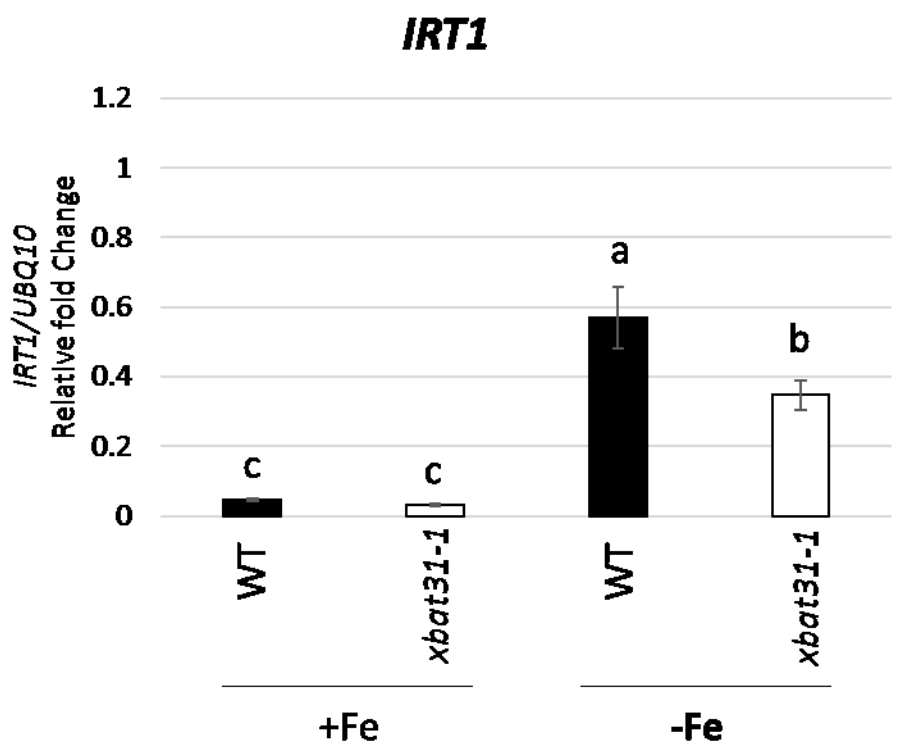

Figure 17 - Expression of *IRT1* in *xbat31-1* Seedlings under Fe-deficient Condition.

qRT-PCR was used to quantify transcript levels of *IRT1* in 9-day-old wild type (WT) and *xbat31-1* seedlings grown with (+) and without (-) Fe for 5 days before performing the assay. *UBQ10* was used as a housekeeping gene in reactions. Different letters indicate p-value ≤0.05 using One-Way ANOVA Tukey comparison. Error bars indicate ± SE from 4 biological replicates.

3.7 *xbat31-1* is Tolerant to Fe-deficiency Stress Condition

Wild type Arabidopsis exposed to Fe-deficient condition display a number of phenotypes including reducing growth and increasing chlorosis in leaves. To determine the effects of -Fe conditions on *xbat31-1*, 9 days-old seedlings exposed to 5 days of Fe deprivation were compared to WT seedlings under the same condition. By assessing primary root growth, fresh weight and total chlorophyll content, *xbat31-1* was found to be more tolerant to Fe-deficiency. No difference in growth was found in *xbat31-1* seedlings when grown under standard MS or +Fe (Supplemental Figure 6). *XBAT31* mutants display longer primary root, greater fresh weight and less chlorotic leaves compared to WT (Figure 18 A and Supplemental Figure 5 A). *xbat31* showed 75% decrease in primary root elongation, a 33% reduction in biomass and only 10% reduction of in total chlorophyll content (Figure 18 B, C and D). On the other hand, WT showed 80% decrease in primary root elongation, a strong reduction in biomass of 44% and a severe reduction of 34% in total chlorophyll content (Figure 18 B, C and D). These results suggest that *xbat31-1* is less sensitive to Fe stress compared to WT seedlings.

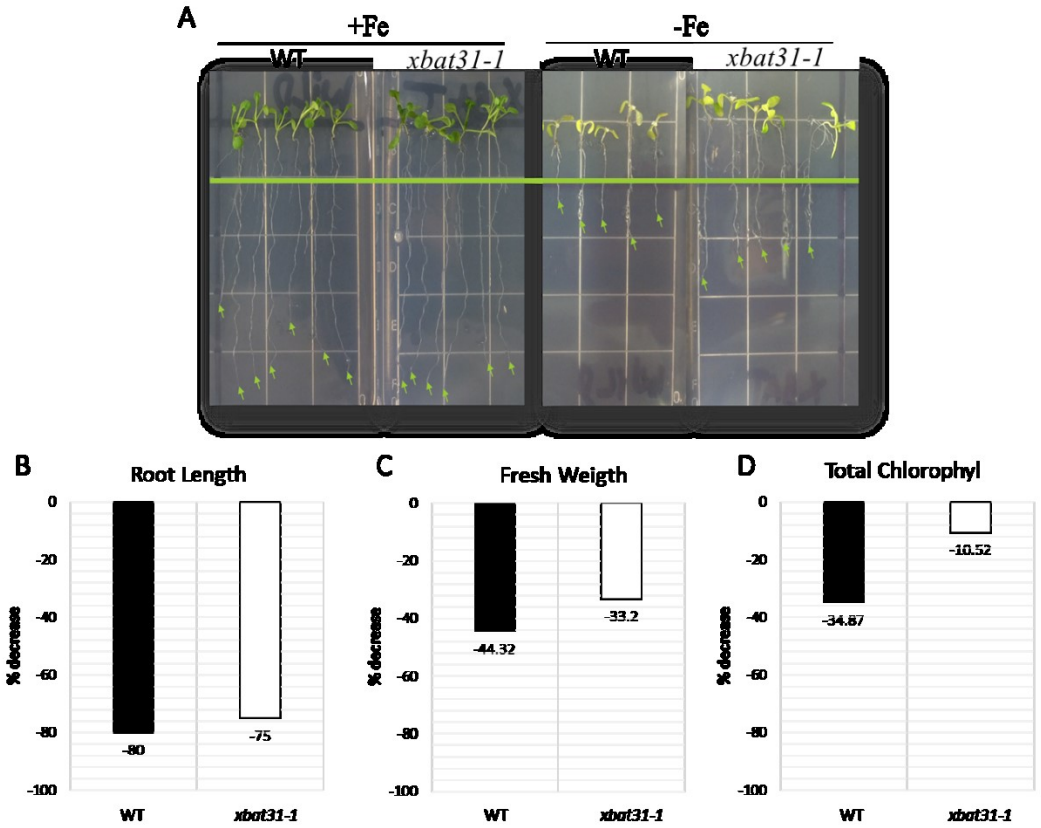

Figure 18 - Growth of *xbat31-1* and Wild Type (WT) Seedlings under Iron-deficient Condition.

xbat31-1 and wild type (WT) seedlings were grown with (+) and without (-) Fe. Representative (A) 9-day-old *xbat31-1* and WT seedlings grown under +Fe and -Fe conditions. Green line indicates root length at time of transfer. Quantification of percent (%) decrease in primary root length (B), fresh weight (C) and total chlorophyll content (D) in seedlings grown under -Fe compared to +Fe. Graphs are based on 3 separate trials with 15 replicates per trial with statistical analysis showed in Sup. Figure 5.

3.8 *xbat31-1* Show Higher Enzyme Activity for AHA2 and FRO2 under -Fe condition

Under Fe-deficiency stress plants promote acidification of the rhizosphere and an increase in the Fe(III) reduction rate (Hindt et al., 2017). Gene expression analysis of *xbat31-1* have demonstrated a significant strong up-regulation of *AHA2* and *FRO2* comparing *xbat31-1* with WT under -Fe condition. AHA2 and FRO2 are responsible for rhizosphere acidification and Fe(III) reduction, respectively (Figure 19). To determine if the enzymatic activity is also strongly up-regulation, we investigated rhizosphere acidification by measuring AHA2 activity and Fe(III) reduction rate by measuring FRO2 activity. *xbat31-1* displayed significant higher acidification of the rhizosphere under +Fe and -Fe conditions compared to WT (Figure 19 A and Supplemental Figure 6). In addition, *xbat31-1* showed a slightly significant increase in Fe(III) reduction rate under +Fe and -Fe conditions, compared to WT (Figure 19 B and Supplemental Figure 7). Results from -Fe condition of AHA2 and FRO2 enzymatic assays are correlated with the results obtained from -Fe condition gene expression analysis of *xbat31-1*, suggesting that AHA2 and FRO2 are more abundant in the mutant compared to WT.

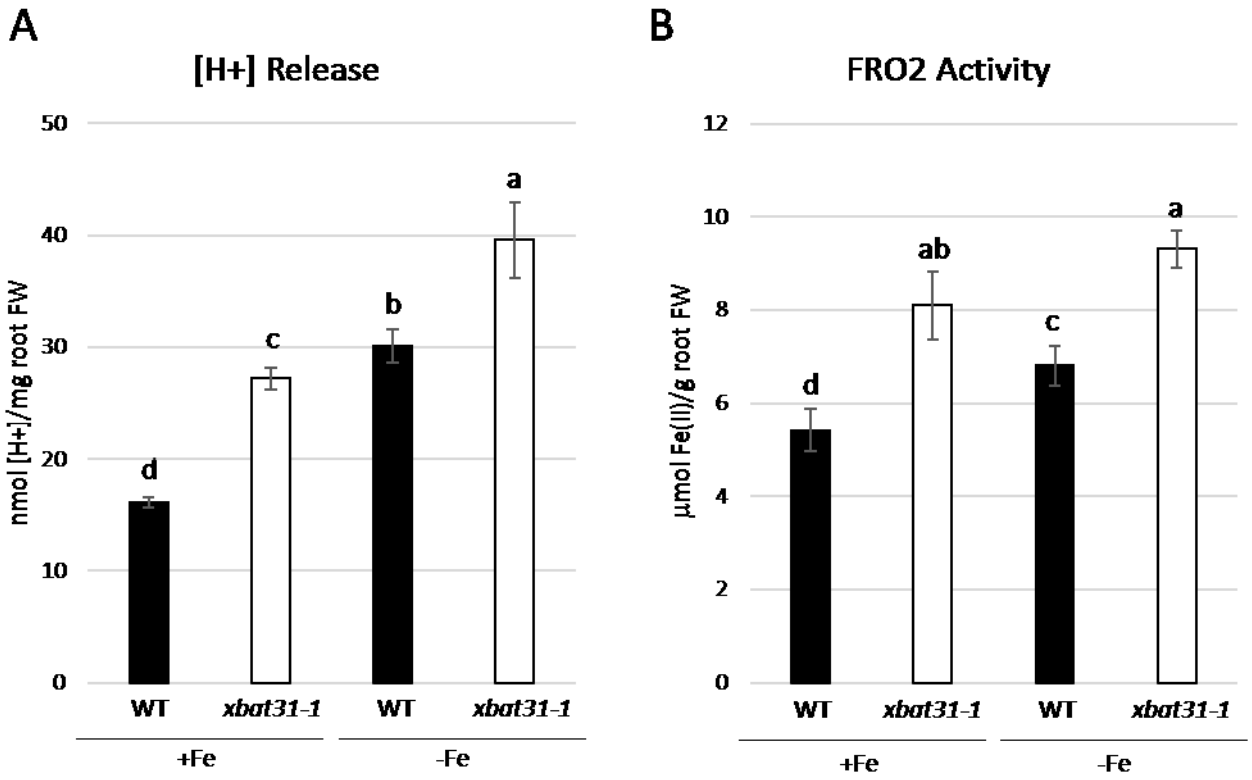

Figure 19 - Activity of Iron Related Enzymes in *xbat31-1* Seedlings Compared to Wild Type (WT).

AHA2 activity (A) as measured by rhizosphere acidification and FRO2 activity (B) as measured by reduction rate of Fe(III) into Fe(II) in 9-day-old seedlings grown in liquid MS media with (+) and without (-) iron (Fe). Different letters indicate p-value ≤0.05 using One-Way ANOVA Tukey comparison. Error bars indicate ±SE from 2 trials with up to 7 technical replicates per trial.

3.9 Metal Content in *xbat31-1* Shoots and Roots

Metal concentration in shoots of plants overexpressing *Fe-utilization related* genes, such as *FIT* and *IRT1,* tends to be higher than WT under -Fe conditions (Yuan et al., 2008). *IRT1* overexpressers showed a significant higher accumulation of Fe, Mn, Co and Zn in shoots under +Fe, a significant higher accumulation of Mn, Co and Zn in shoots under -Fe, and no significant difference in accumulation of Fe under -Fe compared to WT (Barberon et al., 2011). *xbat31-1* had elevated levels of *FIT, FRO2* and *AHA2*; and reduced levels of *IRT1* expression under -Fe condition. Inductively coupled plasma mass spectrometry (ICP-MS) was used to assess metal content in shoots of 9-day-old *xbat31-1* seedlings grown under +Fe and -Fe conditions. Shoots of *xbat31-1* had significant lower concentration of Fe, Mn and Co compared to WT under -Fe condition and did not show any significant change in metal concentrations under +Fe conditions (Figure 20 and Supplemental Table 1). Significant lower transcript levels of *IRT1* in *XBAT31* mutant compared to WT would possible be correlated with lower metal content in *xbat31-1* shoots however it is necessary investigate IRT1 protein levels to be able to make further assumptions.

Metal concentration in roots of plants exposed to -Fe stress, sometimes complement the results obtained from shoots under the same condition. For example, in *IRT1* overexpressers, Fe and Co content from shoots and roots of plants under -Fe condition are similar (Barberon et al., 2011). However, in *irt1-1*seedlings metal content in shoots and roots under -Fe condition did not fully complement each other (Barberon et al., 2011). In order to determine if *xbat31-1* roots follow the same metal content profile of shoots, ICP-MS was used to measure metal concentration in 9-day-old *xbat31-1* roots. Roots of *xbat31-1* did not show any significant difference from Fe, Co, Mn or Zn concentration under -Fe

condition when compared to WT under the same condition (Figure 20 and Supplemental Table 1). These results do not fully complement the results of metal content in shoots which had been reported previously (Vert et al., 2002).

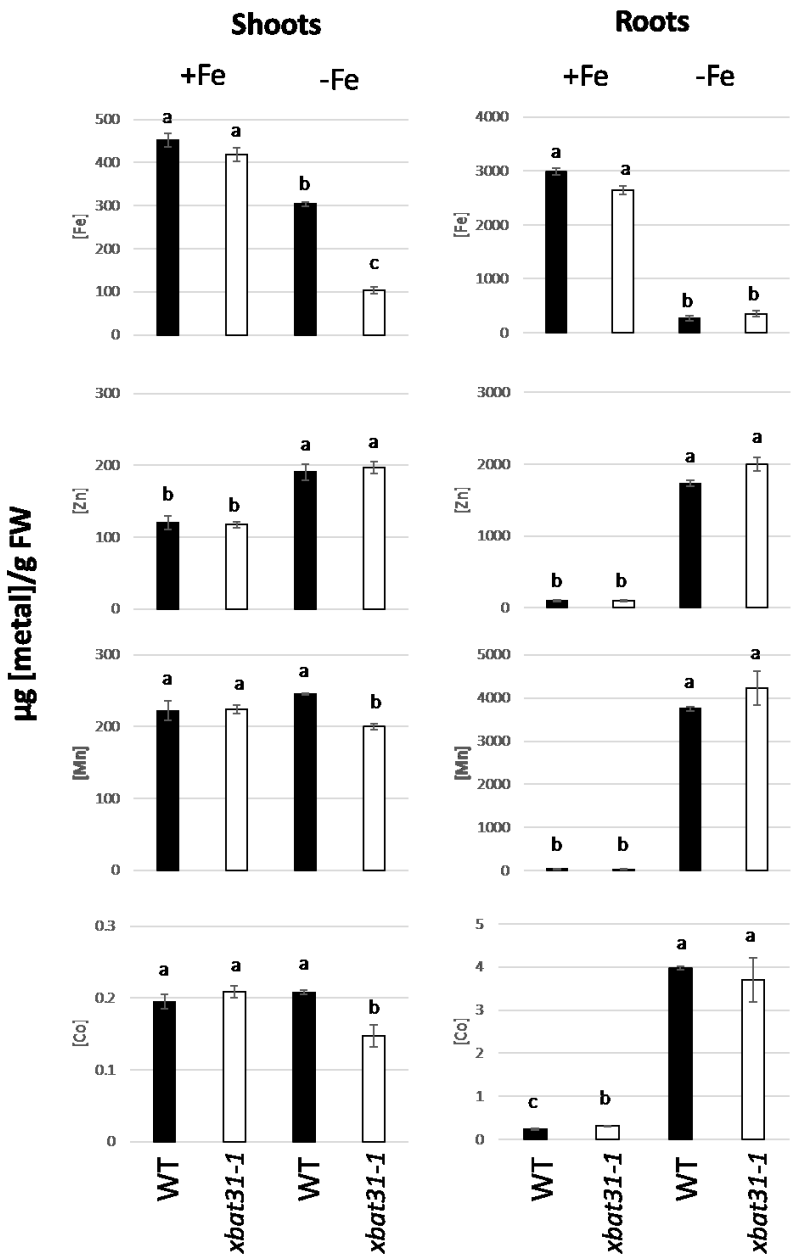

Figure 20 - Metal Content of Wild Type (WT) and *xbat31-1* Seedlings.

Metal content analysis of shoots (first column) and roots (second column) using 9-day-old WT *and xbat31-1* seedlings grown with (+) and without (-) Fe. *xbat31-1* seedlings showed significant less concentration of Fe, Mn and Co in shoots under -Fe condition compared to WT, and a significant higher accumulation of Co in roots under +Fe condition compared to WT. Different letters indicate p-value ≤0.05 using One-Way ANOVA Tukey comparison. Error bars indicate ±SE from 2 biological replicates, each measured 3 times.

3.10 *xbat31-1* is not Overly Stressed Compared to Wild Type under Fe-deficient Condition

Under Fe-deficient condition, dicotyledonous have shown an abnormal expression and activity of different peroxidases isoenzymes leading to induce secondary oxidative stress (Ranieri et al., 2001). In addition, leaves of maize and common bean root nodules had demonstrated to increase lipid peroxidation under Fe-deficient condition (Abdelmajid et al., 2007; Sun et al., 2007). Lower iron content in *xbat31-1* seedlings compared to wild type grown under Fe-deficient condition suggest that the mutant may be experiencing more stress. Electrolyte leakage, malondialdehyde (MDA) and catenoids content are indicators of the level of stress that demonstrates membrane intactness or cell damage (Bartley, 1995; McNulty et al., 2007; Sohrabi et al., 2012). To assess stress-induced injury, lipid peroxidation rate and oxidative protection in *xbat31-1* under +Fe and -Fe conditions, we measured electrolyte leakage, MDA content and carotenoid concentration, respectively. *xbat31-1* seedlings showed no significant difference in electrolyte leakage, carotenoids concentration or MDA content compared to WT under the same conditions (Figure 21). By displaying the same stress levels as WT, is possible to conclude that *xbat31-1* is coping with the low iron content similar to WT under the tested conditions.

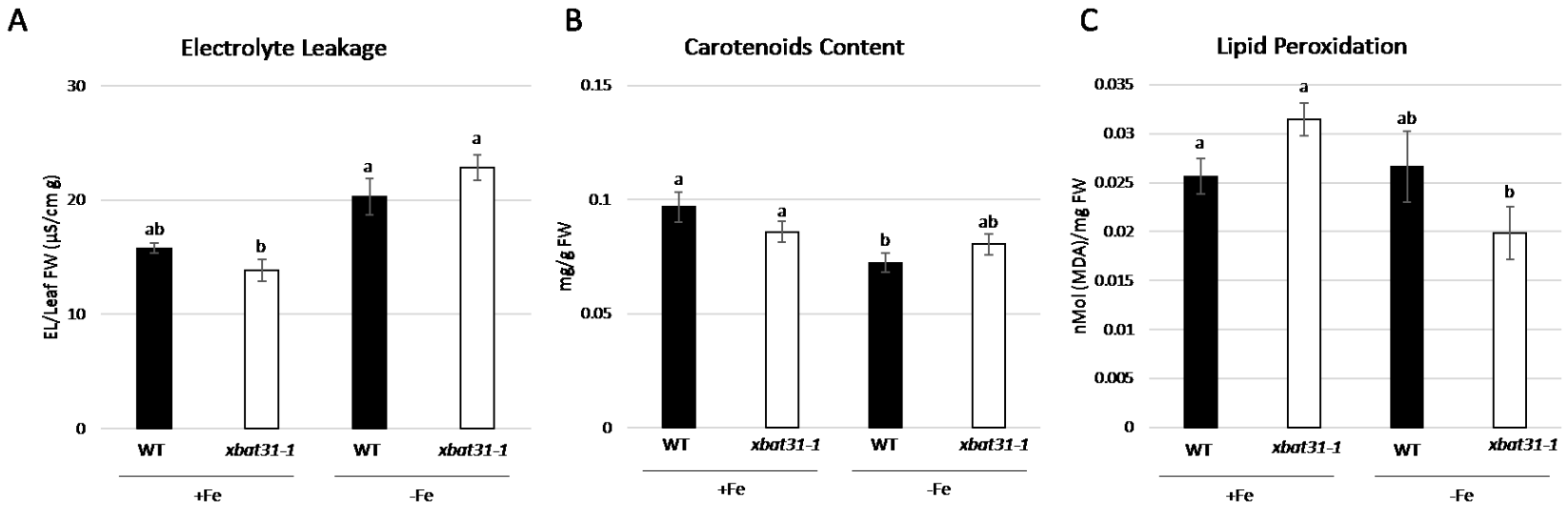

Figure 21 - Stress Responses Indicators in Wild Type (WT) and *xbat31-1* Seedlings.

WT and *xbat31-1* seedlings were grown with (+) and without (-) Fe for 9 days before assays were carry out. No significant difference was observed between WT and *xbat31-1* in electrolyte leakage measurement (A), carotenoids content (B) or lipid peroxidation analysis using MDA (malondialdehyde) measurements (C). Different letters indicate p-value ≤ 0.05 using One-Way ANOVA Tukey comparison. Error bars indicate ±SE from 2 trials with up to 7 technical replicates per trial.

3.11 *xbat31-1* is Tolerant to Heat Stress

Heat stress is another major type of abiotic stress which affect plant growth by affecting its metabolism and consequently affect its productivity (Hasanuzzaman et al., 2013). The XBAT31 interactor CPL1 was shown to be involved in tolerance of heat stress. *CPL1* mutants showed a hypersensitivity to heat stress, while overexpressers are tolerant in high temperatures (Guan et al., 2014). To assess the response of *xbat31-1* to heat stress, 7-days-old seedlings were exposed to 50ºC for different times and then left at room temperature for a recovery period of 7 days. As showed in Figure 22, *xbat31-1* is significantly more tolerant to heat stress compared to WT during 10 and 20min of exposure. 93% of *xbat31-1* seedlings survived when expose for 10min to 50°C in contrast with WT which showed a survival rate of 72% under the same condition. In 20min of exposure to 50°C, *xbat31-1* showed a survival rate of 57% compared to WT which showed a survival rate of 20% under the same condition. These results suggest that XBAT31 is involved in heat stress tolerance which must be further investigated with details.

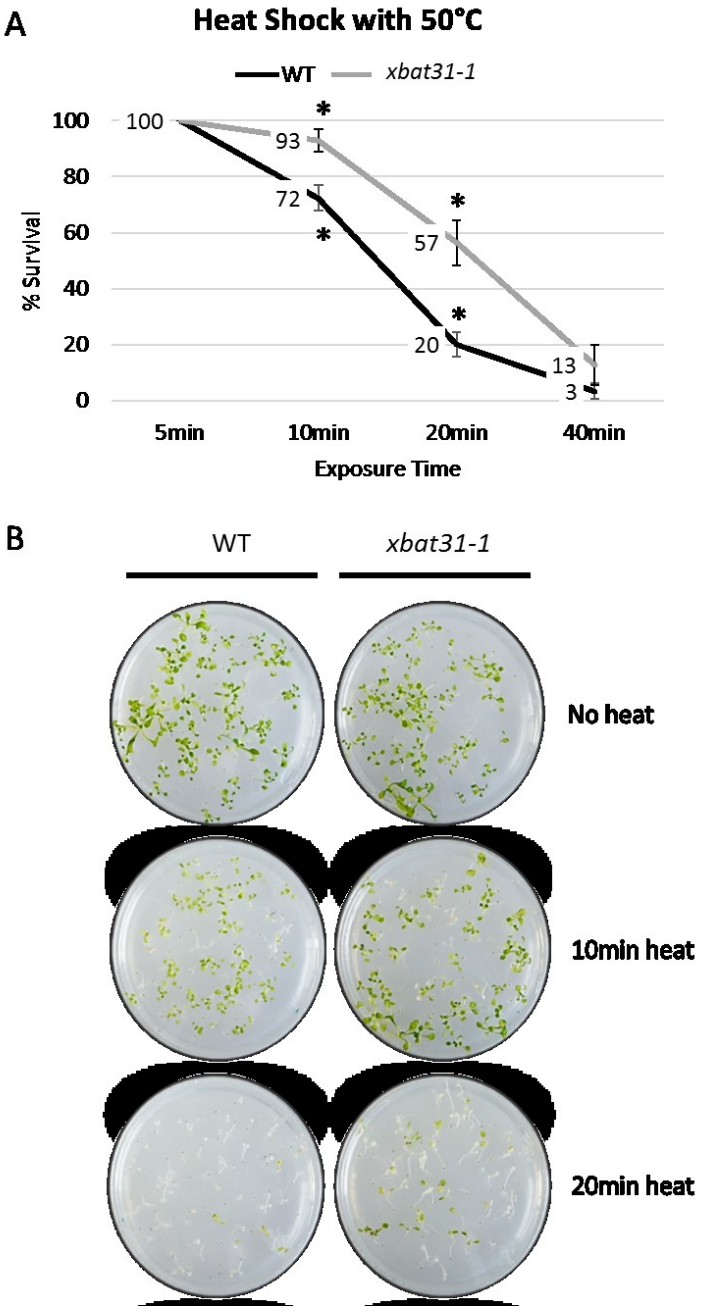

Figure 22 - Heat Stress Response Analysis of *xbat31-1*.

Percent (%) survival (A) of 2-weeks-old wild type (WT) and *xbat31-1* seedlings grown under standard media (solid MS media) following exposure to 50ºC for 5, 10, 20 and 40 minutes and 7-days-recovery period. Asterisks (*) indicate p-value ≤0.05 using One-Way ANOVA Tukey comparison. Error bars indicate ±SE from 2 trials with 2 technical replicates (plates with up to 50 seedlings) per trial. Representative pictures (B) of of 2-weeks-old WT and *xbat31-1* seedlings after exposure to 50ºC for the indicated time and 7-days-recovery period.

CHAPTER 4: DISCUSSION

The first indication of a biological role for the RING-type E3 XBAT31 comes from the identification of CPL1 and BRL2 potential interactors (Bang et al., 2008; Ceserani et al., 2009). BRL2 is involved in vascular development (Ceserani et al., 2009). However, *xbat31-1* does not display any alteration in leaf vascular development suggesting that the E3 is not involved in this process (Stone et al., unpublished data). We then investigated if XBAT31 is required for abiotic stress tolerance, specifically responding to iron deficient conditions. The results identified a role for the ubiquitin ligase as a positive regulator of plant Fe-deficiency response. In addition, the E3 was shown to regulate plant heat stress tolerance.

4.1 XBAT31.1 RING-type E3 is a Regulator of Fe-deficiency Response

XBAT31 undergoes alternative splicing to produce two transcripts; *XBAT31.1* and *XBAT31.2*. Under Fe-deficient condition, *XBAT31.1* is up-regulated, with no significant change in *XBAT31.2* transcript levels. These results suggest that *XBAT31.1*, but not *XBAT31.2*, may be involved in plant response to iron deficient growth conditions. In fact, loss of *XBAT31* gene expression render plants to be less sensitive to the negative effects of reduction in iron levels on plant growth. *xbat31-1* displayed significant longer growth for primary root, greater fresh weight and higher chlorophyll content, compared to wild type seedlings exposed to iron deprivation. *XBAT31* mutants also possess significant higher FRO2 and AHA2 enzyme activities when compared to the wild type. These results point to a role for the E3 in regulating Fe-deficiency response. Since the expression of both

XBAT31.1 and *XBAT31.2* are reduced in *xbat31-1*, we cannot conclusively state that *XBAT31.2* in not involved in plant responses to Fe-deficiency stress. However, finding that *XBAT31.2* transcript is not induced by low iron conditions suggests that the E3 isoform is not involved in regulating the stress response pathway.

The response of *xbat31-1* to iron deficient conditions is similar to those previously reported for BRUTUS (BTS), another RING-type E3. *BTS* acts as a negative regulator of Fe-stress response and mutants are less sensitive to Fe-deprivation with longer roots, higher fresh weight and chlorophyll content (Hindt et al., 2017; Matthiadis and Long, 2016; Selote et al., 2015). Similar to *xbat31-1*, *BTS* mutants also showed increased rhizosphere acidification and higher FRO2 enzyme activity (Hindt et al., 2017; Matthiadis and Long, 2016; Selote et al., 2015). Interestingly, under Fe-deficient condition, *BTS* mutants have significantly lower IRT1 concentration but no significant change in Fe concentration in roots, shoots or seeds compared to the wild type (Hindt et al., 2017). In contrast, under Fe-deficient condition, transcript levels of *IRT1* is significantly lower in *xbat31-1* compared to WT, which correlates with the observed lower levels of Fe, Mn and Co in shoots. The levels of Fe, Mn and Co in *xbat31-1* roots were similar to that found in the WT seedlings. The lower levels of Fe, Mn and Co in *xbat31-1* shoots (and not roots) agrees with previously reported results for *IRT1* mutants (Barberon et al., 2011).

The response of *xbat31-1* to Fe-deficient condition are also in accordance with those observed for another RING-type E3, IDF1, which is a negative regulator of IRT1 protein abundance in the plasma membrane. Similar to *xbat31-1, IDF1* mutants showed enhanced tolerance of Fe-deprivation, displaying larger shoots, greater fresh weight and increased AHA2 protein levels compared to WT (Shin et al., 2013). In contrast to *xbat31-*

1, transcript levels of *IRT1* in *idf1-1* is similar to that of WT. Unexpectedly, the *IDF1* mutants had higher concentration of iron in shoots, which could be the result of greater accumulation of IRT1 protein at plasma membrane (Shin et al., 2013). IRT1 protein levels have not been described for *xbat31-1* in this study. However, the *XBAT31* mutants have significantly lower concentration of Fe, Mn and Co in shoots under Fe-deficient condition, which is an important indicator of lower IRT1 levels. Further investigation of IRT1 protein levels must be performed with *xbat31-1* in order to assure that the observed reduction in transcript levels would reflect in lower protein accumulation, leading to lower metal concentration under -Fe condition.

The enhanced up-regulation of *FIT* in *xbat31-1* should strongly induce all downstream genes involved in Fe uptake, including *FRO2, AHA2* and *IRT1*. As expected, enhanced up-regulation is observed for *FRO2* and *AHA2* in *xbat31-1*. In contrast, the up-regulation of *IRT1* in *xbat31-1* under Fe-deficient condition is significantly lower than that observed for the WT plants. This suggests that *IRT1* expression remains inhibited in *xbat31-1* despite the reduction in iron availability. XBAT31.1 is a functional E3 and may be responsible for destroying a negative regulator of *IRT1* expression to promote the Fe-deficiency response (Figure 23B). In the absence of XBAT31.1, the negative regulator would remain and continue to inhibit *IRT1* expression despite the efforts of *FIT* and other factors to increase *IRT1* transcript levels and accumulation of the protein at the plasma membrane (Figure 23C).

Under non-stress growth conditions, iron availability may facilitate a feedback loop that helps to maintain the inhibitory activity of CPL1, which represses FIT expression and consequently the expression of other downstream genes (Figure 23A). Low iron

availability would promote the inhibition of CPL1 leading to the expression and accumulation of FIT, which would then promote the expression of downstream *Fe-utilization related* genes (*FRO2, AHA2* and *IRT1*) (Figure 23B). The up-regulation of *Fe-utilization related* genes leads to greater metal uptake, which may then promote a feedback loop that downregulates all Fe-uptake machinery (Figure 23B). This feedback signal is needed in order to tightly regulate Fe uptake and prevent Fe toxicity. In *xbat31-1* seedlings, the lower metal acquisition and transport may alter the feedback loop leading to even further upregulation of the *Fe-utilization related* genes. This may explain the enhanced upregulation of *FIT*, *FRO2* and *AHA2* observed for *xbat31-1* seedlings (Figure 23C).

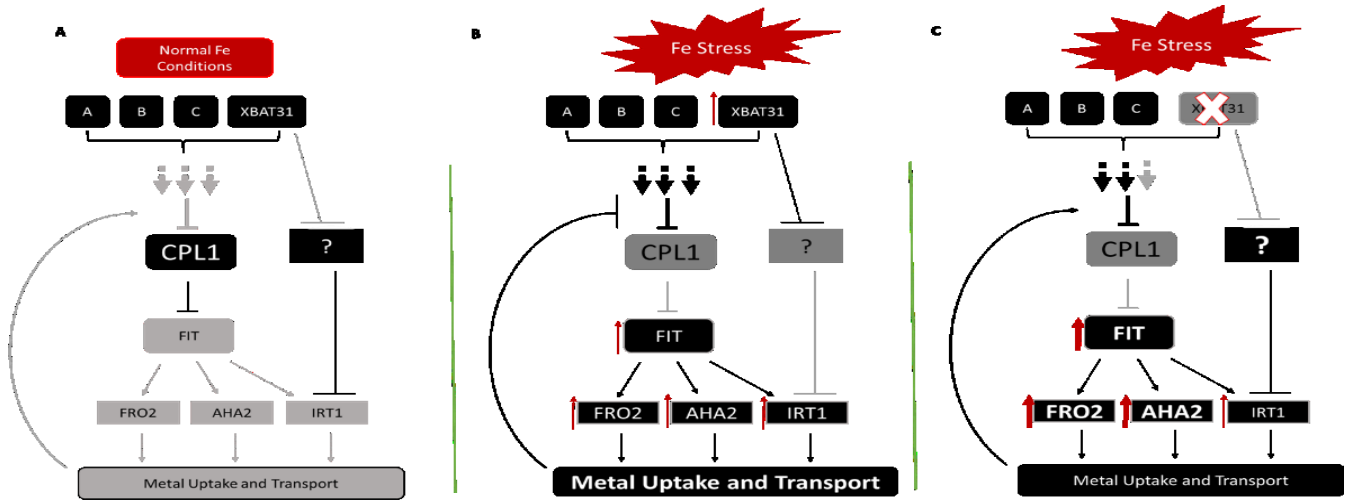

Figure 23 - Model for the Role of XBAT31.1 in Iron Stress Response.

When iron is available (A) in sufficient/nonstress conditions, *CPL1* and other negative regulators (?) inhibit the expression of *Fe-utilization related* genes including *FIT, FRO2, AHA2* and *IRT1*. *XBAT31.1* transcript levels are low, therefore E3 ligase activity is low. A positive feedback loop may help to maintain the low levels of *Fe-utilization related* genes. Under reduced iron availability (B) in deficient/stress conditions, iron sensors promote the stress response leading to the inhibition of CPL1 and other negative regulators (?), which results in the upregulation (red arrows) of *Fe-utilization related* genes including *FIT, FRO2, AHA2* and *IRT1*. *XBAT31.1* transcript levels also increase (red arrow) and the E3 ligase produced is predicted to promote the degradation of a negative regulator (?), loss of which promotes the upregulation of iron regulated genes such as *IRT1*. Following iron uptake, a negative feedback loop would assist in attenuating the response ensuring that the appropriate levels of iron is taken up by the plant. A reduction in *XBAT31.1* levels (C) under iron stress conditions may result in reduced iron sensing and accumulation of a negative regulator (?). This would lead to continued growth of the mutant (e.g. longer roots and greater chlorophyll content) and reduction in the level of *IRT1* upregulation compared to WT plants. The lower *IRT1* levels would lead to less iron uptake, explaining the lower iron content in *xbat31-1*. The lower iron uptake may promote a feedback loop that further increases the expression *Fe-utilization related* genes (e.g. *FIT, FRO2* and *AHA2*) in an effort to further promote iron uptake. This would explain the increase in transcript levels of *Fe-utilization related* genes observed in *xbat31-1*.

4.2 XBAT31.1 May Function as an Iron Sensor in Plants

Based on our results we propose that XBAT31.1 may also function as a Fe-sensor (Figure 23B). This conclusion is based on the findings that *xbat31-1* seedlings are able to grow better than WT under Fe-deficient condition as demonstrated by longer roots, greater fresh weight and more chlorophyll content despite the lower concentration of metals in shoots. This phenotype is unique to *xbat31-1*, as other mutants such as *irt1* and *cpl1-1/2* that also have low iron content are unable to tolerate iron deficient conditions (Emre Aksoy et al., 2013; Barberon et al., 2011). Previous results have shown that higher levels of Fe lead to less sensitivity to Fe-stress, which is the case of *IDF1* and *BTS* mutants; or even high Fe-toxicity effects, which is the case for *PYE* mutants (Long et al., 2010; Selote et al., 2015; Shin et al., 2013). In contrast, *XBAT31* mutants are less sensitive to Fe-stress despite possessing less concentration of Fe, Mn and Co in shoots under Fe-deficiency. These results suggest that the *XBAT31* mutant may be unable to sense the reduced iron levels and as a result does not efficiently induce the appropriate response, such as arresting growth and development. These results suggest that reducing *XBAT31* transcript levels render plants to be less sensitive to Fe-stress independent of their internal metal profile.

4.3 XBAT31 and CPL1 Interaction under Stress Conditions

XBAT31 is known to interact with CPL1, which is involved in response to Fe-deficiency and heat stresses (Aksoy et al. 2013; Bang et al. 2008; Guan et al. 2014). This interaction suggests that CPL1 may be a substrate for the UPS, where XBAT31.1 mediates the ubiquitination and subsequent degradation of CPL1. In this case, the loss of XBAT31.1 would result in the accumulation of CPL1. Since *CPL1* mutants respond in the same

manner as *xbat31-1* to Fe-deficient condition, it is unlikely that XBAT31.1 ubiquitinates and targets CPL1 for degradation to promote response to Fe-deficiency stress (Aksoy et al., 2013). On the other hand, *CPL1* overexpressers respond in the same manner to heat stress as *xbat31-1*, which suggests that XBAT31.1 regulates the abundance of CPL1 in plant response to heat stress. CPL1 overexpressers are more thermotolerant than WT (Guan et al., 2014). The same results have been found for *xbat31-1* in this study. *XBAT31* mutants subjected to 50°C heat shock for 10 and 20 min showed increased tolerance as determine by greater survivability compared to the WT. Heat stress can cause several injuries in plants, which include loss of membrane integrity, accumulation of ROS and disrupted growth and development (Guan et al., 2014). ROS accumulation is known to be involved in cell-death signaling in plants (Jalmi and Sinha, 2015). Overexpression of *XBAT31* in *Nicotiana benthamiana* leaves has been reported to induce programmed cell death with significant higher electrolyte leakage (Huang et al., 2013). These results altogether contribute to a proposal that XBAT31 would target CPL1 for proteasome degradation during exposure to high temperature to promote tolerance. However further investigation, using *in vitro* and in plant assays, must be performed to assure that CPL1 will be degraded by XBAT31.1 under heat stress.

CHAPTER 5: CONCLUSION AND FUTURE WORK

This study demonstrated that XBAT31.1 is a functional ubiquitin ligase with roles in regulating plant response to Fe-deficiency and thermotolerance. Importantly, the *XBAT31* mutants were shown to have dampen the expression of *IRT1* and the uptake of iron when plants were exposed to Fe-deficient condition. Taking all results into consideration, XBAT31.1 is proposed to function as an iron sensor and to control the abundance of a negative regulator of *IRT1* expression. Future work is needed in order to demonstrate the expected reduction in IRT1 protein levels in *xbat31-1*, which would explain the reduction of metal uptake. In addition, still necessary further study in XBAT31.1 to assess its ability to bind iron (and/or other metals) to determine if the E3 is indeed an iron sensor. Further analysis is also required to identify targets for XBAT31.1 E3 activity during the Fe-deficiency response. Furthermore, the interaction between XBAT31 and CPL1 should be better characterized to define if XBAT31 is mediating ubiquitination and consequently CPL1 degradation under heat stress.

REFERENCES

Abdelmajid, K., Karim, B.H., Chedly, A., 2007. Symbiotic response of common bean (Phaseolus vulgaris L.) to iron deficiency. Acta Physiol. Plant. 30, 27–34. https://doi.org/10.1007/s11738-007-0087-5

Aksoy, E., Jeong, I.S., Koiwa, H., 2013. Loss of Function of Arabidopsis C-Terminal Domain Phosphatase-Like1 Activates Iron Deficiency Responses at the Transcriptional Level. Plant Physiol. 161, 330–345. https://doi.org/10.1104/pp.112.207043

Aksoy, E., Koiwa, H., 2013. Function of Arabidopsis CPL1 in cadmium responses © 2013 Landes Bioscience . Do not distribute © 2013 Landes Bioscience . Do not distribute 10–12. https://doi.org/10.4161/psb.24120

Bang, W.Y., Kim, S.W., Jeong, I.S., Koiwa, H., Bahk, J.D., 2008. The C-terminal region (640-967) of Arabidopsis CPL1 interacts with the abiotic stress- and ABA-responsive transcription factors. Biochem. Biophys. Res. Commun. 372, 907–912. https://doi.org/10.1016/j.bbrc.2008.05.161

Barberon, M., Zelazny, E., Robert, S., Conéjéro, G., Curie, C., Friml, J., Vert, G., 2011. Monoubiquitin-dependent endocytosis of the transporter controls iron uptake in plants. Proc. Natl. Acad. Sci. U. S. A. 108, e450–e458. https://doi.org/10.1073/pnas.1100659108/-/DCSupplemental.www.pnas.org/cgi/doi/10.1073/pnas.1100659108

Bartley, G.E., 1995. Plant Carotenoids: Pigments for Photoprotection, Visual Attraction, and Human Health. Plant Cell Online 7, 1027–1038. https://doi.org/10.1105/tpc.7.7.1027

Bedford, L., Paine, S., Sheppard, P.W., Mayer, R.J., Roelofs, J., 2011. Assembly, Structure and Function of the 26S proteasome 20, 391–401. https://doi.org/10.1016/j.tcb.2010.03.007.Assembly

Briat, J., Fobis-loisy, I., Grignon, N., Lobrcaux, S., Pascal, N., Savino, G., Thoiron, S., Wircn, N. Von, Wuytswinkel, O. Van, 1995. Cellular and molecular aspects of iron metabolism in plants. Biol Cell 69–81.

Briat, J.F., Lobreaux, S., 1997. Iron transport and storage in plants. Trends Plant Sci. 2, 187–193. https://doi.org/10.1016/S1360-1385(97)85225-9

Brumbarova, T., Bauer, P., 2009. Iron Uptake and Transport in Plants. Plant Membr. Vacuolar Transp. 109, 149–172. https://doi.org/10.1021/cr900112r.Iron

Brumbarova, T., Bauer, P., Ivanov, R., 2015. Molecular mechanisms governing Arabidopsis iron uptake. Trends Plant Sci. 20, 124–133. https://doi.org/10.1016/j.tplants.2014.11.004

Callis, J., 2014. The Ubiquitination Machinery of the Ubiquitin System. Arab. B. 12, e0174. https://doi.org/10.1199/tab.0174

Carvalho, S.D., Saraiva, R., Maia, T.M., Abreu, I.A., Duque, P., 2012. XBAT35, a novel arabidopsis RING E3 ligase exhibiting dual targeting of its splice isoforms, is involved in ethylene-mediated regulation of apical hook curvature. Mol. Plant 5, 1295–1309. https://doi.org/10.1093/mp/sss048

Ceserani, T., Trofka, A., Gandotra, N., Nelson, T., 2009. VH1/BRL2 receptor-like kinase interacts with vascular-specific adaptor proteins VIT and VIK to influence leaf venation. Plant J. 57, 1000–1014. https://doi.org/10.1111/j.1365-313X.2008.03742.x

Chappelle, E.W., Kim, M.S., Mcmurtrey, J.E., 1992. Ratio Analysis of Reflectance Spectra (rars) - {{}A{}}n Algorithm For the Remote Estimation of the Concentrations of Chlorophyll-a, Chlorophyll-b, and Carotenoids In Soybean Leaves. Remote Sens. Environ. 39, 239–247.

Chen, L., Hellmann, H., 2013. Plant E3 ligases: Flexible enzymes in a sessile world. Mol. Plant 6, 1388–1404. https://doi.org/10.1093/mp/sst005

Chen, Z.J., Sun, L.J., 2009. Nonproteolytic Functions of Ubiquitin in Cell Signaling. Mol. Cell 33, 275–286. https://doi.org/10.1016/j.molcel.2009.01.014

Cho, S.K., Ryu, M.Y., Kim, J.H., Hong, J.S., Oh, T.R., Kim, W.T., 2017. RING E3 ligases : key regulatory elements are involved in abiotic stress responses in plants 50, 393–400.

Chu, H.-H., Chiecko, J., Punshon, T., Lanzirotti, A., Lahner, B., Salt, D.E., Walker, E.L., 2010. Successful Reproduction Requires the Function of Arabidopsis YELLOW STRIPE-LIKE1 and YELLOW STRIPE-LIKE3 Metal-Nicotianamine Transporters in Both Vegetative and Reproductive Structures. Plant Physiol. 154, 197–210. https://doi.org/10.1104/pp.110.159103

Clemens, S., Weber, M., 2016. The essential role of coumarin secretion for Fe acquisition from alkaline soil. Plant Signal. Behav. 11, 1–6. https://doi.org/10.1080/15592324.2015.1114197

Cohen, C.K., Fox, T.C., Garvin, D.F., Kochian, L. V., 1998. The Role of Iron-Deficiency Stress Responses in Stimulating Heavy-Metal Transport in Plants. Plant Physiol. 116, 1063–1072. https://doi.org/10.1104/pp.116.3.1063

Colangelo, E.P., 2004. The Essential Basic Helix-Loop-Helix Protein FIT1 Is Required for the Iron Deficiency Response. Plant Cell Online 16, 3400–3412. https://doi.org/10.1105/tpc.104.024315

Connorton, J.M., Balk, J., Rodríguez-Celma, J., 2017. Iron homeostasis in plants – a brief overview. Metallomics 9, 813–823. https://doi.org/10.1039/C7MT00136C

Couturier, J., Touraine, B., Briat, J.-F., Gaymard, F., Rouhier, N., 2013. The iron-sulfur cluster assembly machineries in plants: current knowledge and open questions. Front. Plant Sci. 4, 1–22. https://doi.org/10.3389/fpls.2013.00259

Dionisio-Sese, M.L., Tobita, S., 1998. Antioxidant responses of rice seedlings to salinity stress. Plant Sci. 135, 1–9. https://doi.org/10.1016/S0168-9452(98)00025-9

Dorantes-Acosta, A.E., S??nchez-Hern??ndez, C. V., Arteaga-V??zquez, M.A., 2012. Biotic stress in plants: Life lessons from your parents and grandparents. Front. Genet. 3, 1–2. https://doi.org/10.3389/fgene.2012.00256

Downes, B.P., Stupar, R.M., Gingerich, D.J., Vierstra, R.D., 2003. The HECT ubiquitin-protein ligase (UPL) family in Arabidopsis: UPL3 has a specific role in trichome development. Plant J. 35, 729–742. https://doi.org/10.1046/j.1365-313X.2003.01844.x

Durrett, T.P., Gassmann, W., Rogers, E.E., 2007. The FRD3-Mediated Efflux of Citrate into the Root Vasculature Is Necessary for Efficient Iron Translocation. Plant Physiol. 144, 197–205. https://doi.org/10.1104/pp.107.097162

Eroglu, S., Meier, B., von Wirén, N., Peiter, E., 2016. The Vacuolar Manganese Transporter MTP8 Determines Tolerance to Iron Deficiency-Induced Chlorosis in Arabidopsis. Plant Physiol. 170, 1030–1045. https://doi.org/10.1104/pp.15.01194

Gayomba, S.R., Zhai, Z., Jung, H., Vatamaniuk, O.K., 2015. Local and systemic signaling of iron status and its interactions with homeostasis of other essential elements. Front. Plant Sci. 6, 1–13. https://doi.org/10.3389/fpls.2015.00716

Guan, Q., Yue, X., Zeng, H., Zhu, J., 2014. The Protein Phosphatase RCF2 and Its Interacting Partner NAC019 Are Critical for Heat Stress-Responsive Gene Regulation and Thermotolerance in Arabidopsis. Plant Cell 26, 438–453. https://doi.org/10.1105/tpc.113.118927

Guerinot, M.L., 2001. Improving rice yields--ironing out the details. Nat. Biotechnol. 19, 417–418. https://doi.org/10.1038/88067

Guerinot, M. Lou, Yi, Y., 1994. Iron: Nutritious, Noxious, and Not Readily Available. Plant Physiol 104, 815–820. https://doi.org/10.1104/pp.104.3.815

Guo, Y., Jia, W., Song, J., Wang, D., Chen, M., Wang, B., 2012. Thellungilla halophila is more adaptive to salinity than Arabidopsis thaliana at stages of seed germination and seedling establishment. Acta Physiol. Plant. 1–8. https://doi.org/10.1007/s11738-012-0925-y

Haniff, J., Das, A., Onn, L.T., Chen, W.S., Nordin, N.M., Rampal, S., Bahrin, S., Ganeslingam, M., Kularatnam, K.I.K., Zaher, Z.M.M., 2007. Anemia in pregnancy in Malaysia: A cross-sectional survey. Asia Pac. J. Clin. Nutr. 16, 527–536. https://doi.org/10.1016/S2214-109X(13)70001-9

Hasanuzzaman, M., Nahar, K., Alam, M.M., Roychowdhury, R., Fujita, M., 2013. Physiological, biochemical, and molecular mechanisms of heat stress tolerance in plants. Int. J. Mol. Sci. 14, 9643–9684. https://doi.org/10.3390/ijms14059643

Hasegawa, H., Rahman, M.A., Saitou, K., Kobayashi, M., Okumura, C., 2011. Influence of chelating ligands on bioavailability and mobility of iron in plant growth media and their effect on radish growth. Environ. Exp. Bot. 71, 345–351. https://doi.org/10.1016/j.envexpbot.2011.01.004

Hell, R., Stephan, U.W., 2003. Iron uptake, trafficking and homeostasis in plants. Planta 216, 541–551. https://doi.org/10.1007/s00425-002-0920-4

Hindt, M.N., Akmakjian, G.Z., Pivarski, K.L., Punshon, T., Baxter, I., Salt, D.E., Guerinot, M. Lou, 2017. BRUTUS and its paralogs, BTS LIKE1 and BTS LIKE2, encode important negative regulators of the iron deficiency response in Arabidopsis thaliana. Metallomics 9, 876–890. https://doi.org/10.1039/C7MT00152E

Huang, X., Liu, X., Chen, X., Snyder, A., Song, W.Y., 2013. Members of the XB3 Family from Diverse Plant Species Induce Programmed Cell Death in Nicotiana benthamiana. PLoS One 8. https://doi.org/10.1371/journal.pone.0063868

Jakoby, M., Wang, H.Y., Reidt, W., Weisshaar, B., Bauer, P., 2004. FRU (BHLH029) is required for induction of iron mobilization genes in Arabidopsis thaliana. FEBS Lett. 577, 528–534. https://doi.org/10.1016/j.febslet.2004.10.062

Jalmi, S.K., Sinha, A.K., 2015. ROS mediated MAPK signaling in abiotic and biotic stress-striking similarities and differences. Front. Plant Sci. 6, 1–9. https://doi.org/10.3389/fpls.2015.00769

Jean, M. Le, Schikora, A., Mari, S., Briat, J.F., Curie, C., 2005. A loss-of-function mutation in AtYSL1 reveals its role in iron and nicotianamine seed loading. Plant J. 44, 769–782. https://doi.org/10.1111/j.1365-313X.2005.02569.x

Jeong, I.S., Fukudome, A., Aksoy, E., Bang, W.Y., Kim, S., Guan, Q., Bahk, J.D., May, K.A., Russell, W.K., Zhu, J., Koiwa, H., 2013. Regulation of abiotic stress signalling by arabidopsis C-terminal domain phosphatase-like 1 requires interaction with a K-homology domain-containing protein. PLoS One 8. https://doi.org/10.1371/journal.pone.0080509

Johnson, D.C., Dean, D.R., Smith, A.D., Johnson, M.K., 2005. Structure, Function, and Formation of Biological Iron-Sulfur Clusters. Annu. Rev. Biochem. 74, 247–281. https://doi.org/10.1146/annurev.biochem.74.082803.133518

Joosten, E., 2017. Iron deficiency anemia in older adults: A review. Geriatr. Gerontol. Int. 1–7. https://doi.org/10.1111/ggi.13194

Kim, S.A., Guerinot, M. Lou, 2007. Mining iron: Iron uptake and transport in plants. FEBS Lett. 581, 2273–2280. https://doi.org/10.1016/j.febslet.2007.04.043

Kobayashi, T., Itai, R.N., Aung, M.S., Senoura, T., Nakanishi, H., Nishizawa, N.K., 2012. The rice transcription factor IDEF1 directly binds to iron and other divalent metals for sensing cellular iron status. Plant J. 69, 81–91. https://doi.org/10.1111/j.1365-313X.2011.04772.x

Kobayashi, T., Itai, R.N., Ogo, Y., Kakei, Y., Nakanishi, H., Takahashi, M., Nishizawa, N.K., 2009. The rice transcription factor IDEF1 is essential for the early response to iron deficiency, and induces vegetative expression of late embryogenesis abundant genes. Plant J. 60, 948–961. https://doi.org/10.1111/j.1365-313X.2009.04015.x

Kobayashi, T., Nagasaka, S., Senoura, T., Itai, R.N., Nakanishi, H., Nishizawa, N.K., 2013. Iron-binding haemerythrin RING ubiquitin ligases regulate plant iron responses and accumulation. Nat. Commun. 4, 1–12. https://doi.org/10.1038/ncomms3792

Kobayashi, T., Nishizawa, N.K., 2014. Iron sensors and signals in response to iron deficiency. Plant Sci. 224, 36–43. https://doi.org/10.1016/j.plantsci.2014.04.002

Kobayashi, T., Nishizawa, N.K., 2012. Iron Uptake, Translocation, and Regulation in Higher Plants. Annu. Rev. Plant Biol. 63, 131–152. https://doi.org/10.1146/annurev-arplant-042811-105522

Kobayashi, T., Ogo, Y., Itai, R.N., Nakanishi, H., Takahashi, M., Mori, S., Nishizawa, N.K., 2007. The transcription factor IDEF1 regulates the response to and tolerance of iron deficiency in plants. Proc. Natl. Acad. Sci. U. S. A. 104, 19150–19155. https://doi.org/10.1073/pnas.0707010104

Koiwa, H., Barb, A.W., Xiong, L., Li, F., McCully, M.G., Lee, B.-H., Sokolchik, I., Zhu, J., Gong, Z., Reddy, M., Sharkhuu, A., Manabe, Y., Yokoi, S., Zhu, J.-K., Bressan, R. a, Hasegawa, P.M., 2002. C-terminal domain phosphatase-like family members (AtCPLs) differentially regulate Arabidopsis thaliana abiotic stress signaling, growth, and development. Proc. Natl. Acad. Sci. U. S. A. 99, 10893–8. https://doi.org/10.1073/pnas.112276199

Kreamer, N.N.K., Wilks, J.C., Marlow, J.J., Coleman, M.L., Newman, D.K., 2012. BqsR/bqsS constitute a two-component system that senses extracellular Fe(II) in Pseudomonas aeruginosa. J. Bacteriol. 194, 1195–1204. https://doi.org/10.1128/JB.05634-11

Lane, D.J.R., Merlot, A.M., Huang, M.L.H., Bae, D.H., Jansson, P.J., Sahni, S., Kalinowski, D.S., Richardson, D.R., 2015. Cellular iron uptake, trafficking and metabolism: Key molecules and mechanisms and their roles in disease. Biochim. Biophys. Acta - Mol. Cell Res. 1853, 1130–1144. https://doi.org/10.1016/j.bbamcr.2015.01.021

Lingam, S., Mohrbacher, J., Brumbarova, T., Potuschak, T., Fink-Straube, C., Blondet, E., Genschik, P., Bauer, P., 2011. Interaction between the bHLH Transcription Factor FIT and ETHYLENE INSENSITIVE3/ETHYLENE INSENSITIVE3-LIKE1 Reveals Molecular Linkage between the Regulation of Iron Acquisition and Ethylene Signaling in *Arabidopsis*. Plant Cell 23, 1815–1829. https://doi.org/10.1105/tpc.111.084715

Liphadzi, M.S., Kirkham, M.B., 2006. Availability and plant uptake of heavy metals in EDTA-assisted phytoremediation of soil and composted biosolids. South African J. Bot. 72, 391–397. https://doi.org/10.1016/j.sajb.2005.10.010

Liu, H., Ravichandran, S., Teh, O., McVey, S., Lilley, C., Teresinski, H.J., Gonzalez-Ferrer, C., Mullen, R.T., Hofius, D., Prithiviraj, B., Stone, S.L., 2017. The RING-Type E3 Ligase XBAT35.2 Is Involved in Cell Death Induction and Pathogen Response. Plant Physiol. 175, 1469–1483. https://doi.org/10.1104/pp.17.01071

Liu, H., Stone, S.L., 2013. Cytoplasmic degradation of the Arabidopsis transcription factor abscisic acid insensitive 5 is mediated by the ring-type E3 ligase keep on going. J. Biol. Chem. 288, 20267–20279. https://doi.org/10.1074/jbc.M113.465369

Long, T.A., Tsukagoshi, H., Busch, W., Lahner, B., Salt, D.E., Benfey, P.N., 2010. The bHLH Transcription Factor POPEYE Regulates Response to Iron Deficiency in Arabidopsis Roots. Plant Cell Online 22, 2219–2236. https://doi.org/10.1105/tpc.110.074096

Mai, H.-J., et al., 2016. Iron homeostasis in Arabidopsis thaliana: transcriptomic analyses reveal novel FIT-regulated genes, iron deficiency marker genes and functional gene networks. BMC Plant Biol. 16, 211. https://doi.org/10.1186/s12870-016-0899-9

Martin, C., Li, J., 2017. Medicine is not health care, food is health care: plant metabolic engineering, diet and human health. New Phytol. 699–719. https://doi.org/10.1111/nph.14730

Matsuda, O., Sakamoto, H., Nakao, Y., Oda, K., Iba, K., 2009. CTD phosphatases in the attenuation of wound-induced transcription of jasmonic acid biosynthetic genes in Arabidopsis. Plant J. 57, 96–108. https://doi.org/10.1111/j.1365-313X.2008.03663.x

Matthiadis, A., Long, T.A., 2016. Further insight into BRUTUS domain composition and functionality. Plant Signal. Behav. 11, 1–6. https://doi.org/10.1080/15592324.2016.1204508

McNulty, H.P., Byun, J., Lockwood, S.F., Jacob, R.F., Mason, R.P., 2007. Differential effects of carotenoids on lipid peroxidation due to membrane interactions: X-ray diffraction analysis. Biochim. Biophys. Acta - Biomembr. 1768, 167–174. https://doi.org/10.1016/j.bbamem.2006.09.010

Miao, Y., Zentgraf, U., 2010. A HECT E3 ubiquitin ligase negatively regulates Arabidopsis leaf senescence through degradation of the transcription factor WRKY53. Plant J. 63, 179–188. https://doi.org/10.1111/j.1365-313X.2010.04233.x

Moroishi, T., Nishiyama, M., Takeda, Y., Iwai, K., Nakayama, K.I., 2011. The FBXL5-IRP2 axis is integral to control of iron metabolism in vivo. Cell Metab. 14, 339–351. https://doi.org/10.1016/j.cmet.2011.07.011

Morrissey, J., Baxter, I.R., Lee, J., Li, L., Lahner, B., Grotz, N., Kaplan, J., Salt, D.E., Guerinot, M. Lou, 2009. The ferroportin metal efflux proteins function in iron and cobalt homeostasis in Arabidopsis. Plant Cell 21, 3326–38. https://doi.org/10.1105/tpc.109.069401

Mulligan, R.M., Choryt, J., 2017. Signaling in Plants Author (s): R . Michael Mulligan , Joanne Chory and Joseph R . Ecker Published by : National Academy of Sciences Stable URL : http://www.jstor.org/stable/41727 Signaling in plants 94, 2793–2795.

Nakasone, M.A., Livnat-Levanon, N., Glickman, M.H., Cohen, R.E., Fushman, D., 2013. Mixed-linkage ubiquitin chains send mixed messages. Structure 21, 727–740. https://doi.org/10.1016/j.str.2013.02.019

Nodzon, L.A., Xu, W.-H., Wang, Y., Pi, L.-Y., Chakrabarty, P.K., Song, W.-Y., 2004. The ubiquitin ligase XBAT32 regulates lateral root development in Arabidopsis. Plant J. 40, 996–1006. https://doi.org/10.1111/j.1365-313X.2004.02266.x

Ogo, Y., Itai, R.N., Nakanishi, H., Inoue, H., Kobayashi, T., Suzuki, M., Takahashi, M., Mori, S., Nishizawa, N.K., 2006. Isolation and characterization of IRO2, a novel iron-regulated bHLH transcription factor in graminaceous plants. J. Exp. Bot. 57, 2867–2878. https://doi.org/10.1093/jxb/erl054

Palmer, C.M., Hindt, M.N., Schmidt, H., Clemens, S., Guerinot, M. Lou, 2013. MYB10 and MYB72 Are Required for Growth under Iron-Limiting Conditions. PLoS Genet. 9. https://doi.org/10.1371/journal.pgen.1003953

Palmer, L.D., Skaar, E.P., 2016. Transition Metals and Virulence in Bacteria. Annu. Rev. Genet. 50, 67–91. https://doi.org/10.1146/annurev-genet-120215-035146

Pandey, P., Irulappan, V., Bagavathiannan, M. V., Senthil-Kumar, M., 2017. Impact of Combined Abiotic and Biotic Stresses on Plant Growth and Avenues for Crop Improvement by Exploiting Physio-morphological Traits. Front. Plant Sci. 8, 1–15. https://doi.org/10.3389/fpls.2017.00537

Pickart, C.M., Fushman, D., 2004. Polyubiquitin chains: Polymeric protein signals. Curr. Opin. Chem. Biol. 8, 610–616. https://doi.org/10.1016/j.cbpa.2004.09.009

Pizzio, G.A., Paez-Valencia, J., Khadilkar, A.S., Regmi, K., Patron-Soberano, A., Zhang, S., Sanchez-Lares, J., Furstenau, T., Li, J., Sanchez-Gomez, C., Valencia-Mayoral, P., Yadav, U.P., Ayre, B.G., Gaxiola, R.A., 2015. Arabidopsis Type I Proton-Pumping Pyrophosphatase Expresses Strongly in Phloem, Where It Is Required for Pyrophosphate Metabolism and Photosynthate Partitioning. Plant Physiol. 167, 1541–1553. https://doi.org/10.1104/pp.114.254342

Prasad, M.E., Schofield, A., Lyzenga, W., Liu, H., Stone, S.L., 2010. Arabidopsis RING E3 Ligase XBAT32 Regulates Lateral Root Production through Its Role in Ethylene Biosynthesis. Plant Physiol. 153, 1587–1596. https://doi.org/10.1104/pp.110.156976

Prasad, M.E., Stone, S.L., 2010. Further analysis of XBAT32, an Arabidopsis RING E3 ligase, involved in ethylene biosynthesis. Plant Signal. Behav. 5, 1425–1429. https://doi.org/10.4161/psb.5.11.13294

Rampey, R.A., Woodward, A.W., Hobbs, B.N., Tierney, M.P., Lahner, B., Salt, D.E., Bartel, B., 2006. An arabidopsis basic helix-loop-helix leucine zipper protein modulates metal homeostasis and auxin conjugate responsiveness. Genetics 174, 1841–1857. https://doi.org/10.1534/genetics.106.061044

Ranieri, A., Castagna, A., Baldan, B., Soldatini, G.F., 2001. Iron deficiency differently affects peroxidase isoforms in sunflower. J. Exp. Bot. 52, 25–35. https://doi.org/10.1093/jexbot/52.354.25

Rengel, Z., 2015. Availability of Mn, Zn and Fe in the rhizosphere. J. Soil Sci. Plant Nutr. 15, 397–409. https://doi.org/10.4067/S0718-95162015005000036

Robinson, N.J., Procter, C.M., Connolly, E.L., Guerinot, M.L., 1999. A ferric-chelate reductase for iron uptake from soils. Nature 397, 694–697. https://doi.org/Doi 10.1038/17800

Romera, F., Welch, R., Norvell, W., Schaefer, S., 1996. Iron requirement for and effects of promoters and inhibitors of ethylene action on stimulation of Fe(III)-chelate reductase in roots of strategy I species. Biometals 9, 45–50. https://doi.org/10.1007/BF00188089

Rout, G.R., Sahoo, S., 2015. Role of Iron in Plant Growth and Metabolism. Rev. Agric. Sci. 3. https://doi.org/10.7831/ras.3.1

Santi, S., Schmidt, W., 2009. Dissecting iron deficiency-induced proton extrusion in Arabidopsis roots. New Phytol. 183, 1072–1084. https://doi.org/10.1111/j.1469-8137.2009.02908.x

Schmid, N.B., Giehl, R.F.H., Doll, S., Mock, H.-P., Strehmel, N., Scheel, D., Kong, X., Hider, R.C., von Wiren, N., 2014. Feruloyl-CoA 6'-Hydroxylase1-Dependent Coumarins Mediate Iron Acquisition from Alkaline Substrates in Arabidopsis. Plant Physiol. 164, 160–172. https://doi.org/10.1104/pp.113.228544

Schmidt, H., Günther, C., Weber, M., Spörlein, C., Loscher, S., Böttcher, C., Schobert, R., Clemens, S., 2014. Metabolome analysis of Arabidopsis thaliana roots identifies a key metabolic pathway for iron acquisition. PLoS One 9, 1–11. https://doi.org/10.1371/journal.pone.0102444

Schmidt, W., Buckhout, T.J., 2011. A hitchhiker's guide to the Arabidopsis ferrome. Plant Physiol. Biochem. 49, 462–470. https://doi.org/10.1016/j.plaphy.2010.12.001

Selote, D., Samira, R., Matthiadis, A., Gillikin, J.W., Long, T.A., 2015. Iron-Binding E3 Ligase Mediates Iron Response in Plants by Targeting Basic Helix-Loop-Helix Transcription Factors. Plant Physiol. 167, 273–286. https://doi.org/10.1104/pp.114.250837

Sharma, B., Joshi, D., Yadav, P.K., Gupta, A.K., Bhatt, T.K., 2016. Role of Ubiquitin-Mediated Degradation System in Plant Biology. Front. Plant Sci. 7, 1–8. https://doi.org/10.3389/fpls.2016.00806

Shenker, M., Chen, Y., 2005. Increasing Iron Availability to Crops: Fertilizers, Organo-Fertilizers, and Biological Approaches. Soil Sci. Plant Nutr. 51, 1–17. https://doi.org/10.1111/j.1747-0765.2005.tb00001.x

Shenker, M., Chen, Y., 2003. Agronomic approaches for increasing iron availability to food crops. Impacts Agric. Hum. Heal. Nutr. Encycl. Life Support Syst. I, 1–9.

Shin, L.-J., Lo, J.-C., Chen, G.-H., Callis, J., Fu, H., Yeh, K.-C., 2013. IRT1 DEGRADATION FACTOR1, a RING E3 Ubiquitin Ligase, Regulates the Degradation of IRON-REGULATED TRANSPORTER1 in Arabidopsis. Plant Cell 25, 3039–3051. https://doi.org/10.1105/tpc.113.115212

Sivitz, A., Grinvalds, C., Barberon, M., Curie, C., Vert, G., 2011. Proteasome-mediated turnover of the transcriptional activator FIT is required for plant iron-deficiency responses. Plant J. 66, 1044–1052. https://doi.org/10.1111/j.1365-313X.2011.04565.x

Sivitz, A.B., Hermand, V., Curie, C., Vert, G., 2012. Arabidopsis bHLH100 and bHLH101 Control Iron Homeostasis via a FIT-Independent Pathway. PLoS One 7. https://doi.org/10.1371/journal.pone.0044843

Smalle, J., Vierstra, R.D., 2004. the Ubiquitin 26S Proteasome Proteolytic Pathway. Annu. Rev. Plant Biol. 55, 555–590. https://doi.org/10.1146/annurev.arplant.55.031903.141801

Sohrabi, Y., Heidari, G., Weisany, W., Ghasemi-Golezani, K., Mohammadi, K., 2012. Some physiological responses of chickpea cultivars to arbuscular mycorrhiza under drought stress. Russ. J. Plant Physiol. 59, 708–716. https://doi.org/10.1134/S1021443712060143

Stone, S.L., 2014. The role of ubiquitin and the 26S proteasome in plant abiotic stress signaling. Front. Plant Sci. 5, 1–10. https://doi.org/10.3389/fpls.2014.00135

Stone, S.L., Troy, A., Herschleb, J., Kraft, E., Callis, J., Hauksdo, H., 2005. Functional Analysis of the RING-Type Ubiquitin Ligase Family of Arabidopsis 1 [w]. Plant Physiol. 137, 13–30. https://doi.org/10.1104/pp.104.052423.carrying

Sun, B., Jing, Y., Chen, K., Song, L., Chen, F., Zhang, L., 2007. Protective effect of nitric oxide on iron deficiency-induced oxidative stress in maize (Zea mays). J. Plant Physiol. 164, 536–543. https://doi.org/10.1016/j.jplph.2006.02.011

Thrower, J.S., 2000. Recognition of the polyubiquitin proteolytic signal. EMBO J. 19, 94–102. https://doi.org/10.1093/emboj/19.1.94

Ueno, D., Iwashita, T., Zhao, F.J., Ma, J.F., 2008. Characterization of Cd translocation and identification of the Cd form in xylem sap of the Cd-hyperaccumulator Arabidopsis halleri. Plant Cell Physiol. 49, 540–548. https://doi.org/10.1093/pcp/pcn026

Vert, G., Grotz, N., Dédaldéchamp, F., Gaymard, F., Guerinot, M. Lou, Briat, J.-F., Curie, C., 2002. IRT1, an Arabidopsis transporter essential for iron uptake from the soil and for plant growth. Plant Cell 14, 1223–33. https://doi.org/10.1105/tpc.001388.Nongrasses

Wang, H.Y., Klatte, M., Jakoby, M., Bäumlein, H., Weisshaar, B., Bauer, P., 2007. Iron deficiency-mediated stress regulation of four subgroup Ib BHLH genes in Arabidopsis thaliana. Planta 226, 897–908. https://doi.org/10.1007/s00425-007-0535-x

Wang, Y.-S., Pi, L.-Y., Chen, X., Chakrabarty, P.K., Jiang, J., De Leon, A.L., Liu, G.-Z., Li, L., Benny, U., Oard, J., Ronald, P.C., Song, W.-Y., 2006. Rice XA21 binding protein 3 is a ubiquitin ligase required for full Xa21-mediated disease resistance. Plant Cell 18, 3635–3646. https://doi.org/10.1105/tpc.106.046730

World Health Organization, 2013. Prevention of Iron Deficiency Anaemia in Adolescents Role of Weekly Iron Acid Supplementation, Pediatrics. https://doi.org/10.3390/nu6125915

Xiong, L., Lee, H., Ishitani, M., Tanaka, Y., Stevenson, B., Koiwa, H., Bressan, R.A., Hasegawa, P.M., Zhu, J.-K., 2002. Repression of stress-responsive genes by FIERY2, a novel transcriptional regulator in Arabidopsis. Proc. Natl. Acad. Sci. U. S. A. 99, 10899–904. https://doi.org/10.1073/pnas.162111599

Xu, Y., 2016. Envirotyping for deciphering environmental impacts on crop plants. Theor. Appl. Genet. 129, 653–673. https://doi.org/10.1007/s00122-016-2691-5

Yi, Y., Guerinot, M. Lou, 1996. Genetic evidence that induction of root Fe(III) chelate reductase activity is necessary for iron uptake under iron deficiency. Plant J. https://doi.org/10.1046/j.1365-313X.1996.10050835.x

Yuan, X., Zhang, S., Liu, S., Yu, M., Su, H., Shu, H., Li, X., 2013. Global Analysis of Ankyrin Repeat Domain C3HC4-Type RING Finger Gene Family in Plants. PLoS One 8, 1–12. https://doi.org/10.1371/journal.pone.0058003

Yuan, Y., Wu, H., Wang, N., Li, J., Zhao, W., Du, J., Wang, D., Ling, H.-Q., 2008. FIT interacts with AtbHLH38 and AtbHLH39 in regulating iron uptake gene expression for iron homeostasis in Arabidopsis. Cell Res. 18, 385–397. https://doi.org/10.1038/cr.2008.26

Zhai, Z., Gayomba, S.R., Jung, H. -i., Vimalakumari, N.K., Pineros, M., Craft, E., Rutzke, M.A., Danku, J., Lahner, B., Punshon, T., Guerinot, M.L., Salt, D.E., Kochian, L. V., Vatamaniuk, O.K., 2014. OPT3 Is a Phloem-Specific Iron Transporter That Is Essential for Systemic Iron Signaling and Redistribution of Iron and Cadmium in Arabidopsis. Plant Cell 26, 2249–2264. https://doi.org/10.1105/tpc.114.123737

Zhang, J., Liu, B., Li, M., Feng, D., Jin, H., Wang, P., Liu, J., Xiong, F., Wang, J., Wang, H.-B., 2015. The bHLH Transcription Factor bHLH104 Interacts with IAA-LEUCINE RESISTANT3 and Modulates Iron Homeostasis in Arabidopsis. Plant Cell 27, 787–805. https://doi.org/10.1105/tpc.114.132704

Zheng, L., Ying, Y., Wang, L., Wang, F., Whelan, J., Shou, H., 2010. Identification of a novel iron regulated basic helix-loop-helix protein involved in Fe homeostasis in Oryza sativa. BMC Plant Biol. 10, 166. https://doi.org/10.1186/1471-2229-10-166

Zimmermann, P., 2004. GENEVESTIGATOR. Arabidopsis Microarray Database and Analysis Toolbox. Plant Physiol. 136, 2621–2632. https://doi.org/10.1104/pp.104.046367

APPENDIX

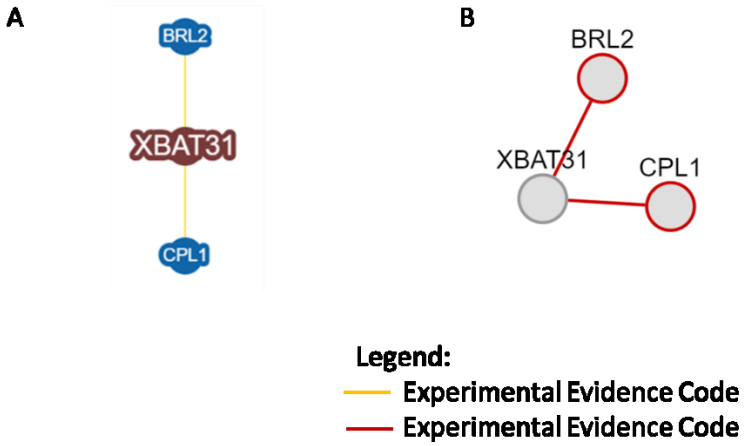

Figure 24 - Sup. Figure 1 - XBAT31 Protein Interactors.

Experimentally confirmed interaction between XBAT31 and BRL2 (Ceserani et al. 2009) and CPL1 (Bang et al. 2008). Modified from BioGRID (A) (Biological General Repository for Interaction Datasets: https://thebiogrid.org) and from ARABPORT (B) (The Arabidopsis Information Portal: https://apps.araport.org/thalemine/begin.do). The databases did not define which version of XBAT31 is used in the interactions.

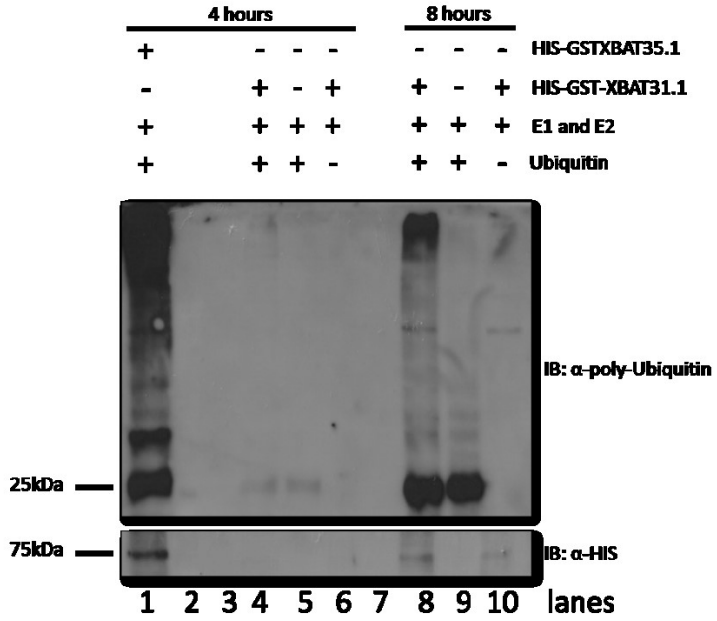

Figure 25 - Sup. Figure 2 - *In vitro* Ubiquitination Assay Showing XBAT31.1 Ubiquitin Ligase Activity.

In the second trial, HIS-GST-XBAT31.1 was incubated with yeast E1, Arabidopsis E2 HIS-AtUBC8 and ubiquitin. A high molecular weight smear detected by immunoblotting (IB) with ubiquitin antibodies indicates the presence of ubiquitinated proteins (lanes 4 and 8). The omission of ubiquitin (lanes 6 and 10) or HIS-GST-XBAT31.1 (lanes 5 and 9) from the assay prohibited protein ubiquitination. HIS-GST-XBAT35.1 was used as a positive control (lane 1). Anti-HIS was used to demonstrate the presence of the HIS-GST-XBAT31.1 and HIS-GST-XABT35.1 in the assay.

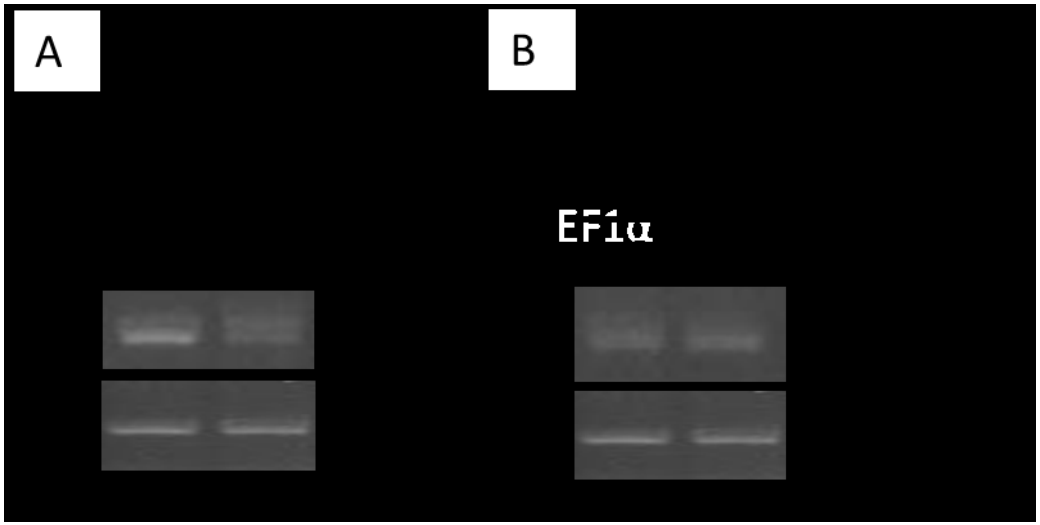

Figure 26 - Sup. Figure 3 - Expression of *XBAT31* Isoforms under Iron Deficient and Sufficient Conditions.

Second trial of *XBAT31.1* (A) and *XBAT31.2* (B) expression analysis using RT-PCR from RNA extracted of 9-day-old wild type (WT) seedlings grown with (+) and without (-) Fe. *EF1α* was used as a control.

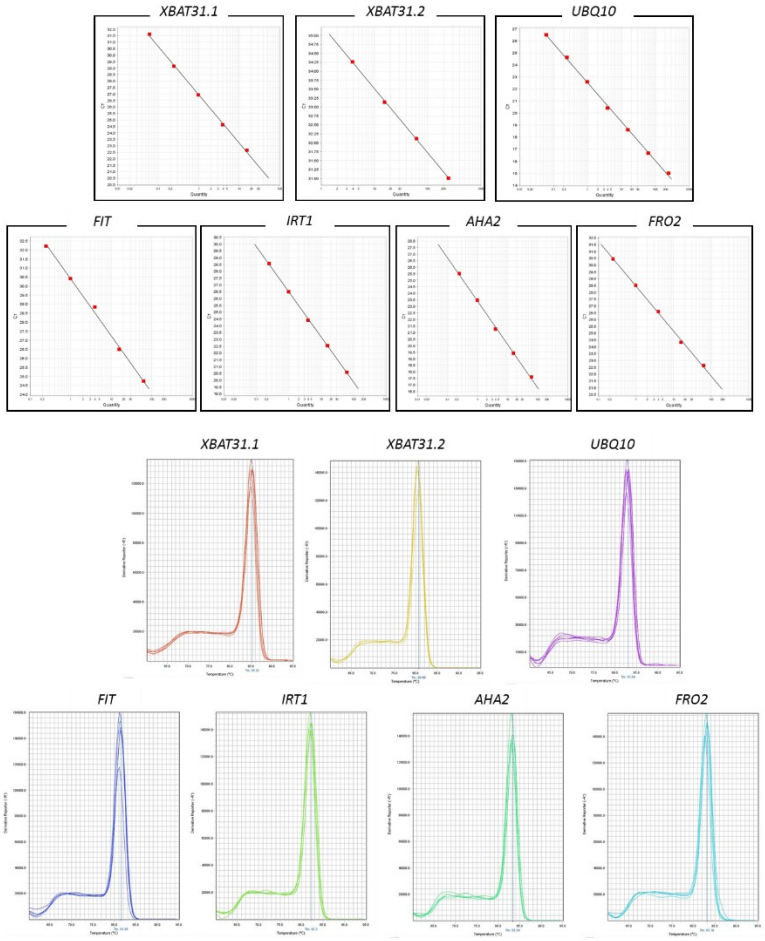

Figure 27 - Sup. Figure 4 – Standard and Melt Curves for qRT-PCR of *XBAT31.1, XBAT31.2* and *Fe-utilization related* Genes.

Fe-utilization related genes include: *FIT, FRO2, AHA2* and *IRT1*. *UBIQUITIN 10 (UBQ10)* was used as a housekeeping gene in qRT-PCR experiments. All 7 gene primers presented an amplification efficiency between 90-110%.

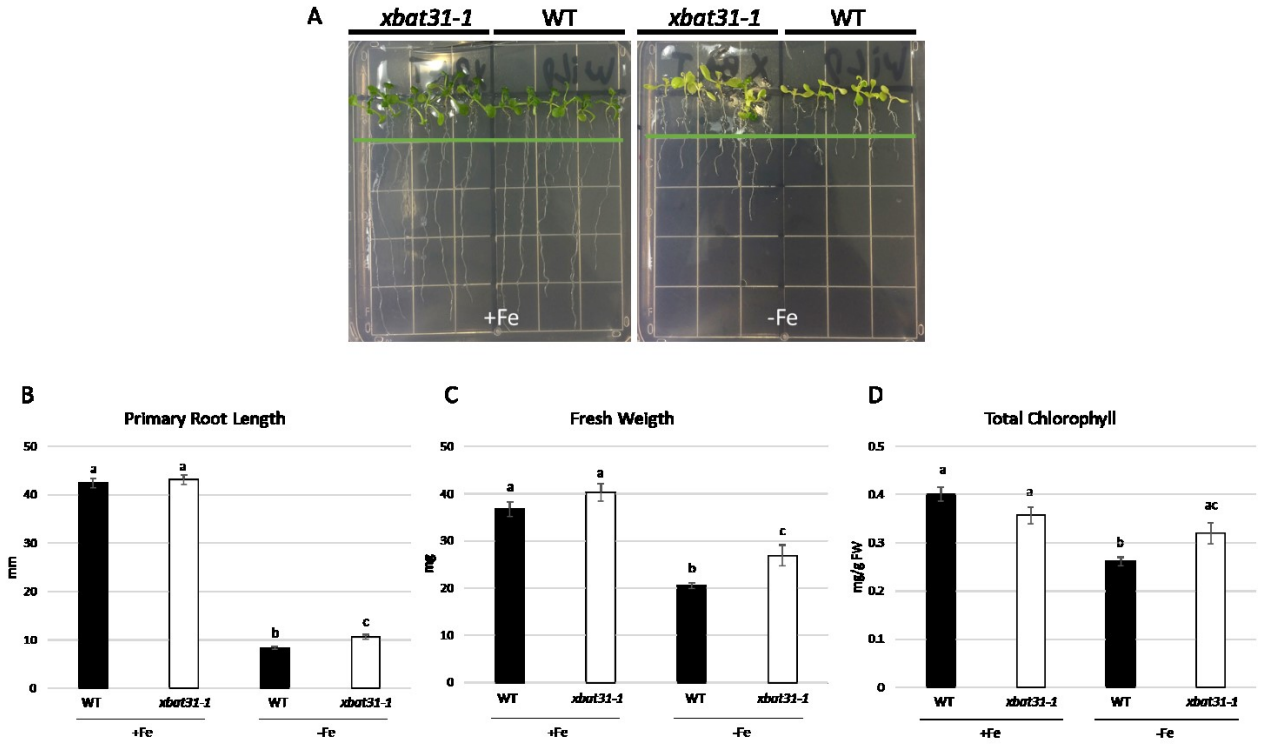

Figure 28 - Sup. Figure 5 - Growth of *xbat31-1* and Wild Type (WT) Seedlings under Iron Sufficient (+Fe) and Iron Deficient (-Fe) Conditions.

xbat31-1 and wild type (WT) seedlings were grown with (+) and without (-) Fe. Representative (A) 9-day-old *xbat31-1* and WT seedlings grown under +Fe and -Fe conditions. Green line indicates root length at time of transfer. Quantification primary root length (B), fresh weight (C) and total chlorophyll content (D) of WT and xbat31-1 seedlings. Different letters indicate p-value ≤ 0.05 using One-Way ANOVA Tukey comparison. Error bars indicate ±SE from 3 trials with 15 replicates per trial.

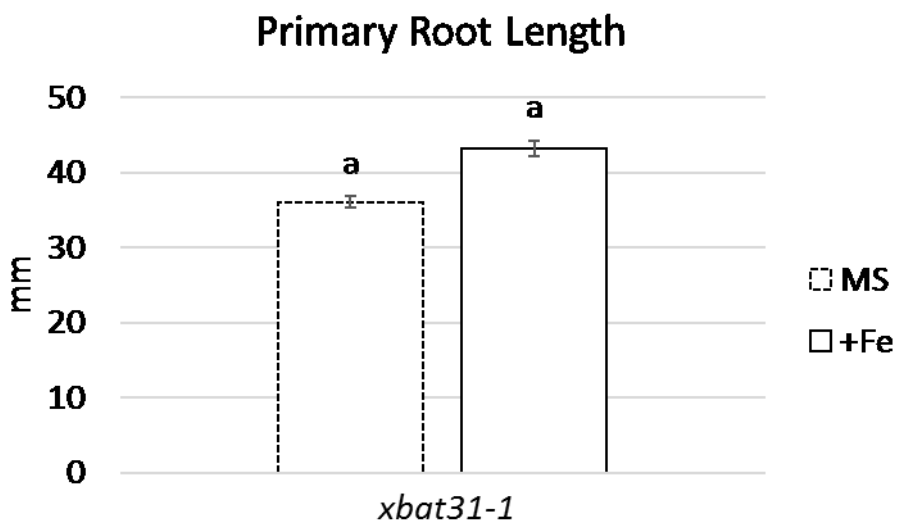

Figure 29 - Sup. Figure 6 - Growth of *xbat31-1* under Standard (MS) and Iron Sufficiency (+Fe) Conditions.

XBAT31 mutants were grown under standard media (solid MS media without any complementation of Fe-EDTA) and +Fe (solid MS media supplemented with 100µM of Fe-EDTA). *xbat31-1* seedlings did not show any significant difference in growth under both medias. Same letter means p-value >0.05 using One-Way ANOVA Tukey comparison. Error bars indicate ± 1 SE from up to 10 technical replicates per trial in a total of 2 trials.

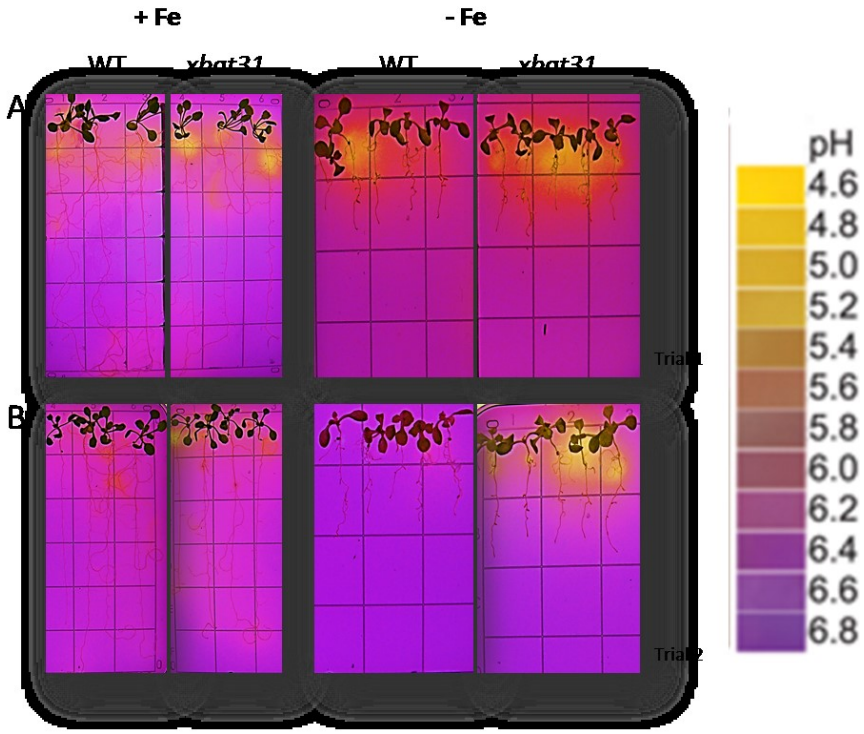

Figure 30 - Sup. Figure 7 - Rhizosphere Acidification Assessment of WT and *xbat31-1*.

Rhizosphere acidification of WT and *xbat31-1* seedlings was asses using Bromocresol Purple (BP) media (pH indicator). 9-day-old xbat31-1 and WT seedlings grown under +Fe and -Fe conditions were placed in BP plates for 24h. Increasing in acidification levels would lead to media to become yellow and alkalinisation would lead to media to become dark purple. First trial (A) and second trial (B) indicated increase in rhizosphere acidification of *xbat31-1* seedlings compared to WT.

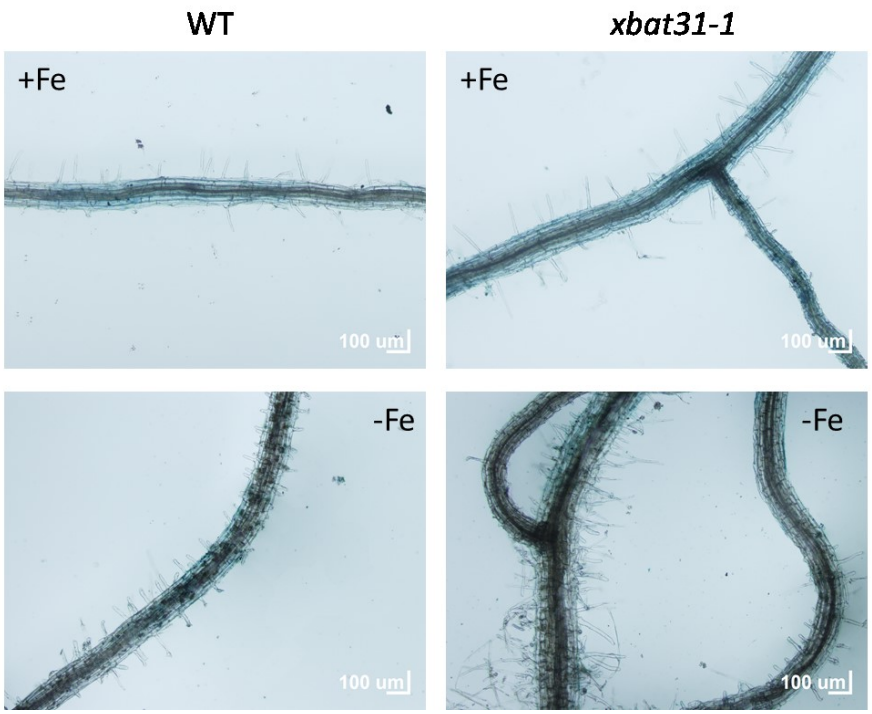

Figure 31 - Sup. Figure 8 - Perls Stain of WT and *xbat31-1*.

Accumulation of Fe(II) in roots of WT and *xbat31-1* seedlings was asses using ferrocyanide (Perls solution). Roots of 9-day-old *xbat31-1* and WT seedlings grown under +Fe and -Fe conditions were incubated with ferrocyanide (Perls solution) for 30 min. Increasing in concentration of Fe(II) in roots would lead to a dark blue color. Pictures indicated no change in vascular tissue deposition of Fe(II) between WT and xbat31-1 under +Fe or –Fe conditions.

Table 7 - Sup. Table 1.1 - Ratio of Metal Content in Wild Type (WT) and *xbat31-1* Seedlings (Shoots).

Part 1. Ratio between +Fe (WT/*xbat31-1*) and –Fe (WT/*xbat31-1*) from 2 biological replicates, each measured 3 times, including standard error (SE) and p-values of shoot metal content. Significant increase (ratio > 1) or decrease (ratio < 1) is indicated by p-value ≤0.05 using One-Way ANOVA Tukey comparison. xbat31-1 seedlings showed significant decrease in Fe, Mn and Co concentrations in shoots under -Fe condition compared to WT, and no significant difference in other metals concentration.

WT – Shoots										
+Fe	24Mg	31P	44Ca	55Mn	56Fe	59Co	65Cu	66Zn	60Ni	111Cd
Average	2272.00	11694.00	6533.11	222.20	452.58	0.19	22.55	120.17	3.88	0.41
SE	136.81	623.84	369.90	13.49	15.63	0.01	0.74	9.11	1.34	0.07
xbat31 – Shoots										
+Fe										
Average	2286.33	12277.78	6892.56	223.98	419.06	0.21	21.57	117.17	5.41	0.29
SE	50.16	264.22	80.14	5.94	15.56	0.01	0.20	3.90	1.38	0.05
P.value	0.923	0.402	0.356	0.906	0.148	0.321	0.229	0.766	0.438	0.156
Ratio (xbat/WT)	1.01	1.05	1.06	1.01	0.93	1.07	0.96	0.98	1.39	0.70

Table 8 - Sup. Table 1.2 - Ratio of Metal Content in Wild Type (WT) and *xbat31-1* Seedlings (Shoots).

Part 2. Ratio between +Fe (WT/*xbat31-1*) and –Fe (WT/*xbat31-1*) from 2 biological replicates, each measured 3 times, including standard error (SE) and p-values of shoot metal content. Significant increase (ratio > 1) or decrease (ratio < 1) is indicated by p-value ≤0.05 using One-Way ANOVA Tukey comparison. xbat31-1 seedlings showed significant decrease in Fe, Mn and Co concentrations in shoots under -Fe condition compared to WT, and no significant difference in other metals concentration.

WT – Shoots										
-Fe	24Mg	31P	44Ca	55Mn	56Fe	59Co	65Cu	66Zn	60Ni	111Cd
Average	2056.89	9765.78	6177.56	245.26	303.48	0.21	23.25	190.38	7.56	2.32
SE	40.54	144.92	137.20	1.53	4.88	0.00	1.63	10.85	1.22	1.06
xbat31-1 – Shoots										
-Fe										
Average	2109.89	9451.22	6302.89	200.06	103.20	0.15	25.44	196.70	5.49	1.03
SE	54.95	133.62	203.20	4.58	8.13	0.02	1.44	8.22	1.29	0.18
P-value	0.449	0.130	0.616	**0.000**	**0.000**	**0.004**	0.339	0.653	0.262	0.246
Ratio										
(*xbat31-1*/WT)	1.03	0.97	1.02	0.82	0.34	0.71	1.09	1.03	0.73	0.44

Table 9 - Sup. Table 2.1 - Ratio of Metal Content in Wild Type (WT) and *xbat31-1* Seedlings (Roots).

Part 1. Ratio between +Fe (WT/*xbat31-1*) and –Fe (WT/*xbat31-1*) from 2 biological replicates, each measured 3 times, including standard error (SE) and p-values of roots metal content. Significant increase (ratio > 1) or decrease (ratio < 1) is indicated by p-value ≤0.05 using One-Way ANOVA Tukey comparison. xbat31-1 seedlings showed a significant increase in Co concentration in roots under -Fe condition, and a significant increase in Cu concentration under +Fe condition compared to WT. No significant difference was found for other metals concentration.

WT – Roots										
+Fe	24Mg	31P	44Ca	55Mn	56Fe	59Co	65Cu	66Zn	60Ni	111Cd
Average	625.88	7244.67	2249.00	33.44	2986.17	0.25	32.73	99.48	3.14	0.30
SE	10.09	250.75	63.29	1.23	61.51	0.02	0.95	7.74	0.31	0.07
xbat31-1 – Roots										
+Fe										
Average	534.57	7043.50	2432.50	29.96	3024.33	0.31	29.37	98.32	3.52	0.26
SE	57.29	388.21	56.22	3.28	173.09	0.00	1.86	9.52	0.26	0.06
P-value	0.148	0.673	0.055	0.336	0.840	**0.000**	0.139	0.926	0.361	0.682
Ratio										
(*xbat31-1*/WT)	**0.85**	**0.97**	**1.08**	**0.90**	**1.01**	**1.20**	**0.90**	**0.99**	**1.12**	**0.87**

Table 10 - Sup. Table 2.2 - Ratio of Metal Content in Wild Type (WT) and *xbat31-1* Seedlings (Roots).

Part 2. Ratio between +Fe (WT/*xbat31-1*) and –Fe (WT/*xbat31-1*) from 2 biological replicates, each measured 3 times, including standard error (SE) and p-values of roots metal content. Significant increase (ratio > 1) or decrease (ratio < 1) is indicated by p-value ≤0.05 using One-Way ANOVA Tukey comparison. xbat31-1 seedlings showed a significant increase in Co concentration in roots under -Fe condition, and a significant increase in Cu concentration under +Fe condition compared to WT. No significant difference was found for other metals concentration.

WT – Roots										
-Fe	24Mg	31P	44Ca	55Mn	56Fe	59Co	65Cu	66Zn	60Ni	111Cd
Average	981.93	7268.00	2987.33	3750.33	266.77	4.04	22.59	1732.50	10.27	0.75
SE	47.29	31.07	116.53	42.40	45.20	0.04	1.78	40.58	1.98	0.14
xbat31-1 – Roots										
-Fe										
Average	1115.87	7444.11	2797.00	4226.67	354.63	3.70	30.53	2000.83	15.05	0.58
SE	59.75	169.96	28.74	395.47	61.35	0.52	1.79	99.40	4.49	0.04
P-value	0.098	0.323	0.144	0.259	0.266	0.531	**0.010**	0.733	0.353	0.278
Ratio										
(*xbat31-1*/WT)	**1.14**	**1.02**	**0.94**	**1.13**	**1.33**	**0.92**	**1.35**	**1.15**	**1.47**	**0.78**

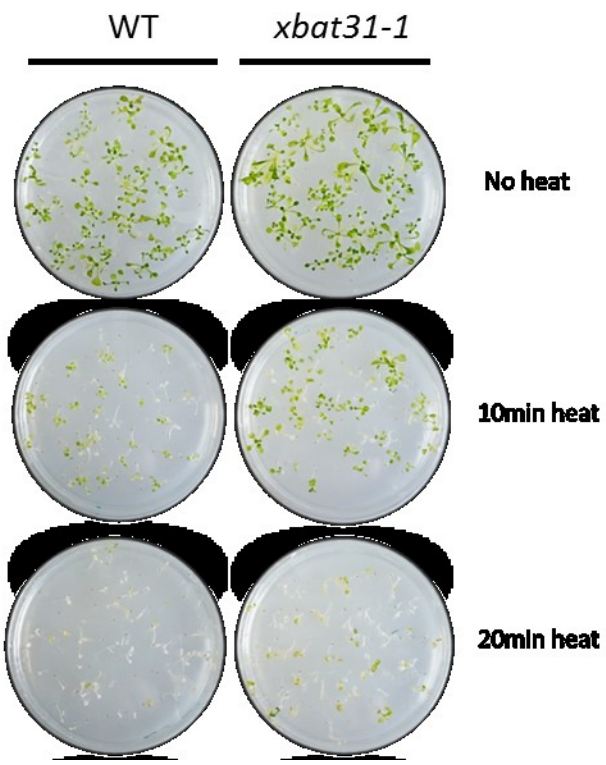

Figure 32 - Sup. Figure 9 - Heat Stress Response Analysis of *xbat31-1*.

Second trial rrepresentative pictures of 2-weeks-old WT and *xbat31-1* seedlings grown under standard media (solid MS media) following exposure to 50ºC for 5, 10, 20 and 40 minutes and 7-days-recovery period after exposure to 50ºC for the indicated time and 7-days-recovery period